MECHANISMS OF INTERPLAY BETWEEN UGTs AND EFFLUX TRANSPORTERS IN FLAVONOID DISPOSITION

A

Dissertation

Presented to the Faculty of

The University of Houston

College of Pharmacy

Department of Pharmacological & Pharmaceutical Sciences

In Partial Fulfillment of the Requirement for the Degree of

DOCTOR OF PHILOSOPHY

By

Wen Jiang

November, 2011

ABSTRACT

Objective: The overall objective is to investigate the mechanism(s) of interplay between UDP-glucuronosyltransferases (UGTs) and efflux transporters in flavonoid disposition. The goals of this research project were to 1) develop and characterize a cell model suitable to study the simplest interplay between one UGT (i.e., UGT1A9) and an efflux transporter (i.e., BCRP); 2) study the interplay between UGT1A9 and BCRP in flavonoid disposition using the established and well-characterized HeLa cell model; 3) compare the interplay between UGTs and efflux transporters in the flavonoid disposition among different cellular and animal models; 4) determine the kinetic parameters of efflux of flavonoid glucuronides that are transported by the specific efflux transporter in the established HeLa cell model.

Methods: For objective 1), HeLa cells were stably transfected with *UGT1A9* gene which was cloned in the pcDNA3.1 (+/-) vector. The developed "engineered" HeLa cells were characterized at expression levels by the Western blotting and RT-PCR, and at functional levels by metabolism and excretion assay. For objective 2), the engineered HeLa cells overexpressing UGT1A9 were treated with several flavonoids in the presence or absence of efflux transporter inhibitors or siRNA of UGT1A9. For objective 3), Caco-2 cells, the engineered MDCKII-BCRP or MDCKII-MRP2 cells (the MDCKII series cells transiently transfected with *UGT1A9*) was treated with flavonoids with or without Ko143, a potent chemical inhibitor of BCRP. In addition, FVB and Bcrp (-/-) mice were

orally given the selected flavonoid at dose of 20mg/kg. For objective 4), the engineered HeLa cells grown on the 6-well plates were treated with several commercially available mono-hydroxyflavones and other selected compounds using concentrations sufficient to describe kinetics of glucuronide efflux.

Results: 1) In the engineered HeLa cells, which were shown to be functional stable for at least five generations, UGT1A9 and BCRP were predominantly expressed. The glucuronidation of model flavonoids (e.g. genistein and apigenin) catalyzed by UGT1A9 overexpressed in the engineered HeLa cells was following the same kinetic mechanism as that by UGT1A9 Supersome^{TM}, although the UGT1A9 isoform from the HeLa cells usually had a larger K_m and smaller V_{max} than those from the Supersome^{TM}. In addition, the glucuronide excretion in the engineered HeLa cells was mainly attributed to the predominant expressed BCRP, because neither the broad specific MRP inhibitor LTC_4, nor the potent siRNAs against MRP2 and MRP3 was effective in inhibiting the glucuronide efflux. 2) To study the mechanism of kinetic interplay between UGTs and efflux transporters in flavonoid disposition, we found that in the engineered HeLa cells, the siRNA-mediated UGT1A9 silencing could result in substantial decreases in glucuronide excretion (40-86%, $p<0.01$), cellular glucuronide levels (45-98%, $p<0.01$), and cellular glucuronidation activity or f_{met} (40-87%, $p<0.01$). However, the BCRP function (measured using glucuronide clearance or CL) was not or marginally affected by siRNA silencing. On the other hand, dose-dependent inhibition of BCRP by Ko143 could lead to the dramatic increase in the intracellular glucuronide levels (4-8 folds), moderate decrease in glucuronide

excretion (<60%), and substantial inhibition of CL (>75%). The effect of Ko143 (5μM) on f_{met} was compound-dependent. 3) To compare the engineered HeLa cells with other cell or animal models, we found that inhibition of BCRP by Ko143 (5μM) did not affect the phase II metabolism of flavonoids but affected the distribution of flavonoid sulfates in Caco-2 cells. In the engineered MDCKII-BCRP or –MRP2 cells, which were transiently transfected with *UGT1A9*, the excretion rates of wogonin glucuronide, intracellular levels of glucuronides and f_{met} were all significantly increased. In Bcrp knockout mice, the $AUC_{0\text{-}480min}$ values of wogonin and its conjugates were markedly improved (10 folds, $P<0.05$), compared with FVB mice. 4) In determining the kinetics parameters of glucuronides transported by BCRP, we found that the correlation of K_m' between vesicles and engineered HeLa cells appeared to be better than other kinetics parameters such as J_{max} (or maximal efflux rate constant).

Conclusion: Engineered HeLa cells which are stably transfected with *UGT1A9* are an appropriate tool to study the mechanisms of kinetic interplay between UGTs and efflux transporters and to rapidly identify the glucuronide substrate of BCRP. The bioavailability of flavonoid such as wogonin could be improved experimentally by disrupting the function of BCRP in a mouse pharmacokinetic model in vivo.

ACKNOWLEDGEMENT

It is my great pleasure to acknowledge everyone who has accompanied me during my journal for the Ph.D. degree.

Foremost, I would like to express my sincere appreciation and gratitude to my major advisor - Dr. Ming Hu, for the continuous guidance and support of my study and research, for his patience, enthusiasm, motivation, and immense knowledge. Dr. Hu has provided me a free and enjoyable environment, in which I can pursue my own interests with fun and dedication. His scientific guidance, expertise and keen sense ensure that I am not only on the right track, but also can be exposed to the scientific frontier. His optimism has moved and inspirited me. He is a role model that I will follow for the rest of my life as a young scientist.

My special thanks go to Drs. Diana Chow, Romi Ghose, Vincent Tam, and Rong Yu for their continuous encouragement and valuable advice. I am so blessed to have everyone of you as a member of my Ph.D. committee.

I would also like to thank previous and current labmates, members from PPS department who lent me help during the entire period of my Ph.D. study.

Last but not the least, I really appreciate my parents-Fuxi Jiang and Yizhi Liu, who are always on my side to encourage me and have provided me a better environment for pursuing my interests freely since I was a kid; my husband, Lingyi Zeng, who has always been there, not only carefully taking care of me, but also readily listening to, comforting and motivating me when I feel frustrated; my

relatives, especially my grandparents and aunts, who have been giving me faith and warmth during each period of my development.

I would like to cite one of my favorite songs by Josh Groban to end this acknowledgement:

" You raise me up, so I can stand on mountains;

You raise me up, to walk on stormy seas;

I am strong, when I am on your shoulders;

You raise me up… To more than I can be."

TABLE OF CONTENTS

LIST OF FIGURES

LIST OF TABLES

CHAPTER 1: LITERATURE REVIEW AND INTRODUCTION TO THE THESIS PROJECT

Flavonoids are naturally-occurring polyphenolic compounds which are easily accessible via our daily diet. Accumulating evidence has showed that flavonoids have various “claimed” beneficial effects such as chemoprevention, cardiovascular disease prevention, antioxidant, anti-virus and anti-inflammation [1-5]. However, the big challenge that prevents flavonoids from exhibiting their beneficial properties is their poor bioavailability (<5%) [1-4].

It is well known that the extensive phase II metabolism by either uridine-5’-diphospho-glucuronosyltransferases (UGTs) or sulfotransferases (SULTs) and the sequential excretion of phase II metabolites by efflux transporters are the two main reasons for the low bioavailability of flavonoids. However, it has not been directly proven yet whether and how the phase II enzymes and efflux transporters are working coordinately to limit the bioavailability of flavonoids. Therefore, our study will first prove the existence of interplay between phase II enzymes and efflux transporters. Due to the unsuccessful experience with the current in vitro models, we will develop a suitable cell model, in which only one UGT isoform and one efflux transporter were predominantly expressed, to demonstrate the existence as well as the simple mechanisms of the interplay (Chapter 4). We then will use the newly developed cell model to study how the

interplay affects the disposition of flavonoids (Chapter 5) and compare the results with those obtained in Caco-2 cells and modified MDCKII series cells (Chapter 6). Next, a mouse model will be used to determine whether the disrupting one player in the interplay can improve the bioavailability of flavonoids (Chapter 6). In addition, we will also try to expand the application of the newly developed HeLa cell model to determine whether and how changes in flavonoid glucuronide structures affect its efflux kinetics parameters (Chapter 7).

In this chapter (Chapter 1), the first section (1.1) gives us a detailed introduction of flavonoids with respective to their chemical structures and classification, natural sources, beneficial properties and low bioavailability. The second section (1.2) introduces the metabolic pathways of flavonoids and the involving enzymes with a focus on UGTs. The third section (1.3) introduces the efflux transporters involved in excretion of flavonoid and their metabolites. The last section (1.4) discusses the variety of interplays between drug metabolizing enzymes and transporters.

1.1. Flavonoids

1.1.1. Introduction of flavonoids

Flavonoids are a class of polyphenolic compounds produced as secondary plant metabolites. Flavonoids are widely distributed in nature and consist of various

compounds with similar backbone structures. The typical sources of flavonoids include vegetables, fruits, beans, grains and herbs. Therefore, it is easy for an average person to intake flavonoids from daily diet. Studies indicated that typical daily intake of flavonoids was in the range of 20-50mg/day in several Western populations [5-7]. The most attractive property of flavonoids is due to their multiple "claimed" beneficial effects to human.

1.1.2. Chemical structure and classification

In nature, flavonoids are usually presented as glycosides and to a less extent as aglycones and some of their methylated derivatives. For aglycones, they share the backbone consisting of three carbon rings: a benzene ring (A) linked with a six-membered ring (C), in which the 2 position carries a phenyl ring (B) as a substituent [8]. For glycosides, the sugars are normally attached to the hydroxyl groups at position 3 or 7 of A ring. The common sugars or carbohydrates linked with aglycones are D-glucose, glucorhamnose, galactose, L-rhamnose or arabinose [8]. For methylated derivatives, the methylation usually occurs at position 5' and 3' of the B ring or at position 7 of the A ring [9]. According to their chemical structures, flavonoids (aglycones) are classified into several subfamilies: flavones, flavonols, flavanone, flavanonol, flavanol, isoflavones, anthocyanidin and chalcones (Fig. 1) [10]. In the future study, flavonoids from flavones and isoflavone are our focus. Without any specification, flavonoids are referred to aglycones.

1.1.3. Source

Flavonoids are enriched in many plants which are consumable for human such as vegetables, fruits, beans, grains, herbs and spices. The typical vegetables with high enrichment of flavonoids are including broccoli [11], parsley [12], spinach [13] and onions [14] etc. The common fruits are including orange, varieties of berries and apples [15]. In addition to daily diets, some beverages also contain high amounts of flavonoids such as tea [16] , juice [17] and red wine [18] . For U.S. adults, the estimated mean daily total flavonoid intake was 189.7 mg/d, which was mainly from flavan-3-ols (83.5%) followed by flavanones (7.6%), flavonols (6.8%), anthocyanidins (1.6%), flavones (0.8%) and isoflavones (0.6%) [5].

1.1.4. “Claimed” beneficial effects

More and more evidence suggested that high consumption of flavonoids-rich diet was associated with a lower incidence and mortality rate of various degenerative diseases such as cancer [5, 19], cardiovascular disease [5, 20] and immune dysfunction [5, 21]. This is because flavonoids have various biological activities, which are suggested to be beneficial to human. The most extensive studied biological activities of flavonoids include anti-cancer, anti-inflammatory, antioxidant, antineoplastic, antimicrobial, cardiotonic and lipid lowering activity [8].

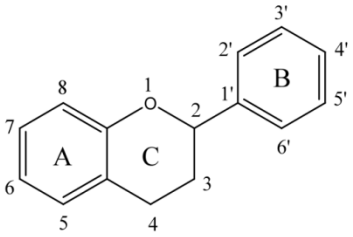

Backbone of flavonoids

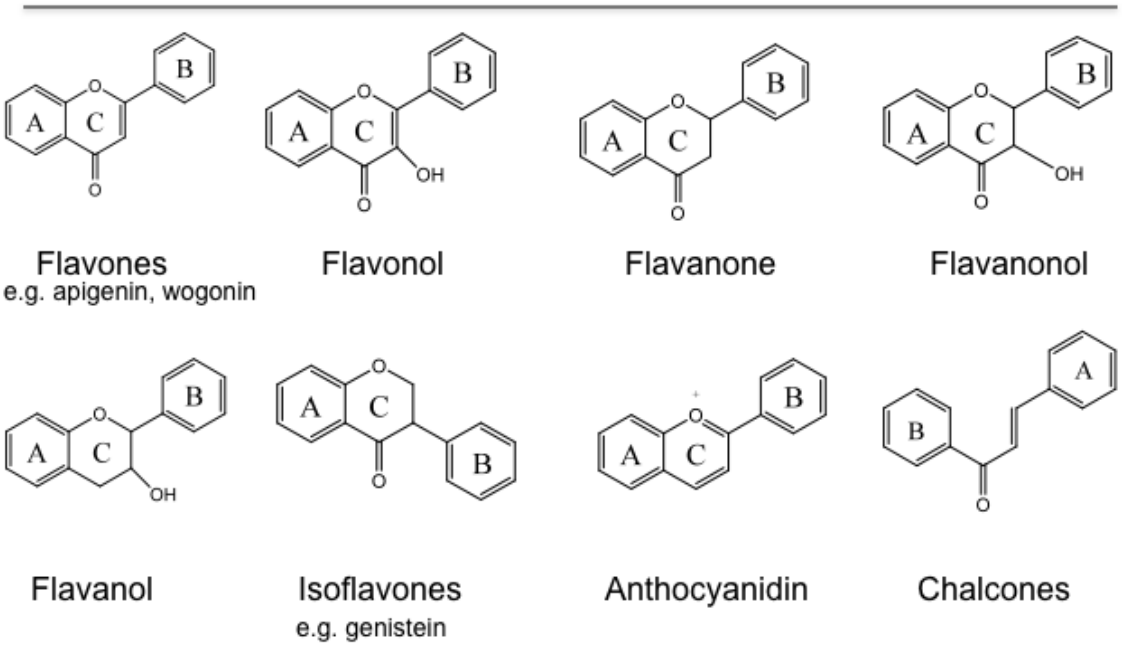

Fig. 1 Chemical structures of flavonoids from various subfamilies. The most used model flavonoids from flavones and isoflavones subfamilies are listed along with representative chemical structures.

1.1.5. Disposition of flavonoids and their low bioavailability

To exert biological activities, flavonoids must be absorbed and remain as aglycones in the body, since flavonoid metabolites are rarely reported as the active species [22] . In addition, aglycones are believed to be able to passively diffuse across the gut wall, though evidences suggest that the absorption of intact glycosides may also occur, albeit at significantly slower rate [23-24]. For most flavonoid glycosides, they must be hydrolyzed to aglycones either by microorganisms residing in intestine or by brush-border enzymes (e.g. lactase phloridzin hydrolase, LPH) before their absorption [25-27]. The absorption of flavonoids is a rapid process. During absorption, flavonoids are subjected to metabolism (especially phase II) by intestine conjugating enzymes. Even after passing through the intestinal epithelium intactly, flavonoid aglycones would still be subjected to the similar rapid metabolism (especially phase II) by the liver conjugating enzymes. Therefore, phase II metabolism plays a significant role in absorption and metabolism of flavonoids. On the other hand, phase I metabolism (e.g. cytochrome P450) other than hydrolysis makes minor contribution to flavonoid clearances after absorption [28].

Most of the flavonoids undergo two types of phase II metabolisms in both enterocytes and hepatocytes: glucuronidation by uridine-5'-diphosphate glucuronosyltransferases (UGTs) and/or sulfation by sulfotransferases (SULTs) [29]. As a result, flavonoid glucuronides and/or sulfates are formed, respectively. These phase II metabolites of flavonoids could be subsequently excreted into lumen or bile by efflux transporters such as multidrug resistance protein 2

(MRP2) [30] and breast cancer resistance protein (BCRP) [31]. Interestingly, the excreted glucuronides and sulfates in the intestine can be hydrolyzed by microflora or β-glucuronidases back to flavonoid aglycones, which can undergo absorption and metabolism again. Therefore, it is not surprising to speculate that the low bioavailability of flavonoids (<5%) is due to the presence of a potent disposition network that is mainly consisting of phase II conjugating enzymes and efflux transporters [32].

1.2. Metabolism of flavonoids

1.2.1. Drug metabolizing enzymes

Drug metabolizing enzymes (DME) are a diverse group of proteins responsible for biotransforming a series of xenobiotics including drugs and pollutants as well as some endogenous substances (e.g. bilirubin and estradiol) [33]. DME play a significant role in maintaining the normal physiological function of human by preventing accumulation of toxins inside the body. DME are divided into two groups: phase I enzymes and phase II enzymes, which are responsible for phase I metabolism and phase II metabolism, respectively [34].

1.2.2. CYP450 and phase I metabolism

Phase I enzymes can catalyze the reaction incorporating or unmasking functional groups, such as hydroxylgroups, primary amines and carboxylic acids, etc. As a result, oxidation, reduction or hydrolysis can happen to the substrates of phase I

enzymes. Among all the phase I enzymes, cytochrome P450 (CYP) superfamily, which consists of membrane-bound proteins with approximate molecular weight of 50KD, catches most attention and extensive investigation due to its wide distribution, large variety and ability to metabolize majority of drugs. CYP450-mediated metabolisms usually result in oxidation reaction with introduction of an oxygen atom into substrate molecules. So far, more than fifty isoforms from CYP450 superfamily are discovered in human, which are further classified into 17 families and 39 subfamilies due to their amino acid sequence similarities [35]. Within this large superfamily, CYP3A4/5, CYP2D6, CYP2C8/9, CYP1A2, CYP2C19, CYP2E1, CYP2B6 and CYP2A6 are well investigated because their substrates are almost including every drug on the markets. Therefore, to prevent potential drug- drug interaction, the US food and drug administration (FDA) drafted the guidance for industry to emphasize the drug metabolism study with respect to CYP450 on the new investigational drugs.

Flavonoids, like other drugs or xenobiotics, can be metabolized by cytochrome P450 (CYP450) enzymes. It was reported that CYP2C9 was the most efficient isoform for the oxidation of galangin followed by CYP1A3 and CYP1A1 [36]. For kaempferide, CYP1A2 was predominantly responsible for its oxidation followed by CYP2C9 and CYP1A1 [37]. However, compared with the phase II metabolic pathways, CYP450-mediated metabolism contributes little to metabolism of flavonoids. In addition, CYP-mediated metabolism of flavonoids has never been shown to be important in vivo or in intact cells. For example, apigenin was metabolized by rat liver microsomes to form three monohydroxylated derivatives,

one of which was luteolin [28]. Further investigation indicated the involvements of CYP1A1, CYP3B and CYP2E1 in apigenin hydroxylation in vitro [28]. However, when apigenin was perfused through an isolated rat liver, none of the phase I metabolites could be recovered in the effluent perfusate [28], suggesting that CYP-mediated metabolism had little significance in flavonoid clearance, when phase II metabolic pathway was functioning. Therefore, metabolism via CYP is not a major clearance mechanism for flavonoids and not mainly responsible for their poor bioavailability in vivo.

1.2.3. Phase II metabolism

In contrast to minor contribution of phase I metabolism, phase II metabolism was predominant for flavonoids both in vitro and in vivo. In the phase II metabolism, conjugating enzymes (also called phase II enzymes) catalyze the reaction incorporating a large conjugates onto the substrates at the position with carboxyl, hydroxyl, amino or sulfhydryl group. The attached conjugates include glucuronic acid, sulfonates, glutathione and amino acids. With the assistance of phase II enzymes, substrates are more hydrophilic with their increasing molecular weight and become inactive. Thus the reactions catalyzed by phase II enzymes are usually regarded detoxification [34]. The well-known phase II enzymes include UDP-glucuronosyltransferases (UGTs), sulfotrasferases (SULTs) and glutathione S-transferases (GSTs), which are responsible for glucuronidation, sulfation and glutathione conjugation respectively. It is believed that glucuronidation could

occur directly to the substrates but not necessarily after oxidation of substrates mediated by CYP 450.

1.2.4. UDP-glucuronosyltransferases (UGTs)

Enzymes from UGT superfamily are located to the endoplasmic reticulum with molecular weight of 50-60KD. These UGTs are able to transfer the glucuronyl group from uridine 5'-diphosphoglucuronic acid (UDPGA) to the substrates which have functional group of oxygen, nitrogen, sulphur and carbon. Since flavonoids are polyphenolic acid with several OH groups, therefore, conjugations of glucuronidc acid mainly occur at the OH and *O*-glucuronides are formed [10]. After the conversion, the substrates become more hydrophilic thus are easily excreted in urine, bile or feces. UGT enzymes share the highly conserved structures. The C-terminal domain with 250 amino acids is identical among all the UGT isoforms and is believed to bind to the cofactor UDPGA [38-39]. On the contrary, the N-terminal domain, which has about 280 amino acids and varies a lot, is believed to bind to the substrates [39-40].

1.2.4.1. Classification and nomenclature

Up to date, there are four families of UGTs *(UGT1, UGT2, UGT3 and UGT8)* identified, which can be further categorized into five subfamilies (UGT1A, UGT2A, UGT2B, UGT3A and UGT8A) [41]. The classification is based on their primary amino acid sequences. Members within same family must share at least

50% homology in their gene sequences, whereas members within same subfamily must share at least 60% homology in their gene sequences [42]. In the UGT nomenclature system, Arabic numerals are used to represent the family followed by a letter representing the subfamily, whereas another group of Arabic numerals are used to denote the individual gene [41].

The UGT1 gene is located to chromosome 2 at 2q37 and consists of 13 promoters, 4 common exons (2-5) and at least 13 variable exons [41]. Each UGT1A promoter regulates the independent expression of a specific UGT1A isoform. Base on the different exons' splicing, UGT1A subfamily can produce the following isoforms-UGT1A1, UGT1A3, UGT1A4, UGT1A5, UGT1A6, UGT1A7, UGT1A8, UGT1A9 and UGT1A10 [39, 41]. In contrast to UGT1 single locus encoding gene, UGT2 genes are encoded as individual structural genes on chromosome 4q13 [41]. The UGT2A1, UGT2A2 and UGT2A3 are three members of UGT2A subfamily [41]. The UGT2B subfamily consists of UGT2B4, UGT2B7, UGT2B10, UGT2B11, UGT2B15, UGT2B17 and UGT2B28 [39, 41]. Compared to UGT1 and UGT2 families, UGT3 and UGT8 are relatively new in the UGT superfamily. UGT3 family is composed of two members: UGT3A1 and UGT3A2, which are encoded by genes of seven exons positioned adjacent to each other on chromosome 5q13.2 [41]. UGT8 family contains its only identified member, UGT8A1, which is encoded by a gene of five exons on chromosome 4q26 [41].

1.2.4.2. Tissue distribution and substrate specificity

The UGT1A subfamily is able to catalyze a broad range of endogenous molecules (e.g. bilirubin), dietary chemopreventives (e.g. isoflavoids), environmental carcinogens and chemotherapeutics. Isoforms from UGT1A subfamily are widely distributed in human and could be detected at almost every tissue/organ in the body [39, 43]. UGT1A1 was highly expressed in liver followed by gastrointestinal tract and bladder [43]. UGT1A3 had the similar expression pattern to UGT1A1, albeit to a less degree [43]. UGT1A4 was also primarily expressed in liver and moderately expressed in gastrointestinal tract, kidney, bladder and ovary [43]. UGT1A5 was moderately expressed in gastrointestinal tract, kidney, bladder and uterus [43]. UGT1A6 had the similar expression to UGT1A5 except non-detection in uterus [43]. Compared to others, UGT1A7 and UGT1A8 were relatively expressed specifically in small intestine, colon, kidney and bladder [43]. UGT1A9 was abundantly expressed in liver and kidney while marginally in small intestine, colon, bladder and testis [43]. UGT1A10, similar to UGT1A7 and UGT1A8, was mainly expressed in gastrointestinal tract and bladder and little expressed in liver, kidney, ovary and uterus [43]. UGT2A1 was mainly expressed in olfactory epithelium [39].

UGT2B subfamily is mainly responsible for catalyzing endogenous steroids and their corresponding derivatives (e.g. dihydrotestosterone and estrogen). Isoforms from this subfamily are expressed in liver, pancreas, mammary gland, prostate, kidney, adrenal, skin adipose tissue and lung [39]. UGT2B4 was primarily expressed in liver, moderately in breast and marginally in kidney, bladder,

adrenal gland, uterus and testis [43]. UGT2B7 was detected in all tissues, highly in liver followed by small intestine, colon, kidney, bladder and uterus [43]. UGTB10 was highly and specifically expressed in liver and bladder and marginally expressed in uterus and testis [43]. UGT2B11 was highly expressed in liver, bladder and breast and moderately in kidney and uterus [43]. UGT2B15 was abundantly expressed in liver and bladder followed by in gastrointestinal tract breast, ovary and testis [43]. UGT2B17 was highly expressed in liver, stomach, colon and testis [43]. UGT2B28 was predominantly expressed in bladder and marginally in liver, stomach and breast [43].

In contrast to those isoforms from UGT1A and UGT2B subfamilies, which primarily account for the glucuronidation of most xenobiotics and endogenous substrances, UGT8A1 plays a role in biosynthesis of the glycosphingolipids, cerebrosides, and sulfatides of the myelin sheath of nerve cells by catalyzing transfer of galactose from uidine diphospho (UDP) galactose to ceramide [44].

UGT3A1 which is detected in the liver and kidney, and to a lesser, in the gastrointestinal tract, can catalyze the transfer of N-acetylglucosamine from UDP N-acetylglucosamine to ursodeoxycholic acid [45]. This special UGT isoform can also use other UDP sugars such as UDP glucose, UDPGA, UDP galactose and UDP xylose as cosubstrates. The substrates of this isoform also include 17-estradiol, 4-nitrophenol and 1-naphthol [45].

1.2.4.3. UGTs-mediated metabolism of flavonoids

Flavonoids are extensively metabolized by varieties of UGT isoforms. It was reported that UGT1A1, UGT1A8, UGT1A9 and UGT1A10 mainly contributed to the glucuronidation of isoflavones including daidzein, genistein, glycitein, formononetin, biochanin A and prunetin in a concentration-dependent way [46]. UGT1A8 and UGT1A10 usually had overlapping substrates due to their sequence similarity of the primary amino acids (94%), and the former displayed a higher glucuronidation rate toward flavones (7-hydroxyflavone, chrysin and apigenin), a flavanone (naringenin) and an isoflavone (genistein) than UGT1A10 [47]. UGT1A9 was reported to share the same flavonoid selectivity with UGT1A3, but the catalyzing efficiency of UGT1A9 was higher than that of UGT1A3 [48] . Both isoforms preferred the glucuronidation at 7-OH. Especially, UGT1A9 was able to metabolize most flavonoids at a relatively fast glucuronidation rate. As for UGT1A6, it was the predominant isoform responsible for glucuronidation of luteolin (40% substrate conversion) at 7 position and able to catalyze chrysin efficiently with a low K_m value [49]. In another study, UGT1A7 was found to be involved in glucuronidation of eupatilin, which was also the substrate of UGT1A1, UGT1A3, UGT1A8, UGT1A9 and UGT1A10 [50].

In addition to UGT1A isoforms, UGT2B isoforms can also metabolize flavonoids, though they may not be as efficient as UGT1A isoforms. Evidence showed that galangin, chrysin, 7-hydroxyflavone and naringin were substrates for UGT2B17, among which galangin had the highest conversion value (58pmole/min/mg protein), whereas apigenin, baicalein, fisetin, quercetin, genistein and biochanin

A were not conjugated by UGT2B17 [51] . It was demonstrated that luteoin and quercetin were substrates of UGT2B15 and UGT2B7 with glucuronidation primarily occurring at position 7 and 3', respectively and the latter isoform had a relatively higher conversion than the former one [49]. Generally, as substrates of UGT2B7, flavonol has higher glucuronidation activity than flavones and isoflavones [52].

1.2.4.4. Clinical relevance and polymorphism

It was reported that metabolism was a leading reason that accounted for the clearance mechanisms for the top 200 drugs prescribed in the United States in 2002 [53] . In particular, glucuronidation by UGTs was a clearance mechanism for approximately 1 in 10 drugs in the top 200, second to the metabolism mediated by CYP450 [53]. Though the number of drugs that appeared to have glucuronidation as a clearance mechanism was not as many as that cleared by CYP450, they were sufficient in number for consideration of the effects (or lack thereof) of drug-drug or drug-food interactions [53].

Moreover, genetic polymorphism, which has been taken into consideration for drug pharmacokinetics, physiology and toxicology, is not an uncommon phenomenon for UGTs. Most UGT isoforms were reported to have the genetic polymorphism, such as UGT1A1, UGT1A6, UGT1A7, UGT1A8, UGT1A9, UGT2B4, UGT2B7 and UGT2B15 [54-55]. The famous example is promoter polymorphisms of UGT1A1, which can result in the inheritable diseases- Crigler-

Naijar or Gilbert syndrome. From pharmacokinetic point of view, the direct consequence of polymorphism of UGTs is to change the drug metabolism arising from the glucuronidation activity change. It was reported that mycophenolic acid (MPA) dose-corrected trough concentrations were 70% lower in patients who carried the UGT1A9-275T>A/-2152C>T polymorphism and also received cyclosporine [56]. Another study showed that compared to controls, MPA exposure was significantly lower for UGT1A9 -275/-2152 carriers, with no significant changes in phenolic glucuronide of mycophenolic acid (MPAG) [55]. Moreover, the estimates of enterohepatic (re)cycling (area under the concentration-time curve ($AUC_{6\text{-}12\ h}/AUC_{0\text{-}12h}$)) were significantly lower for MPA and its glucuronides in UGT1A9 -275/-2152 subjects [55]. Therefore, the polymorphism of UGTs is of significance for the given clinical drugs and flavonoids that mainly cleared via glucuronidation.

1.2.5. SULT-mediated metabolism of flavonoids

SULTs, another important phase II enzyme superfamily for flavonoid metabolism, can catalyze the formation of a flavonoid sulfate by transferring a sulfonate group from the coenzyme 3-phosphoadenosine-5'-phophosulfate (PAPS) to the substrates. SULTs expressed in the cytosol are responsible for the metabolism of flavonoids. In human, SULT superfamily can be divided into three subfamilies consisting of thirteen members: SULT1A family (SULT1A1, 1A2, 1A3, 1A4, 1B1, 1C2, 1C4 and 1E1), SULT 2B family (SULT2B1 v1 and v2), and SULT4A1 (SULT4A1 v1 and v2) [57]. Among all the SULTs, SULT1A1, SULT1A2, SULT1A3

and SULT1E1, which are distributed in liver and gastrointestinal tract, are well studied [58-59].

Compared with extensive study on the glucuronidation of flavonoids, research on sulfation of flavonoids, which is regarded as a metabolic pathway that can compete with glucuronidation, is relatively scant. Previously, sulfation primarily catalyzed by SULT1A1 and SULT1A3, was the major pathway in metabolism of (-)-epicatechin (EC) in human liver and intestine without detectable glucuronidation [60]. This sulfation result was consistent with another report showing that SULT1A1 and SULT1A3 metabolized EC in addition to hesperetin, eriodictyol, (+) catechin [61]. On the other hand, rapid sulfation and glucuronidation of EC in rats implied a large species difference in metabolism compared to humans [60]. In addition, it was reported that three SULT isoforms (SULT1A1, SULT1A3 and SULT1E1) were involved in sulfation of galangin, among which SULT1A1 displayed the most sulfation efficiency. On the contrary to above three SULT isoforms, SULT2A1 had no activity against galangin [62].

In Caco-2 cells, it is common to observe that flavonoids (e.g. genistein, apigenin [63] and baicalein [64]) are undergoing both glucuronidation and sulfation. And sulfation might be attributed to SULT isoforms expressing in Caco-2 cells such as SULT1A1, SULT1A2 and SULT1A3 [65].

1.3. Relevant efflux transporters

1.3.1. ATP-binding cassette transporters (ABC transporters)

ABC transporters are ubiquitous integral membrane proteins that transport various ligands actively across the membrane (either uptake or efflux) with hydrolysis of ATP. ABC transporters play a critical role in cell physiology. In humans, total forty-eight ABC transporters were identified, which shared some typical sequences and organization of ATP-binding domains [66]. Usually, a full ABC transporter has two types of domains: nucleotide-binding domain (NBD, also called ATP-binding domain) and transmembrane domain (TMD) [66]. The NBD, which is located in the cytoplasma, contains two characteristic motifs (Walker A and B), separated by approximately 90-120 amino acids [67]. The TMD contains 6-11 membrane-spanning α-helices with provision of substrate specificity [67]. To achieve export, ABC transporters require a minimum of four domains: two TMDs form the ligand binding sites and provide specificity, and two NBDs bind and hydrolyze ATP to drive the translocation of the bound ligand [66].

The existing eukaryotic ABC transporters are categorized into seven subfamilies, which can be further classified into subgroups on the basis of their amino acid sequences [67]. All human and mouse ABC genes have standard nomenclature, developed by the Human Genome Organization (HUGO) at a meeting of ABC gene researchers. Details of the nomenclature scheme can be found at: http://www.genenames.org/genefamily/abc.html [67] In the following, several ABC transporters (ABCB1, ABCC and ABCG2) will discussed on details, which are of more interest for researchers and more clinically relevant to drug-drug interactions.

1.3.2. P-glycoprotein (ABCB1)

P-glycoprotein (P-gp), encoded by *ABCB1* gene with molecular weight of 170KD, is the first human ABC transporter that cloned and characterized through its ability to confer a multi-drug resistant phenotype to cancer cells [67-68] . P-gp consists of two homologous segments, each of which contains six transmembrane domains (TMDs) and a nucleotide binding domain (NBDs) with ATPase activity [69]. P-gp is highly expressed in blood-brain barriers, liver, kidney and intestine [70]. Its function is to transport molecules out of cells. The substrates of P-gp cover variety of lipophilic and cationic substances, including chemotherapeutic agents, steroids, peptides, lipids and drugs [70]. Therefore, P-gp is not involved in efflux of flavonoid glucuronides, which are organic anions.

1.3.3. MRPs (ABCCs)

The multidrug resistance protein (MRP) subfamily of ABC transporters, also called ABCC subfamily, contains twelve full transporters with a diverse functional spectrum [67]. Among all the MRP proteins, MRP1, MRP2 and MRP3 bear a close structural resemblance (40%-50%). Especially, MRP1 and MRP3 share the highest sequence identity (58%). To a less extent, MRP6 has a similar structural resemblance to MRP1-3 (40-46%) [71]. On the other hand, MRP4, MRP5, MRP11 and MRP12 proteins are smaller than the other MRP-1like proteins and their sequences are more divergent [67]. MRP1, MRP2 and MRP3 transport drug

conjugates and glutathionine and other organic anions; MRP8 and MRP9 bind sulfonylurea and regulate potassium channels involved in modulating insulin secretion [67]; MRP4 and MRP5 confer a unique resistance to nucleosides including purine and nucleotide analogues [71]. In the following, MRP2 and MRP3 will be discussed on details because they are more relevant to the efflux of phase II metabolites of flavonoids.

MRP2 is the second member of MRP subfamily with molecular weight about 190KD (alias cMOAT) [71-75]. The *MRP2* gene is located to chromosome 10q24 [76]. MRP2 has 2 NBDs and 17 TMDs [77]. As a factor leading to the chemotherapy resistance, MRP2 is highly expressed in carcinoma cells or tumor tissues. The MRP2 is also distributed in normal tissues such as liver, kidney and gut [77]. In human intestine, the mRNA expression of MRP2 is high in the proximal region such as jejunum, and very low in distal region such as ileum and colon [78] . As for its cellular localization, MRP2 is exclusively expressed at the apical membrane of those polar cells such as Caco-2 and MDCK cells. The main function of MRP2 is to actively transport substances out of the cells depending on the hydrolysis of ATP. The substrates of MRP2 are various, including chemotherapy drugs (e.g., camptothecins, methotrexate and cisplatin) [71, 79-80], drug conjugates (e.g. grepafloxacin glucuronides [81] and moxifloxacin glucuronides/sulfates [82]) and endogenous compounds (e.g. tetrahydrofolate and bilirubin glucuronides [83]). Considering its endogenous substrates, MRP2 plays a significant role in human physiology. Dubin-Johnson syndrome, a hereditary disorder characterized by modest elevations of bilirubin conjugates in serum without increases of liver

enzymes, is the consequence of dysfunctional MRP2 caused by several mutations in the gene [84]. Currently, there is no specific inhibitor for MRP2. LTC_4 (leukotriene C4) and estrodio-17ß-glucuronides, both of which are the substrates of MRP2, are used as MRP inhibitors in addition to MK-571[71, 77].

MRP3 is the third member of MRP subfamily and also has two NBDs and 17 TMDs [77]. The *MRP3* gene is located to chromosome 17q21.3 [85]. Unlike cellular localization of MRP2, MRP3 is at the basolateral membrane of polar cells. In humans, MRP3 is highly expressed in the adrenal glands and the intra-hepatic bile ducts followed by moderately to marginally in the small intestine, kidney and pancreas [77]. The substrate spectrum of MRP3 is similar to MRP2, including amphiphilic anions. LTC_4 and estrodio-17ß-glucuronides are also the substrates of MRP3, however, they have less affinity to MRP3 than to MRP2 [71]. In addition, MRP3 is highly up-regulated in the livers of rats made cholestatic by bile duct ligation [86] or in cholestatic human liver [87], suggesting MRP3 is inducible and play a role in the removal of toxic organic anions from livers under cholestatic conditions .

1.3.4. BCRP (ABCG2)

Breast cancer resistance protein (BCRP), encoded by *ABCG2* gene located to chromosome 4q22, consists of 655 amino acids with molecular weight of 72KD [88]. Unlike other members from ABC transporter superfamily, BCRP is a “half ABC transporter” because it only contains one NBD and six TMDs [89]. To

function properly, BCRP must form homodimers or homooligomers [90]. BCRP has many physiological functions such as the extrusion of porphyrins from haematopoietic cells and hepatocytes and secretion of vitamin B2 (riboflavin). In addition to physiological function, BCRP also has a role in limiting oral bioavailability of drugs and transport across the blood-brain barrier, blood–testis barrier and the maternal-fetal barrier of some selected substrates [91-92].

1.3.4.1. Tissue distribution

BCRP is expressed not only in cancer cells but also in normal tissues. Substantial evidence showed that BCRP was highly expressed in placenta, central nervous system, liver, adrenal gland, prostate, testes and uterus as well as lowly expressed in the gastrointestinal tract, lung, kidney and pancreas as determined by northern blot [88] [92]. BCRP seemed missing in heart [88]. The tissue distribution of BCRP is consistent with its physiological function. In addition, the expression of BCRP in intestine or liver is always higher than that of MRP2 [93-94].

1.3.4.2. Substrate and inhibitor

BCRP has a large scale of substrates, which are steadily expanding since its discovery. It is well known that chemotherapy agents are the predominant substrates of BCRP, including mitoxantrone (a hallmark of cells expressing BCRP), flavopiridol, topotecan, irinotecan and its active metabolite SN-38 [92, 95]. Other known substrates of BCRP are from various drugs such as antivirals (e.g.

abacavir and lamivudine), HMG-CoA reductase inhibitors (e.g. rosuvastatin and cerivastatin), carcinogens (e.g. Aflatoxin B1and PhIP), antibiotics (e.g. erythromycin and nitrofurantoin), tyrosine kinase inhibitors (e.g. imatinib and gefitinib) and calcium channel blockers (dipyridamole and nitrendipene) [92, 95]. In addition to the substrates listed above, which are all xenobiotics, the endogenous substrates of BCRP are known as bile acids and its phase II metabolites, porphyrins, milk and vitamin K3 and B2 etc [91, 96-97].

In addition to clinical drugs, flavonoids were also reported to be the substrates of BCRP. The investigation on quantitative structure activity relationships suggested that the presence of a 2, 3-double bond in ring C, ring B attached at position 2, hydroxylation at position 5, lack of hydroxylation at position 3 and hydrophobic substitution at positions 6, 7, 8 or 4', are important structural properties for potent flavonoid–BCRP interaction [98] .

As for inhibitors of BCRP, fumitremorogin C was the first reported one [92, 99]. Later on, dipyridamole was also identified as an inhibitor of BCRP [100]. So far, the most potent and specific inhibitor of BCRP is Ko143, which has the IC_{50} around 200nM [101-103]. Therefore, Ko143 is more and more used as specific inhibitor of BCRP.

1.3.4.3. Polymorphism

Up to date, over 80 naturally occurring sequence variations have been identified in the *ABCG2* gene [104]. With more extensive investigations, more

polymorphisms of *ABCG2* are identified. Though there is no link between human diseases and the mutation of the gene, the sequence variations of *ABCG2*, especially single nucleotide polymorphism (SNP), is believed to play a very critical role in pharmacokinetics of drugs. For example, the nonsynonymous 421C>A resulting in a glycine to lysine (Q141K) amino acid change, was found to be related to decreasing expression of ABCG2 in plasma membrane, thus altered the pharmacokinetics of chemotherapeutic agents such as topotecan , diflomotecan and 9-aminocamptothecin [105-107]. The occurring frequency of Q141K was low in African-American (2-5%) followed by moderate in Europeans (11-14%), Hispanic (10%) or Middle Eastern (13%), whereas was high in Asian such as Chinese and Japanese (35%) [108]. Accordingly, drugs taken by the related populations must pay more attention on the dose to avoid the potential toxicity. Other reported SNP of *ABCG2* are including V12M, Q126Stop, I206L and N590Y [109].

1.4. Interplay between DME and transporters

The considerable overlap in the substrate specificity and tissue localization of DME and transporters has led the hypothesis that DME and transporters are working together in limiting the bioavailability of drugs [91, 110-111]. The first interplay between DME and transporters was hypothesized two decades ago [111]. The interplay was between CYP3A and P-gp, which played complementary roles in drug absorption and disposition. With more efforts put on this field due to the significant effect of interplay on the bioavailability and drug-drug interactions,

the current study on the interplay was expanded to phase II enzymes (e.g. UGTs and SULTs) and other transporters (e.g. BCRP and organic anion transporting polypeptide (OATP)) [32, 112-113]. The interplay means that induction or inhibition of one player has an influence not only on itself, but also on the observed effect or expression of the other. As a result, the activity on the substrates can be either reinforced or counteract [114]. Simply speaking, the interplay suggests the codependence of DME and transporters. Three aspects of interplay were studied: cooperation in drug absorption and disposition; co-regulation by common nuclear receptors and control of intracellular levels of substrates or of DME by transporters [114].

The better understanding of interplay between DME and transporters can give us a hint in improving drug bioavailability and in reducing potential drug-drug interactions. So far, the interplay has been investigated thoroughly either by experiments or by computer simulations. The in vitro models used to study DME and transporters separately are not suitable for the interplay investigation. A model integrating both DME and transporters is the ideal one since the relative contribution from each player on the drug elimination or on the other player can be assessed and the potential drug-drug interactions can be predicted [114]. Therefore, animals and intact cells (e.g. organ perfusion and Caco-2 cells), in which both DMEs and transporters are present, are widely accepted and used. The advantages of the two systems are that pathways are readily perturbed with use of inhibitors or inducers, and that individual events are confined to the organ/tissue of interest [115].

As for simulation and modeling method, physiologically based pharmacokinetic modeling (PBPK) are preferred by many researchers due to its powerful applications in understanding rate-limiting step, in allowance of thorough simulation, and in study the effect of physiological factors on the DME and transporter (e.g. blood flow and DME distribution within organ) [114-116].

1.4.1. Interplay between CYP3A and P-gp

CYP3A is the most prominent oxidative CYP450 enzymes present in liver and small intestine. CYP3A can metabolize about 50% of the currently marketed drugs [117]. P-gp is a well-known efflux transporter, which is present in the luminal membrane of gut epithelial cells. Both CYP3A and P-gp are regulated by nuclear receptors such as pregnane X receptor (PXR), and they share some substrate specificity [111, 118-119]. Accordingly, the overlap in substrate specificity, expression regulator and the tissue distribution led the investigators to hypothesize that CYP3A and P-gp work in a coordinated manner to serve as an absorption barrier, which later on is defined as interplay between CYP3A and P-gp. It is believed that the synergistic effect resulting from the interplay between CYP3A and P-gp accounts for more extensive first-pass of drugs such as cyclosporine A.

In views of Dr. Benet, the P-gp, as a controller, determines the drug metabolism in intestines without inhibiting or inducing CYP3A enzymes [120]. Under normal function of P-gp, the drugs effluxed by P-gp without instant metabolism by CYP3A, have the potentials to be metabolized by CYP3A later after being

reabsorbed. If P-gp is inhibited, the risk for drugs of being metabolized by multiple times is reduced; on the contrary, if P-gp is induced, the drugs have increasing opportunities to be metabolized by CYP3A. As a result, drug pharmacokinetics is greatly affected by the interplay between CYP3A and P-gp. For example, it was found in rat single pass intestinal perfusion model, that the fraction metabolized for K77 (substrate of Pgp and CYP3A4) was decreased (95% to 85%) in presence of GG918 (an inhibitor of Pgp) [121]. In another case, the bioavailability of docetaxel was dramatically increased (>70-fold) in double knockout mice (Cyp3a/Mdr1a/1b$^{-/-}$) followed by in single Cyp3a$^{-/-}$ mice (12-fold) and Mdr1a/1b$^{-/-}$ mice (3-fold) [122] . However, there was no functional synergism between Cyp3a and Mdr1 as their expectation that one player's function would be more efficiently when the other player's function is active than when the other is not active [122].

In addition to the observation of interplay in animal model, the conclusions about interplay between CYP 3A and P-gp in Caco-2 cells are controversial [115]. On the one hand, it was suggested that the increase in the mean residence time (MRT) accompanying increased secretion laid the basis for increased metabolism [115, 123-130]. This idea was similar to the conclusion obtained on the basis of animal model. On the other hand, the opposite point was suggested that the increased secretion could evoke a decrease in metabolism due to the competition between enzyme and apical efflux transporter for the drug within the cell [115, 131-133]. In other words, the reciprocal relationship exists between the clearances related to

enzymes and apical transporters, both of which compete for the substrates within cells. This competition was also described as “see-saw” phenomenon [115].

1.4.2. Interplay between phase II enzymes and BCRP/MRP

Compared to interplay between CYP3A and P-gp, interplay between phase II enzymes and BCRP/MRP was relatively new and proposed recently [31-32, 134]. As an extending idea on the basis of interplay between CYP3A and Pgp, interplay between phase II enzymes and BCRP/MRP describes a sequential process in which substrates are metabolized by phase II enzymes and the produced phase II metabolites are transported out of cells by efflux transporters like BCRP or MRP. This kind of interplay was proposed according to the study of flavonoid disposition in both animal and cell models. This is because flavonoids as substrates can passively diffuse into cells and be catalyzed to glucuronides and sulfates via glucuronidation and sulfation, respectively. The glucuronides and sulfates then exit cells by efflux transporters due to their hydrophilicity (Fig. 2). The involving efflux transporters include BCRP, MRP2 and MRP3 [31, 63, 135]. Previously, the efflux step of flavonoid conjugates (phase II metabolites) was regarded most likely as the rate-limiting step for the interplay due to the discrepancy of results between in vitro glucuronidation assay and Caco-2 cell model or rat perfusion model [134]. For example, glucuronidation of biochanin A was found to be faster than formononetin in rat intestinal and liver microsomes; however, excretion of formononetin conjugates was more efficient than biochanin

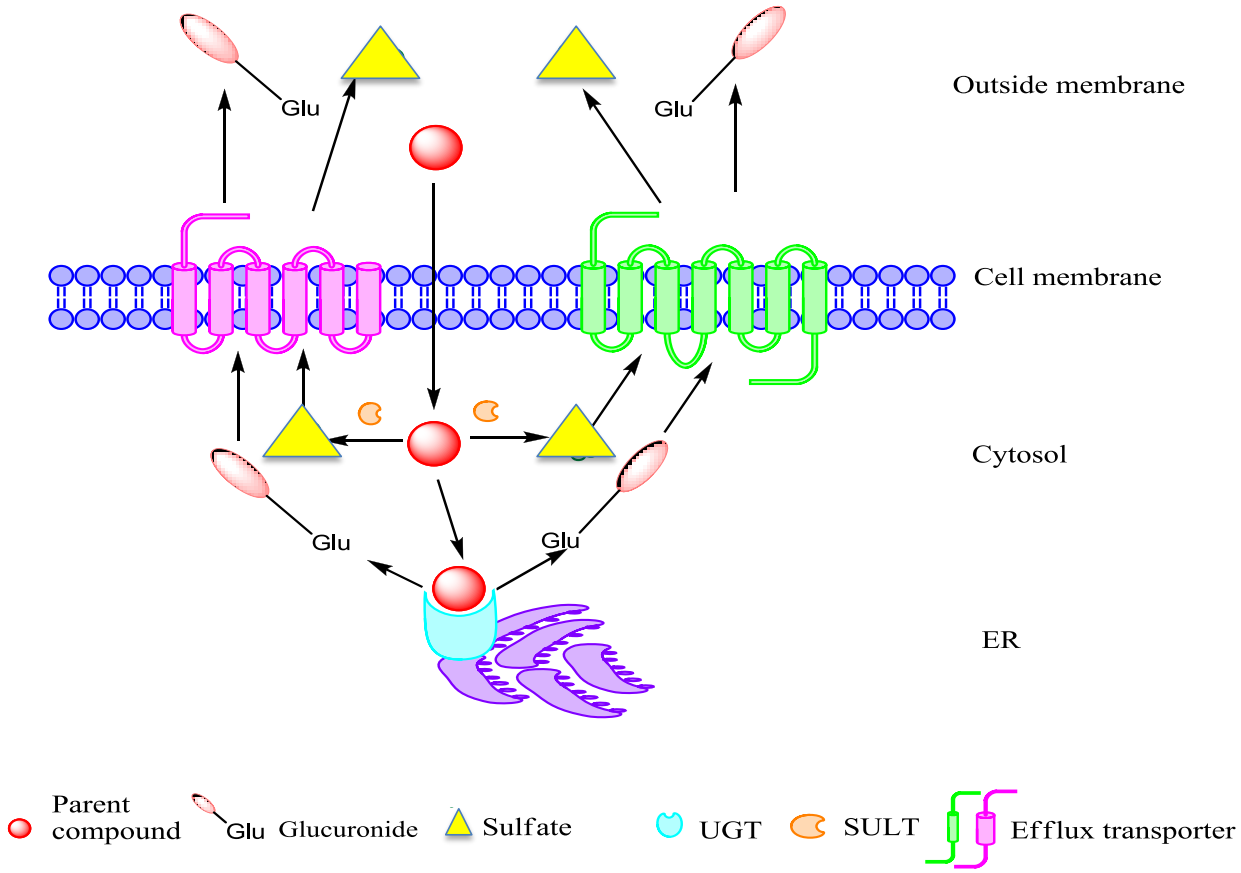

Fig. 2 Cellular interplay between phase II enzymes and efflux transporters in disposition of flavonoids.

A in rat intestine perfusion model and Caco-2 cell model [134]. Nevertheless, this cannot be used as direct evidence for the interplay. On the other hand, the compensation occurring in traditional cell model (e.g.Caco-2 cells) and animal model prevents the mechanism study of the interplay, therefore, it is hard to reach a solid and convincing conclusion about the interplay between phase II enzymes and BCRP/MRP. So far there is one mechanism proposed to describe the interplay between phase II enzymes and MRP in the futile cycling on the basis of the animal study [136]. The authors suggested that a reduction in the excretion of estradiol 17ß-D-glucuronide (as substrate, $E_2$17G) and estradiol 3-sulfate-17ß-D-glucuronide (as produced metabolites) by Mrp2 exert an impact on the futile cycling kinetics and reduced the net metabolism of $E_2$17G. Therefore, it is necessary for us to build a model, which is suitable to study the mechanism of interplay between phase II enzymes and BCRP/MRP experimentally.

1.4.3. Interplay between DME and uptake transporters

As one of the players in interplay, transporters are not necessarily referred to efflux transporters as mentioned above. In many occasions, interplay between DME and uptake transporters is more important for drug disposition, especially when biliary excretion is a major elimination route of drugs and their metabolites [113]. On the contrary to the interplay between DME and efflux transporters, in which metabolism occurs before or at the same time as excretion, drugs involved in the interplay between DME and uptake transporters are always uptaken first by transporters followed by either phase I or phase II metabolism. As matter of

fact, the interplay between DME and uptake transporters is often linked with another interplay between DME and efflux transporters, which consists of a more complex interplay among uptake transporters, DME and efflux transporters.

The typical uptake transporters involved in the interplay are members of the organic anion transporting polypeptide (OATP) family, including OATP1B1, OATP1B3 and OATP2B1[113]. These uptake transporters, which are encoded by the *SLCO* genes (formerly *SLC21*) [137], in addition to the other organic anion transporters such as OAT2 and OAT7, are responsible for uptaking a wide range of anionic substances. Whereas OATP1B1 and OATP1B3 are predominantly, if not exclusively, expressed in hepatocytes (basolateral membrane) [138-140], OATP2B1 is expressed in othe cell types and tissues as well [137][141-142]. The proposed transportation mechanism for OATPs is anion exchange and the possibly involved physiological counter-ions are controversial [143].

An example of interplay between DME and OATP was observed when bilirubin was uptaken by OATP1B1 followed by metabolized by UGT1A1 [144-145]. The participation of OATP1B1 was confirmed by the findings that inhibition of OATP1B1 in humans leads to unconjugated hyperbilirubinemia [144]. Another example of the interplay was about Telmisartan, which was a non-peptide benzimidazole angiotensin II receptor antagonist and exclusively eliminated via liver [146]. Similar to bilirubin, Telmisartan was first carried into liver cells by OATP1B3 [147]. Then Telmisartan inside cells was metabolized to glucuronides by UGTs in liver [146]. Last but not the least, Bromosulfophthalein, which was a triphenylmethane derivative used to measure hepatobiliary elimination, was

reported to be substrate of both OATP1B1 and OATP1B3 [113, 142]. After being uptaken, Bromosulfophthalein was metabolized by glutathione S-transferase. The final fate of above metabolites (bilirubin glucuronide [148], Telmisartan glucuronide [148] and Bromosulfophthalein glutathione conjugate [149]) was to exit hepatocytes by efflux transporters.

CHAPTER 2: OBJECTIVES AND HYPOTHESIS

The bioavailability of flavonoids is very poor after oral administration and this low bioavailability limits their pharmacological functions in vivo. There are two leading reasons for low bioavailability: one is the extensive phase II metabolism of flavonoids; the other is the rapid excretion of their phase II metabolites (also called flavonoid conjugates). Substantial evidence indicated that extensive phase II metabolism was from the result of glucuronidation and/ or sulfation, which were catalyzed by UGTs and SULTs, respectively. On the other hand, once flavonoids are metabolized to glucuronides and sulfates through glucuronidation and sulfation, respectively, these flavonoid conjugates are more hydrophilic than parent compounds. Therefore, the hydrophilic conjugates must depend on the active transporters to be removed from the cells. Studies from different groups suggested that BCRP and MRP2, two members from ABC transporter superfamily, are mainly responsible for the excretion of conjugates [31, 63]. Thus we assume that it is the kinetic interplay between phase II enzymes and efflux transporters that limits the bioavailability of flavonoids. In other words, UGTs/SULTs and BCRP/MRP2 work coordinately to prevent flavonoids from reaching into or remaining in the blood circulation system as aglycones.

The mechanism of interplay between phase II enzymes and efflux transporters, especially mechanism of interplay between UGTs and efflux transporters are not investigated as extensively as the interplay between CYP3A and P-gp due to the

limitation of various models. Animal model and cell model are widely used to study the interplay between UGTs and efflux transporters. For animal model, flavonoids escaping interplays in one organ can undergo interplays in another organ; for Caco-2 cells, flavonoids avoiding the interplay between UGTs and efflux transporters, may go through the interplay between SULTs and efflux transporters. As a result, the compensation observed in these models prevents the in-depth analysis on the interdependence of UGTs and efflux transporters. In addition, the intracellular levels of glucuronides in these models were not seen to be fluctuating with the control of efflux transporters. To understand more about the interdependence of UGTs and efflux transporters and the control of intracellular glucuronides, it is necessary for us to build a simple cell model, which can satisfy our desire to study the mechanism(s) of interplay and the role of interplay in the disposition of flavonoids. Moreover, the mechanism arising from the simple cell model may be applicable to other cellular or animal models in understanding how change in the interplay may impact oral bioavailabilities of flavonoids.

2.1. Objectives

The overall objective is to investigate the mechanism of interplay between UGTs and efflux transporters in flavonoid disposition. The goals of this project were to 1) develop a cell model which was suitable to study the simplest interplay between one UGT isoform and one predominant efflux transporter; 2) determine

the mechanism of simplest interplay in flavonoid dispsotion by using the well-established HeLa cell model; 3) study the interplay between UGTs and the specific efflux transporter in flavonoid disposition by using mouse and other cell models; 4) determine the kinetic parameters of efflux of flavonoid glucuronides mediated by the predominant efflux transporter in the established HeLa cell model.

2.2. Hypothesis

The hypotheses for this thesis are as follows:

H1(a). The function of predominant efflux transporter (MRP2 or BCRP) can affect the glucuronidation activity in intact cells.

H1(o). The function of predominant efflux transporter (MRP2 or BCRP) cannot affect the glucuronidation activity in intact cells.

H2(a). The intracellular levels of glucuronides can be altered either by glucuronidation activity or by function of the predominant efflux transporter.

H2(o). The intracellular levels of glucuronides can be altered neither by glucuronidation activity nor by function of the predominant efflux transporter.

H3(a). The bioavailability of flavonoids can be improved experimentally by disrupting the interplay.

H3(o). The bioavailability of flavonoids cannot be improved experimentally by disrupting the interplay.

H4(a). The established cell line used to study the simplest interplay between one UGT isoform and the predominant efflux transporter can be applied to predict the bioavailability of flavonoids in a mouse model.

H4(o). The established cell line used to study the simplest interplay between one UGT isoform and the predominant efflux transporter cannot be applied to predict the bioavailability of flavonoids in a mouse model.

H5(a). The kinetics parameters of transporter-mediated efflux of glucuronides can be determined in an established cell model.

H5(o). The kinetics parameters of transporter-mediated efflux of glucuronides cannot be determined in an established cell model.

CHAPTER 3: GENERAL METHODOLOGY

3.1. Stability of the flavonoids in HBSS buffer (pH7.4)

For the flavonoids selected for the excretion study, the stability of each flavonoid at three concentrations (2.5, 10 and > 25 μM) was determined in the water bath (37°C) up to 4 hours (maximally time span of experimentation). Briefly, each flavonoid at specific concentration in HBSS buffer was diluted from 100 times concentrated stock solution in DMSO/MeOH as 1:4. For example, 10μM of 7-hydroxyflavone in HBSS buffer was diluted from 1mM stock solution in DMSO/MeOH as 1:4. Samples were collected at 0, 2, 4 hours followed by centrifugation at 15,000rpm for 15min. After centrifugation, samples were injected into UPLC for analysis. For those flavonoids which were not stable for 4 hours at 37°C, 0.1% vitamin C was added. Previously it was shown that the addition of 0.1% vitamin C would not interfere the transport or metabolism of tested flavonoids.

3.2. Cell experiments

HeLa cells, Caco-2 cells and MDCKII series cells are used in the study of interplay between phase II enzymes and efflux transporters. HeLa cells, which are derived from cervical cancer cells, are widely used in cell biology field. This cell line is very easy to culture and grows rapidly. Unlike HeLa cells, Caco-2 cells and MDCKII series cells are polarized cells, which can be grown on the insert.

These two cell lines have been extensively investigated, and are used to study the absorption and metabolism of drugs.

3.2.1. Cell culture

Caco-2 TC-7 cells are routinely cultured in our lab as previously described [134] [63]. Briefly, Caco-2 cells were seeded on the monolayer at density of 100,000cells/cm^2, and maintained at 37ºC under 5% CO_2 in Dulbecco' Modified Eeagle Medium (DMEM) supplemented with 10% fetal bovine serum (FBS). Media were changed every other day. The cells on the monolayers were ready for transport experiments from day 19 to 22 since seeding. For engineered HeLa cells and MDCKII series cells, they are regularly maintained in the same condition as Caco-2 cells and split every three or four days. These two cell lines are only grown on the plates with multiple wells but not on the monolayers.

3.2.2. Preparation of cell lysates

Cells were washed and harvested in 50mM potassium phosphate buffer (KPI, pH7.4) after growing for 3-4 day. The collected cells were sonicated in Aquasonic 150D sonicator (VWR Scientific, Bristol, CT) for 30 min at the maximum power (135 average watts) in an ice-cold water bath (4°C) [150]. Then the cell lysates were centrifuged at 4°C (5min at 6000rpm). The supernatant was taken to

determine the protein concentration by BCA assay (Pierce Biotechnology, Rockford, IL) and to be used in the UGT activity assay or western blotting.

3.2.3. Excretion study

Two types of excretion studies were conducted depending on the cells. For Caco-2 cells (TC-7 clone) grown on the inserts, flavonoids were loaded on the apical side with or without an inhibitor. At predetermined time intervals, samples were taken from both apical and basolateral sides. At the same time, the same volume of loading flavonoids is added back to apical side, whereas the same volume of blank buffer is replenished to basolateral side [63]. For engineered HeLa cells or MDCKII series cells grown on the plates, samples were taken from plates at predetermined time intervals and the same volume of loading flavonoids is replenished to the plate.

3.2.4. Quantification of metabolites inside cells

The Caco-2 cell monolayers were washed twice with ice-cold HBSS buffer after the transport study. Then the monolayers were cut off from the culture inserts and mixed with 1ml of acetonitrile in the microcentrifuge tubes. After being sonicated in Aquasonic 150D sonicator (VWR Scientific, Bristol, CT) for 30 min at the maximum power (135 average watts) in an ice-cold water bath (4°C) [150], the mixtures were centrifuged at 15,500rpm for 20min. The supernatants were

transferred into another microcentrifuge tubes and subsequently evaporated to dryness under air. The residues were reconstituted in 200µl HBSS buffer with addition of 50µl 94% acetonitrile/6%glacial acetic acid containing 100µM testosterone as the internal standard. Samples were ready for UPLC analysis after centrifugation (15min at 15,000 rpm).

The engineered cells were washed with ice-cold HBSS buffer twice after the excretion experiments. Then the cells were collected in 100 or 200µl HBSS buffer and sonicated in the same conditions as described above. UGT1A9 is not expected to function without the co-factors once cells are broken. After centrifugation at 15,500rpm for 20min, supernatants were collected and mixed with the “Stop Solution” consisted of 94% acetonitrile and 6% acetic acid. The samples were ready for UPLC analysis after centrifugation (15min at 15,000 rpm).

3.3. Analysis of flavonoids and their phase II metabolites

3.3.1. Analysis of flavonoids and their conjugates by UPLC

The conditions for UPLC analysis of flavonoids and their glucuronides were modified based on a previously published method [151]. The conditions were: system, Waters Acquity with a binary pump and a 2996 DPA diode array detector (DAD, Waters, Milford, MA); column, Acquity UPLC BEH C18 column (50X2.1mm I.D.1.7 µm (Waters, Milford, MA); mobile phase A, 2.5mM ammonium acetate (pH 7.4); mobile phase B, 100% acetonitrile; gradient, 0-

2.0min, 10-35%B, 2.0-3.0min, 35-70%B, 3.0-3.5min 70%B; 3.5-3.6min, 70-90%B; 3.6-4.1min, 90%B; 4.1-4.6min, 90-10%; injection volume, 10ul; the wavelength to observe flavonoids and their phase II metabolites are compound-dependent. The precision and accuracy is typically within acceptable range (<15%). The detection limits were at least 0.16μM.

3.3.2. Confirmation of phase II metabolites of flavonoids using UPLC-MS/MS

To confirm the glucuronides or sulfates of flavonoids, especially for those with more than one hydroxyl group in their structure, UPLC-MS/MS was used. The UPLC conditions were similar to that described above. The effluent from Waters Acquity UPLC system was introduced into an API 3200 Qtrap triple-quadrupole mass spectrometer (Applied Biosystem/MDS SCIEX, Foster city, CA) mounted with a TurboIonSpray^{TM} source. The mass spectrometer was operated in negative or positive ion mode. The instrument-dependent parameters were optimized and its main working conditions were listed as follows: ion-spray voltage, -4.5kV; ion source temperature, 600°C; nebulizer gas (gas 1), nitrogen, 40psi; turbo gas (gas 2), nitrogen, 40psi; curtain gas, nitrogen, 20psi; collision cell energy, 30volts; collision cell exit potential, 3volts. Minor adjustments may be needed for each flavonoid and its phase II metabolites. The compound-dependent parameters were also optimized. Generally, the mass of each individual peak of separated glucuronides and sulfates was measured using Q1MS mode followed by MS2 scan mode to confirm the identity of each peak as

glucuronide/sulfate by fragmenting the parent ion into glucuronic acid/sulfate and aglycone daughter ion.

3.3.3. Quantification of flavonoid glucuronides

The conversion factors representing the molar extinction coefficient ratio of glucuronides to aglycones, were used to quantify the amounts of flavonoid glucuronides as described previously [151-153]. The conversion factors were determined according to the published method. Briefly, it was determined by comparing (a) the peak area change in glucuronides with (b) the corresponding peak area change in alycones after glucuronides were hydrolyzed by β-glucuronidase. By plugging various K values into the following equations using peak area of glucuronides, concentrations of glucuronides were calculated by equation:

$C_{glu}=C*K$

where C_{glu} and C represent the concentration of glucuronides and corresponding flavonoid aglycones, respectively, whereas K is the conversion factor (=Δ peak area of glucuronides/ Δ peak area of flavonoids)

3.4. Disruption of interplay between UGTs and efflux transporters

To study the interdependence between UGTs and efflux transporters as well as the interplay effects on the disposition of flavonoids, it is necessary for us to

isolate each player and explore its contribution to the interplay by disruption. For cell models, there are two ways for disruption: one is to use chemical inhibitors (e.g. BCRP and or/MRP inhibitor); the other is to use small interfering RNA (siRNA). For animal model, gene knockout mice (e.g. Bcrp(-/-)) is used for disruption. The detailed methods are described in later chapters.

3.5. Statistical analysis

We use triplicates for all the cell experiments and phase II metabolism study (e.g. UGT assay or sulfation assay). We use quintuplets for mouse pharmacokinetics experiments. One way ANOVA followed by Tukey post hoc test and or student t-test are used to compare the results between control group and the test group. Two significance levels are selected as criteria to determine whether the difference between control and test groups is significant: $p<0.05$ and $p<0.01$.

CHAPTER 4: ESTABLISHMENT AND CHARACTERIZATION OF A SIMPLE HELA CELL MODEL SUITABLE FOR THE STUDY OF THE ROLES OF INTERPLAY IN THE FLAVONOID DISPOSITION

4.1. Abstract

The purpose of this study was to develop a simple cell model, which was suitable to study the interplay between one UGT isoform and one efflux transporter in flavonoid disposition. Wild type HeLa cells were selected to be modified by transient or stable transfection of *UGT1A9* gene. The HeLa cells with stable transfection (called engineered HeLa cells) were then characterized at both function and expression levels. The results indicated that the engineered HeLa cells rapidly excreted the glucuronides of genistein and apigenin in a concentration-dependent manner. The ability for engineered HeLa cells to excrete glucuronides was consistent with the abundant expression of UGT1A9 in the engineered HeLa cells but non-detectable expression in the wild type. The kinetic characteristics of flavonoid glucuronidation were similar when using UGT1A9 overexpressed in HeLa cells or the commercially available UGT1A9 Supersome^{TM}. The involvement of MRP2 or MRP3 in the excretion of glucuronides were excluded since neither LTC_4 (a specific inhibitor of MRPs) nor siRNA against MRP2 and MRP3 affected the excretion of flavonoid glucuronides. This was also consistent with the expression pattern of efflux transporters in the HeLa cells: BCRP was expressed relatively higher than MRP2 and MRP3. Moreover, the engineered HeLa cells were stable at least for 5 consecutive generations. All these results suggested that the HeLa cells stably transfected

with *UGT1A9* was potentially a good and simple model to study the interplay between UGT1A9 and BCRP in flavonoid disposition.

Keywords: UGT1A9, HeLa cells, Genistein, Apigenin, flavonoid, BCRP, MRP2, MRP3, interplay

4.2. Introduction

Interplay between drug metabolizing enzymes (DME) and transporters was firstly proposed about 15 years ago that focused on the P-glycoprotein (P-gp) and cytochrome P450 3A (CYP 3A) [111]. It was hypothesized that P-gp and CYP3A played a complementary role in drug absorption and disposition. The interplay occurred at two different levels: molecular level and kinetic level. At the molecular level, the efflux transporters and enzymes are regulated by the same nuclear receptor such as pregnane X receptor (PXR) and the constitutive androstane receptor (CAR); and at the kinetic level, the DME or the intracellular levels of substrates are controlled by transporters. More recently, the interplay was expanded to phase II enzymes such as UDP-glucuronosyltransferases (UGTs) and sulfotransferases (SULTs) and other transporters such as breast cancer resistance protein (BCRP) and multidrug resistance protein 2 (MRP2) [32, 112].

To delineate the interplay between transporters and DME, animal model and cell culture models are widely used. Usually, cell lines transfected with transporters or DME were first studied in vitro, which is then followed by transgenic or relevant gene knockout mice or rats for in vivo study. The most common and popular cell lines are Caco-2 cells and MDCK II cell lines which are both polarized cells and suitable for studying phase II metabolism of xenobiotics including flavonoids. However, the above two cell models are still too complex for us to study the interplay between UGTs and efflux transporters since multiple efflux transporters and other phase II enzymes such as SULTs are also expressed in these cells. A simple model which is suitable for studying the interplay between one UGT

isoform and efflux transporters must have one predominant expressed UGT isoform and negligible activity from other phase II enzymes such as SULTs. At the same time, at least one predominant efflux transporter must express in the cells. Due to such strict criteria, it is necessary for us to develop a simple yet highly functional cell model.

Therefore, HeLa cells, which were derived from epithelial cervical cancer cells, were selected to be modified for the purpose of studying the interplay based on the following reasons: first, they had no detectable glucuronidaiton and negligible sulfation activity in metabolizing most flavonoids; and second, they expressed significant amount of BCRP but very little MRP2 and MRP3. The very low expression of MRP2 was consistent with those reported by a different group of investigators [154]. We were interested in these efflux transporters, since BCRP and MRP2 as well as MRP3 were all capable of mediating the efflux of glucuronides and sulfates [155-158].

Human UGT1A9 was the first UGT isoform selected to be overexpressed in HeLa cells for several reasons: first, UGT1A9 was responsible for metabolism of many clinical drugs such as SN-38 [159] and acetaminophen [160] ; second, and more importantly, our previous data showed that UGT1A9 was able to metabolize many flavonoids at relatively high rates, consistent with results from Pritchett et al [161].; and third, UGT1A9 was more stable than other UGT isoforms [162-163]. In the development, UGT1A9 was introduced to HeLa cells, first by transient transfection to determine the feasibility, followed by stable transfection to reduce the experimental variability.

Previous investigation presumed that it was the interplay between phase II enzymes and efflux transporters that contributed to the low bioavailability of flavonoids [31-32]. The low bioavailability impedes the testing of many of their "claimed" beneficial effects in human including anti-cancer [164], anti-inflammatory [165] and anit-viral [166] as well as prevention of cardiovascular diseases [20]. It is believed that a better understanding of the mechanism of interplay will lead to their bioavailability improvements. Therefore, the purpose of this paper was to build an appropriate cell model and test its potential for the future mechanism study of simplest interplay between UGT1A9 and one efflux transporter in the disposition of flavonoids. Several flavonoids such as genistein (isoflavone) and apigenin (flavones) were used as model flavonoids to determine whether the UGT1A9 overexpressed in HeLa cells was functional. The successful establishment of the HeLa cells overexpressing UGT1A9 followed by characterization is the basis for the further study of interplay mechanism in flavonoid disposition.

4.3. Materials and methods

4.3.1. Materials

HeLa cells and pcDNA3.1(+/-) were a generous gift from Dr. Yu Rong (University of Texas at Houston). Apigenin, genistein and testosterone as well as other flavonoids were purchased from Indofine Chemical Company, Inc. (Hillsborough, NJ). Recombinant human UGT1A9 expressed in baculovirus-infected insect cells (Supersome™) was purchased from BD Biosciences (Woburn, MA). UGT1A9 antibody was purchased from Abnova (Walnut, CA). pCMV6_XL4 vector carrying *UGT1A9* gene was from Origene (Rockville, MD). All the endonucleases were purchased from New England BioLab (Ipswich, MA). All other chemicals and solvents were of analytical grade or better and commercially available.

4.3.2. Transient transfection in HeLa cells

HeLa cells were seeded at $1.0X10^5$ cells/well of a 6- well plate and maintained at 37°C under 5% CO_2 in Dulbecco's modified Eagles medium (DMEM) containing 10% fetal bovine serum (FBS). After 6-7 hours, vector carrying UGT1A9 gene (*NM_021027.2)* was introduced to the cells using the modified calcium precipitation method [167]. The medium containing 10% FBS (DMEM with high glucose) was changed to a medium containing 2% FBS on the next day. The transfected cells on the third day are ready for excretion study.

4.3.3. Construction of plasmid for stable transfection

The commercially available vector pCMV6-XL4 carrying *UGT1A9* gene (NM_021027.2) was digested by Not I (endonuclease) to release the *UGT1A9* gene. Then the UGT1A9 gene was ligated by DNA T4 ligase to the precutting target vector pcDNA3.1 (+/-), which had the neomycin resistant gene for clone selection. After amplification, the plasmid was purified and ready for stable transfection.

4.3.4. Development of stable transfected HeLa cells

After transient transfection, HeLa cells were maintained at 37°C under 5% CO_2 in Dulbecco's modified Eagles medium (DMEM) containing 10% fetal bovine serum (FBS) and Geneticin® (G418, 1.2mg/ml). Media were changed every two or three days until the colonies came out. The colonies were picked up and cultured in a 12-well plate (1colony/well). Once cells reached the 100% confluence, the cells from each well of the 12-well plate were split into two wells of the 6-well plates and allowed to grow until confluence. Those cells that were able to excrete large amounts of glucuronides were considered as the positive clones. Positive cloned cells were further cultured for five generations to test the stability of glucuronide production, and stable and highly active cells were then cryopreserved for future use. Each vial of cryopreserved cells was used for ten passages before a new one was initiated for use. HeLa cells stably transfected with *UGT1A9* were called engineered HeLa cells.

4.3.5. Transfection of siRNA

The engineered HeLa cells were seeded at 0.5 $X10^5$ cells/well in a 12-well plate and maintained at 37°C under 5% CO_2 in DMEM containing 10% FBS. On the next day, siRNA of MRP2 (SC-35963) or MRP3 (SC-40748) was transfected into the engineered HeLa cells by using Lipofactamine™ 2000 (Invitrogen) following the manufacturer's protocol. Cells were ready for experiment on the third day after transfection.

4.3.6. Preparation of cell lysates

The details were described in section3.2.2, Chapter 3. Briefly, cells were washed and harvested in 50mM potassium phosphate buffer (KPI, pH7.4) after growing for 3-4 day. The collected cells were sonicated for 30 min in an ice-cold water bath (4°C) [150]. Then the cell lysates were centrifuged at 4°C (5min at 6000rpm). The supernatant was taken to determine the protein concentration by BCA assay (Pierce Biotechnology, Rockford, IL) and to be used in the UGT activity assay or western blotting.

4.3.7. Western blotting

Cell lysates from wild type and engineered HeLa cells and UGT1A9 Supersomes™ were boiled at 95°C, and denatured protein was then run on a

10% SDS-PAGE gel to test the expression levels of UGTs. Following electrophoresis, the separated proteins on the gel were transferred to a PVDF membrane (Millipore) by a standard protocol. After blocking in 5% nonfat milk for one hour, the membrane was incubated with UGT1A9 antibody at 1:500 dilution in 3% milk at 4°C overnight. After washing for three times, the membrane was incubated with HRP-conjugated 2nd antibody (anti-rabbit) at 1:2000 dilution in 3% milk for one hour. Finally, the membrane was developed by enhanced chemiluminescence kit (Rockford, IL).The same membrane was stripped for detecting glyceraldehyde-3-phosphate dehydrogenase (GAPDH) as loading control. For commercial UGT1A9 Supersome™, the GAPDH could not be detected.

4.3.8. RT-PCR

Cells were collected and the RNA was extracted by using RNeasy Mini Kit of QIAGE (Valencia, CA). RT-PCR was run according to the manufacturer's protocol (OneStep RT-PCR Kit from QIAGEN, Valencia, CA). Briefly, a 50µl mixture containing 2µg total RNA, primers (final 0.6µM, sequences shown in the following), QIAGEN OneStep RT-PCR Enzyme Mix (2µl), dNTP mix (final 400µM of each dNTP) and QIAGEN OneStep RT-PCR Buffer as well as RNase-free water, was reversed transcribed at 50°C for 30min. Then continue to incubate the mixture at 95°C for 13min followed by 35 cycles of running (94°C/0.5min, 50°C/0.5min, 72°C/1min) and final extension at 72°C for 10min. The forward primer of UGT1A9 is 5'GTTGCCTATGGAATTTGA, and the reverse primer is 5'

GGGTGACCAAGCAGAT. The forward primer of BCRP is 5'TTCTCCATTCATCAGCCTCG, and the reverse primer is 5' TGGTTGGTCGTCAGGAAGA. The forward primer of β-actin is 5' GAGAAGATGACCCAGATCATGT, and the reverse primer is 5' TCGTCATACTCCTGCTTGCAG [168]. All these primers were shown to work previously and supplied by Sigma. The MRP2 (SC-35963-PR) and MRP3 (SC-40748-PR) primers were purchased from Santa Cruz biotechnology, Inc.. After RT-PCR, agarose gel electrophoresis and UV visualization were used together to determine the relative amounts of PCR products.

4.3.9. UGT activity assay

The method was modified based on a previously published paper [151]. Briefly, we mixed cell lysates (final protein concentration from 0.053mg/ml to 0.21mg/ml) or human UGT1A9 Supersome™ (final protein concentration from 0.013mg/ml to 0.053mg/ml), magnesium chloride (0.88mM), saccharolactone (4.4mM), and alamethicin (0.022 mg/ml), and different concentrations of genistein (0.5-50μM) or apigenin (0.5-40μM) in a 50mM potassium phosphate (or KPI) solution (pH7.4) diluted from 100X concentrated stock solutions in organic solvent (DMSO/Methanol=1:4). Uridine diphosphoglucuronic acid (3.5 mM) was added last to the previous mixture to the final volume of 170μl, and the mixture was incubated at 37°C for 30min, 45min or 60min. At the end of the reaction, it was stopped by the addition of 50μl solutions consisting of 94% acetonitrile/6% glacial

acetic acid and the internal standard. Samples were ready for HPLC or UPLC analysis after centrifugation (15min at 15,000 rpm).

4.3.10. Excretion experiments

The engineered HeLa cells (the HeLa cells stably transfected with *UGT1A9*) were grown on 6-well plates (2 $X10^5$ cells/well) or on 12-well plates (1 $X10^5$ cells/well) for about 3-4 days. Then the HBSS buffer containing genistein or apigenin (or the loading solution) was used to incubate the cells (2ml/well for a 6-well plate, 1ml/well for a 12-well plate) for a predetermined time interval at 37°C. The sampling times were selected to ensure linear range in the amounts excreted vs. time plots. At each time point, 200µl of incubating media from each well was collected and the same volume of loading solution was used to replenish each well. The collected incubating media were mixed with a stopping solution containing 100uM testosterone as internal standard in 94%acetonitrile/6% acetic acid. Supernatants were ready for UPLC analysis after centrifugation (15min at 15,000rpm).

4.3.11. Determination of cellular glucuronides in engineered HeLa cells

The details were described in section 3.2.4, Chapter 3. Briefly, the engineered HeLa cells were washed with ice-cold HBSS buffer twice after the excretion experiments. Then the cells were collected in 100 or 200µl HBSS buffer and sonicated on ice for 30min. After centrifugation at 15,500rpm for 20min,

supernatants were collected and mixed with 100uM testosterone as internal standard in 94%acetonitrile/6% acetic acid. The samples were ready for UPLC analysis after centrifugation.

4.3.12. Sample analysis by HPLC

The conditions for HPLC analysis of genistein, apigenin and their glucuronides were modified based on a previously published method [63]. The conditions were: system, Hewlett Packard 1090 with dioarray detector and Hewlett Packard Chemstation; column, Aqua (Phenomenex, Gilroy, CA), 5µm, 150X0.45cm; mobile phase A, 0.1% formic acid plus 0.06% triethylamine (pH 2.6); mobile phase B, 100% acetonitrile; gradient, 0-3min 20%B, 2-22min 20-49% B, 22-26min 49% B; injection volume, 200ul; wavelength, 254nm (for genistein and the internal standard) and 340nm (for apigenin). There was a 4-min interval between the end of the run and the next injection to allow the column to be reequilibrated with 20% mobile phase B. The precision is typically better than 5% and accuracy better than 10%.

4.3.13. Sample analysis by UPLC

The details were described in section 3.3.1, Chapter 3.

4.3.14. Quantification of glucuronides

The details were described in section 3.3.3, Chapter 3. Generally, the conversion factors representing the molar extinction coefficient ratio of glucuronides to aglycones, were used to quantify the amounts of flavonoid glucuronides as described previously.

4.3.15. Kinetic study of UGT1A9

Rates of metabolism in UGT1A9 Supersome™ or HeLa cell lysates were expressed as amounts of glucuronides formed/min/mg protein (nmole/min/mg). If the Eadie-Hofstee plot was linear, formation rates (V) of flavonoid glucuronides at various substrate concentrations (C) were fit to the standard Michaelis-Menten equation:

$$V = \frac{V_{max} C}{K_m + C} \qquad (1)$$

where K_m represents the Michaelis constant and V_{max} represents the maximum formation rate. If Eadie-Hofstee plots showed characteristic profiles of atypical kinetics such as autoactivation, biphasic kinetics and substrate inhibition [169-170], the data were fit to other corresponding equations [171], using Excel program. The best-fit model was determined based on Akaike's information criterion (AIC) [172] and the rule of parsimony was applied.

4.3.16. Calculation of f_{met} value and CL

Fraction metabolized or f_{met} value was defined as the fraction of dose metabolized (equation (2)). The f_{met} value was considered as the more appropriate parameter to reflect the extent of metabolism in the presence of a transporter-enzyme interplay [115].

$$f_{met} = \frac{\sum Metabolites}{\sum Metabolites + \sum Parent\ compound} \quad (2)$$

Clearance of efflux transporter (CL) was used here since intracellular concentrations could be very different from the extracellular concentrations of glucuronides.

$$CL = \frac{J}{Ci} = \frac{J_{max}}{K_m' + Ci} \quad (3)$$

where J_{max} is the excretion rates of glucuronides, K_m' is the Michaelis constant reflecting affinity of glucuronides to the efflux transporter, and C_i is the intracellular concentration of glucuronides. The J_{max} and K_m' were previously used as two kinetics parameters for transporters [131]. Assuming that the average volume of engineered HeLa cells was 4µl/mg protein [173], the intracellular concentrations of glucuronides were calculated after the total amounts of intracellular glucuronides were determined experimentally. Other investigators have estimated volume at a value that was a bit larger than 4µl/mg protein [174], so the intracellular concentrations might be slightly overestimated.

4.3.17. Statistical analysis

All the experiments were done in duplicates or triplets and data were analyzed by one-way ANOVA or student's t-test as appropriate and the level of significance is set at $p<0.05$ or $p<0.01$.

4.4. Results

4.4.1. Preparation for development of engineered HeLa cells

To develop engineered HeLa cells, which were stably overexpressing UGT1A9, the *UGT1A9* gene (NM_021027.2) was cloned into pcDNA 3.1 (+/-), which contained the neomycin gene and had the resistance to G418, an antibiotic selection marker. The gene sequence analysis (Appendix A) confirmed that *UGT1A9* gene was indeed cloned into the pcDNA 3.1 (+/-) and had no mutation. At the same time, wild type HeLa cells were treated with different concentrations of G418 to determine the proper concentration for selection. The result from MTT assay indicated that IC_{50} of G418 was around 1-1.5mg/ml (Appendix B). Therefore, in the development of engineered HeLa cells, G418 at 1.2mg/ml was selected to treat the cells after transient transfection.

4.4.2. Glucuronide excretion in control and transiently transfected HeLa cells

To test whether HeLa cells with overexpression of UGT1A9 is a feasible cell model to study interplay, wild type HeLa cells were first transiently transfected with *UGT1A9* followed by incubation with genistein or apigenin. The results indicated (Fig. 3) that there was a new peak eluting before each parent compound in the engineered HeLa cells when comparing to the control HeLa cells. For genistein, the new peak retention time is around 7min; and for the apigenin, the new peak retention time is around 9min. Based on the published

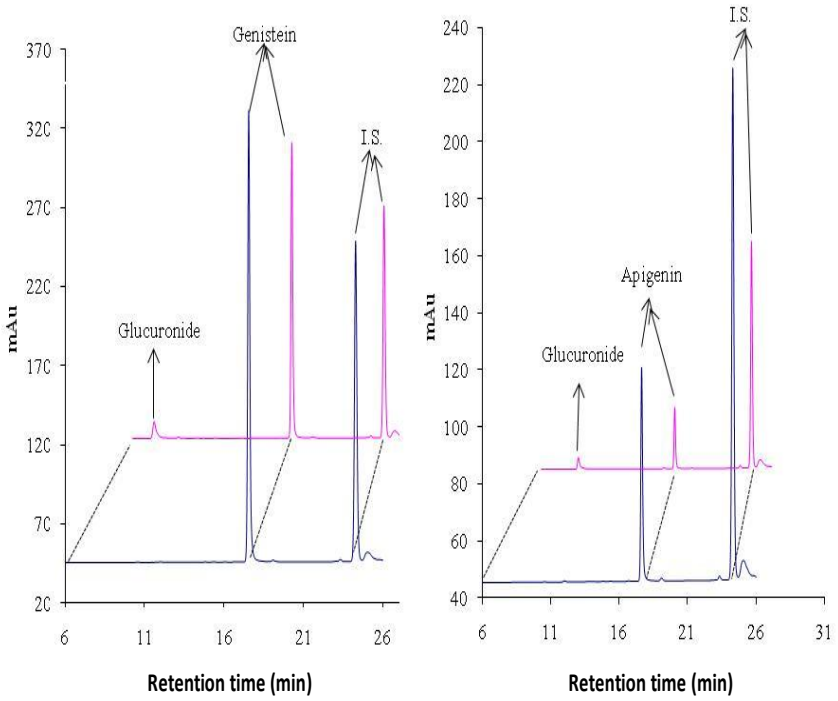

Fig. 3 The HPLC chromatogram of genistein and apigenin as well as their glucuronides. The HeLa cells not transfected or transiently transfected with *UGT1A9* were treated with 10μM genistein or apigenin for overnight at 37°C. The profile without the glucuronide was derived from the control cells whereas the profile with the glucuronide was from the transiently transfected cells. The chromatographic profiles were derived from HPLC analysis of the samples. Glucuronide was also authenticated with UPLC-MS/MS and authentic standards. I.S. was short for the internal standard.

data [175], these new forming peaks represent the glucuronides of each parent compound. On the contrary, only peak representing genistein or apigenin was detected in control HeLa cells. These results were further confirmed by UPLC-MS/MS study. Briefly, a predominant glucuronide of genistein was detected in transiently transfected HeLa cells with pseudomoleucular ion $[M-H]^-$ at m/z 445, which was 176Da higher (characteristic of the addition of glucuronic acid) than that of genistein (m/z 269). Similarly, a predominant glucuronide of apigenin was detected in transiently transfected HeLa cells by using the same UPLC-MS/MS method [31].

4.4.3. Characterization of engineered HeLa cells overexpressing UGT1A9

Engineered HeLa cells overexpressing UGT1A9 were characterized both at molecular and functional levels once the positive clones were obtained. The results from molecular level showed that UGT1A9 were well expressed at both mRNA (Fig. 4B) and protein levels (Fig. 4A) in engineered HeLa cells. Furthermore, our study at functional levels indicated that the engineered HeLa cells could metabolize flavonoids and excrete their corresponding glucuronides, similar to the observation shown in Fig. 3 by using transiently transfected HeLa cells. Moreover, mRNA levels of three efflux transporters: BCRP, MRP2 and MRP3 were determined in untransfected HeLa cells (Fig. 4C). It indicated that BCRP had a relatively higher mRNA expression level than MRP2 or MRP3 in the HeLa cells, consistent with an early observation that MRP2 was poorly expressed in HeLa cells [154].

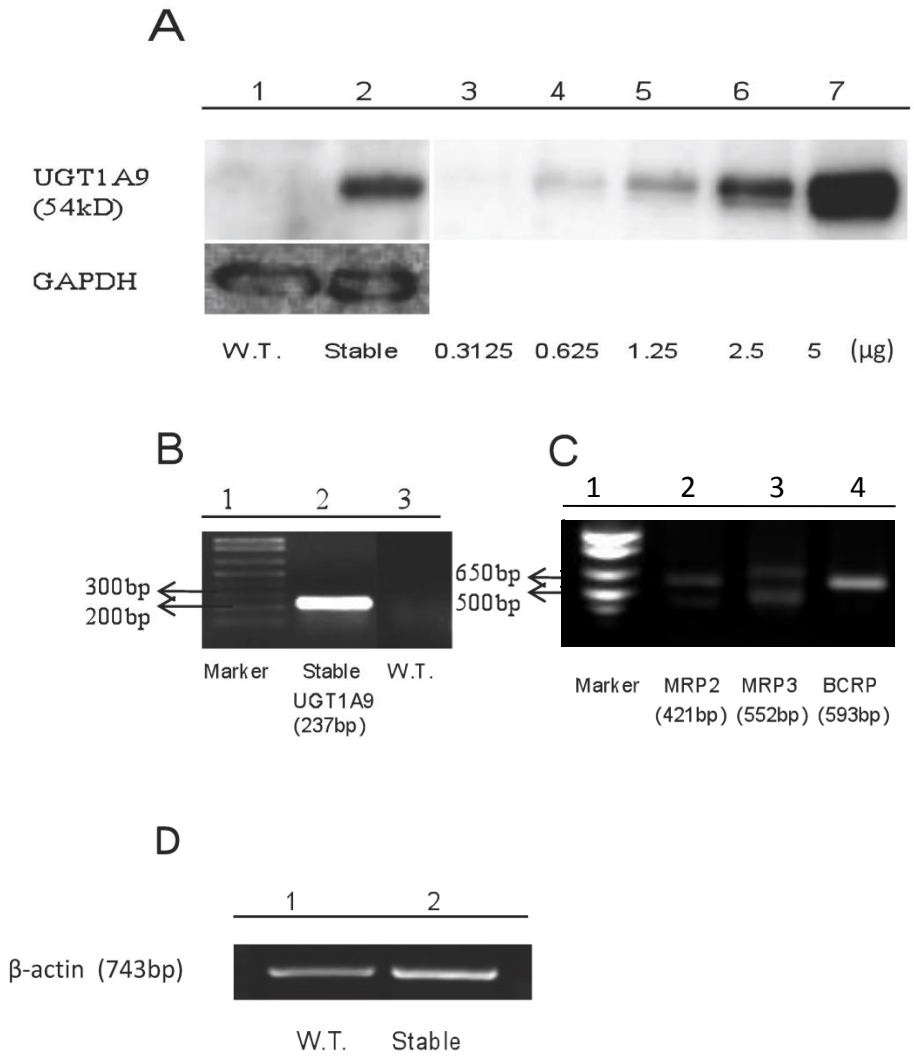

Fig. 4 Western blotting (A) and RT-PCR (B, C and D) of wild-type and engineered HeLa cells. For Western blotting, lane 1 was HeLa cells (wild type), lane 2 was engineered HeLa cells stably overexpressing UGT1A9, and lane 3 to lane 7 were different amounts of commercially available human UGT1A9 Supersomes™ (amount 0.3125μg to 5μg). The total amount of protein loaded on to lane 1 and 2 was 80μg. For RT-PCR (B), lane 1 was marker, lane 2 was engineered HeLa cells stably overexpressing UGT1A9 and lane 3 was the control HeLa cells (wild-type). For RT-PCR (C), lane 1 was marker, and lanes 2 to 4 were all HeLa cells (wild type). For RT-PCR (D), lane 1 was HeLa cells (wild type) and lane 2 was engineered HeLa cells stably overexpressing UGT1A9.

4.4.4. Stability of engineered HeLa cells

To determine how stable the engineered HeLa cells overexpressing UGT1A9 were, cells from five consecutive generations were treated with genistein or apigenin (10μM) for 4 hours. The activities were all normalized to the first generation. It indicated that the activity differences of engineered HeLa cells among the five generations were within 38% (Fig. 5). Therefore, the engineered HeLa cells overexpressing UGT1A9 were stable enough for us to do the following studies.

4.4.5. Enzyme kinetics study using UGT1A9 overexpressed in engineered HeLa cells

The kinetics profiles of UGT1A9 transiently or stably overexpressed in HeLa cells in metabolizing flavonoids (genistein, apigenin, wogonin and 5,4'-dihydroxyflavone) were explored and compared with commercially available human UGT1A9 Supersome™(Fig. 6 and Fig. 7). The K_m and V_{max} values of these kinetic studies were summarized in Table 1a and 1b. In general, UGT1A9 transiently overexpressed in HeLa cells had a K_m value very similar to the one that was stably overexpressed in glucuronidation of genistein or apigenin. However, UGT1A9 overexpressed in HeLa cells had larger K_m values than human UGT1A9 Supersome™ except for wogonin. V_{max} from UGT1A9 overexpressed in HeLa cells are not directly comparable to those of expressed in

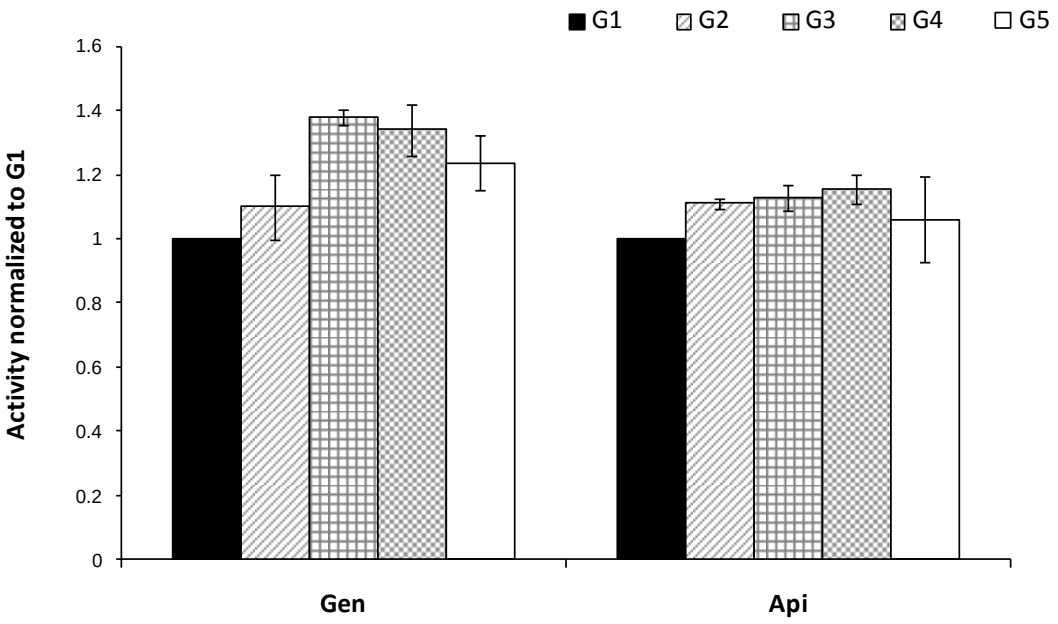

Fig. 5 Stability of expressed UGT1A9 in engineered Hela cells. Genistein (Gen) or apigenin (Api) (10μM) were incubated with engineered HeLa cells for five consecutive generations. The activities were all normalized to the first generation. Each data point was the average of three determinations with error bars representing the standard deviation of the mean (n=3).

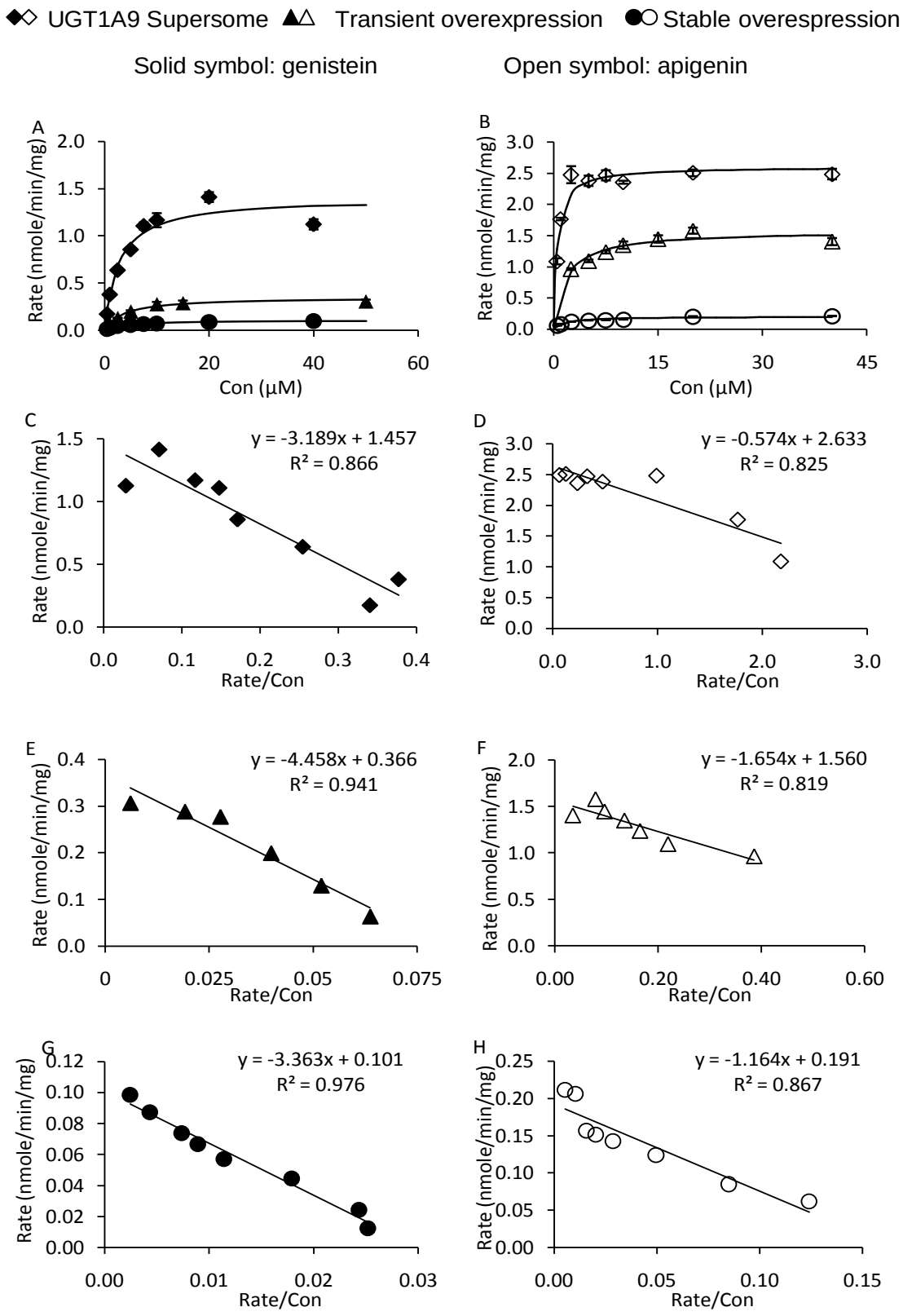
◆◇ UGT1A9 Supersome ▲△ Transient overexpression ●○ Stable overespression
Solid symbol: genistein
Open symbol: apigenin
A
Rate (nmole/min/mg)
Con (μM)
B
Rate (nmole/min/mg)
Con (μM)
C
y = -3.189x + 1.457
R² = 0.866
Rate (nmole/min/mg)
Rate/Con
D
y = -0.574x + 2.633
R² = 0.825
Rate (nmole/min/mg)
Rate/Con
E
y = -4.458x + 0.366
R² = 0.941
Rate (nmole/min/mg)
Rate/Con
F
y = -1.654x + 1.560
R² = 0.819
Rate (nmole/min/mg)
Rate/Con
G
y = -3.363x + 0.101
R² = 0.976
Rate (nmole/min/mg)
Rate/Con
H
y = -1.164x + 0.191
R² = 0.867
Rate (nmole/min/mg)
Rate/Con

Fig. 6 In vitro metabolism study of genistein and apigenin using human UGT1A9 Supersome™ and engineered HeLa cell lysates(UGT1A9-overexpressing HeLa cells). The genistein kinetics were shown in the Panel A. Rates of metabolism were determined from 0.5μM to 50μM, and reaction time was 60min. The related Eadie-Hofstee plots were shown in Panel C (Supersome™), Panel E (transient overexpression) and Panel G (stable overexpression), respectively. The apigenin kinetics were shown in Panel B. Rates of metabolism were determined from 0.5μM to 40μM, and reaction time was 15, 30 or 60min. The related Eadie-Hofstee plots were shown in Panel D (Supersome™), Panel F (transient overeexpression) and Panel H (stable overexpression). Each data point was the average of two (stable overexpresion, n=2) or three (Supersome and transient overexpression, n=3) determinations with error bars representing the standard deviation of the mean.

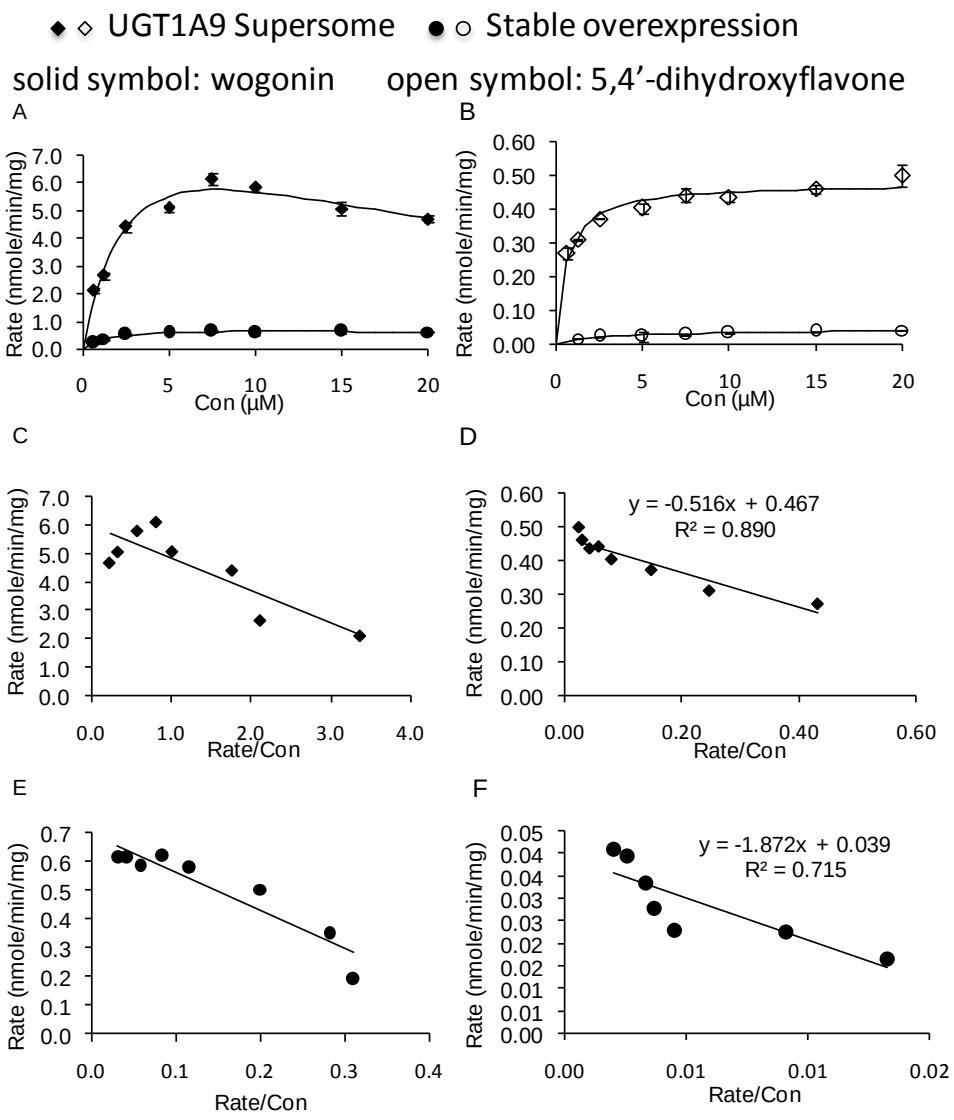

Fig. 7 In vitro metabolism study of wogonin and 5,4'-dihydroxyflavone using human UGT1A9 Supersome™ and engineered HeLa cell lysates (UGT1A9-overexpressing HeLa cells). The wogonin kinetics were shown in the Panel A. Rates of metabolism were determined from 0.625μM to 20μM, and reaction time was 15 or 20min. The related Eadie-Hofstee plots were shown in Panel C (Supersome™), and Panel E (stable overexpression), respectively. The 5,4'-dihydroxyflavone kinetics were shown in Panel B. Rates of metabolism were determined from 0.625μM to 20μM, and reaction time was 25min. The related Eadie-Hofstee plots were shown in Panel F (Supersome™), Panel G (transient overeexpression) and Panel H (stable overexpression). Each data point was (n=3) determinations with error bars representing the standard deviation of the mean.

Table 1a Comparison of kinetics parameters of UGT1A9 from different sources in genistein and apigenin glucuronidation

	Genistein	Apigenin
Structure	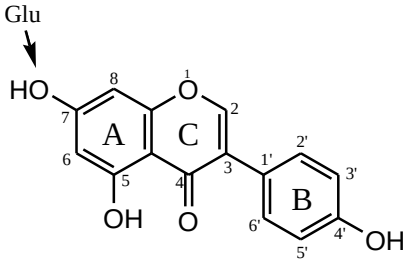	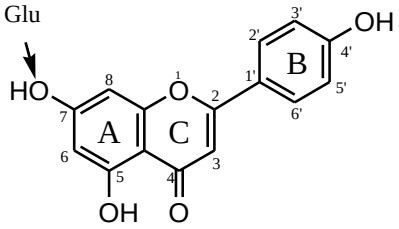

Source	Supersome™	Transient	Stable	Supersome™	Transient	Stable
K_m (μM)	2.72±0.073	3.71±0.65	*3.83±0.18	0.51±0.048	*1.76±0.11	1.68±0.037
V_{max} (nmole/ min/mg)	1.41±0.027	0.35±0.025	0.10±0.0015	2.61±0.023	1.58±0.0054	0.21±0
AIC	-15.82	-36.63	-76.62	-10.44	-18.96	-47.84
R^2	0.97	0.99	0.99	0.91	0.86	0.92

Note: A Student's t-test was used to compare the data (*, p<0.05). For Supersome™ and transient overexpression of UGT1A9, three independent studies (or n=3) were run, whereas for stable overexpression of UGT1A9, only two independent studies (n=2) were run. The arrows indicated the position for glucuronidation occurring in engineered HeLa cells.

Table 1b Comparison of kinetics parameters of UGT1A9 from different sources in wogonin and 5, 4'-dihydroxyflavone glucuronidation

	Wogonin		**5, 4'-dihydroxyflavone**	
Structure	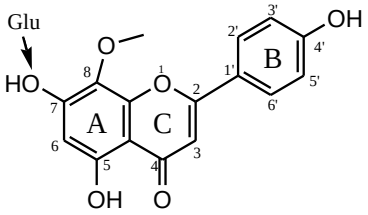		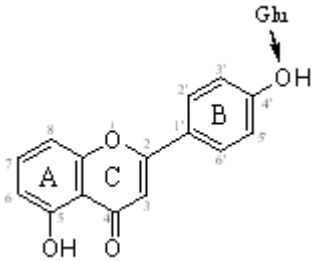	
Source	Supersome™	Stable	Supersome™	Stable
K_m (μM)	3.19± 0.13	*1.63± 0.30	0.59±0.087	*3.12±0.569
Ks (μM)	18.94± 0.58	84.20± 31.57	-	-
V_{max} (nmole/min/mg)	10.47± 0.14	0.80± 0.09	0.48±0.0077	0.045±0.0019
AIC	1.78	-40.17	-42.28	-62.86
R^2	0.96	0.98	0.93	0.85

Note: A Student's t-test was used to compare the data (*, p<0.05). For Supersome™ and stable overexpression of UGT1A9, three independent studies (n=3). The arrows indicated the position for glucuronidation occurring in engineered HeLa cells.

human UGT1A9, since the latter was expressed in insect cells. In any rate, UGT1A9 from all the sources followed the classical Michaelis-Menten profile in metabolizing genistein, apigenin and 5,4'-dihydroxyflavone and followed the substrate inhibition profile in metabolizing wogonin, suggesting that UGT1A9 derived from these various sources are likely the same, although the levels of expressions were clearly different.

4.4.6. Concentration-dependent excretion of glucuronides in engineered HeLa cells

To study whether the concentrations of genistein (2, 5, 10, 20 and 50μM) or apigenin (2, 5, 10, and 20μM) had an effect on the excretion of glucuronides, different concentrations of genistein or apigenin were incubated with engineered HeLa cells (Fig. 8). As expected, the rates of excretion of both genistein and apigenin glucuronides increased whereas their f_{met} decreased with a rise in concentration. The increase in excretion reached a plateau at a relatively low concentration (5 μM), but the decrease in f_{met} persisted throughout. In contrast, the intracellular glucuronide concentrations increased faster than the changes in the loading concentrations, which resulted in a significant and substantial decrease in the cellular clearance of these flavonoid glucuronides as the loading concentration increased.

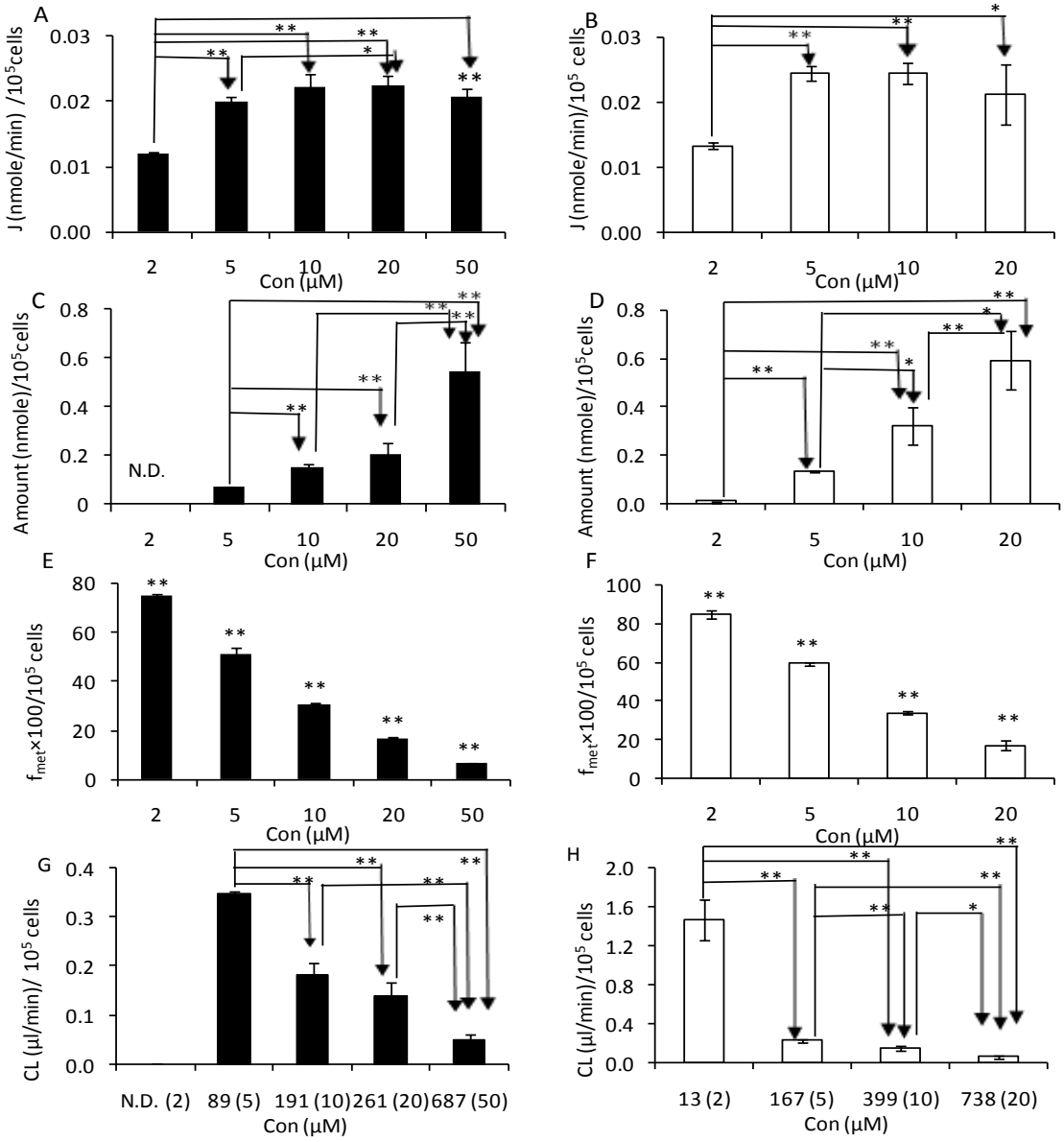

Fig. 8 Effects of concentration on excretion rates (A, B), intracellular amounts (C, D), fraction metabolized (f_{met}) (E, F), and clearance (CL) (G, H) of genistein or apigenin glucuronide. Different concentrations of genistein (A, C, E and G) or apigenin (B, D, F and H) were incubated with engineered HeLa cells. The calculated intracellular concentrations of glucuronides were shown in the X-axis of G and H followed by the actual loading flavonoid concentrations shown in brackets (G and H). Each data point was the average of three determinations with error bar representing the standard deviation of the mean (n=3). P<0.05, *; P<0.01, **.

4.4.7. Effects of LTC_4 on excretion of glucuronides

We used LTC_4, a general inhibitor of MRPs, to determine if it would impact cellular glucuronide excretion as was demonstrated in Caco-2 cells [63]. The results indicated that this general inhibitor did not affect the cellular excretion of either genistein or apigenin glucuronide (Fig. 9).

4.4.8. Effects of siRNA-mediated MRP2 and MRP3 silencing on excretion of glucuronides

siRNA of MRP2 or MRP3 was introduced to the engineered HeLa cells to determine how these treatments might affect the excretion of genistein and apigenin glucuronides and the results indicated that these two siRNAs had no impact on the excretion of genistein or apigenin glucuronides (Fig. 10).

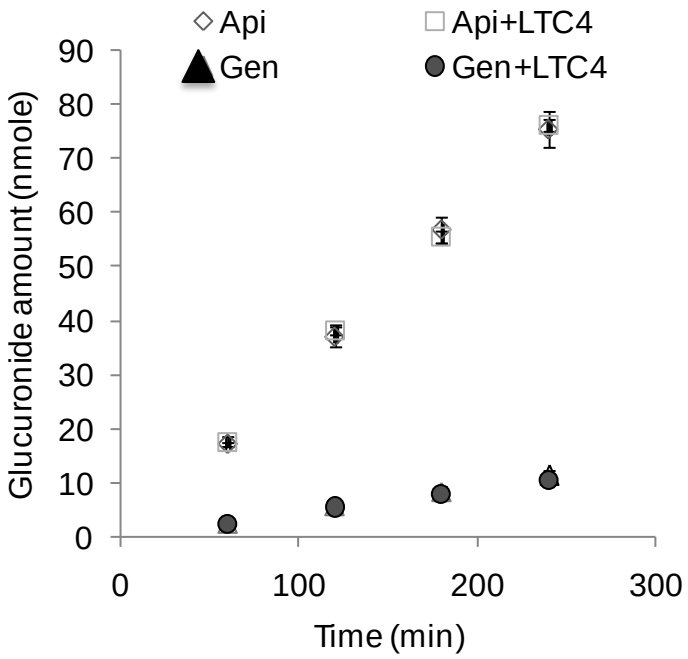

Fig. 9 Effects of LTC_4 (0.1μM) on the excretion of genistein or apigenin glucuronide. Genistein (Gen) or apigenin (Api) (10μM) were incubated with engineered HeLa cells grown on 6-well plates in the presence or absence of LTC_4 at 37°C. The incubating media were taken at 60, 120, 180 and 240min. Each data point was the average of three determinations with error bar representing the standard deviation of the mean (n=3).

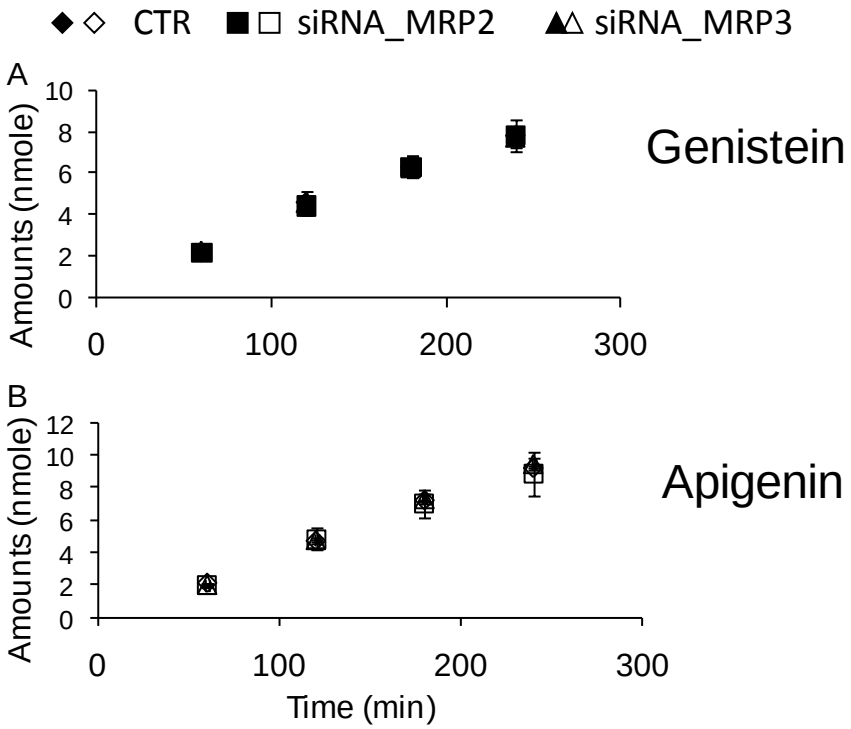

Fig. 10 Effects of siRNA-mediated MRP2/MRP3 silencing on excretion of glucuronides. Genistein (A) or apigenin (B) (10μM) were incubated with engineered HeLa cells in the presence or absence of siRNA of MRP2 or MRP3 (40pmole/well of 12 well-plate) at 37°C. The incubating media were taken at 60, 120, 180 and 240min. Each data point was the average of three determinations with error bar representing the standard deviation of the mean (n=3).

4.5. Discussion

Our results clearly indicated that engineered HeLa cells stably transfected with *UGT1A9* gene was able to be used as a suitable cell model to study the interplay between UGT1A9 and efflux transporters. This is because: first, both interplay players- UGT1A9 and BCRP are predominantly expressed and functional (Fig. 4); second, UGT1A9 overexpressed in HeLa cells following the same kinetics profile in metabolism of flavonoids as commercial UGT1A9 Supersome™ (Fig. 6 and Fig. 7); third, the engineered HeLa cells are functional stable for at least five generations (Fig. 5).

UGT1A9 overexpressed in the engineered HeLa cells played a significant role in the interplay. Without introduction of UGT1A9, there was no detectable excreted glucurnoides out of HeLa cells; however, with introduction of UGT1A9, there were amounts of glucuronides excreted out of engineered HeLa cells (Fig. 3). Moreover, the results also indicated that the glucuronides of genistenin or apigenin excreted out of the engineered HeLa cells were the metabolites of overexpressed UGT1A9. Even though some endogenous UGT isoforms were expressed in the HeLa cells such as UGT1A4 and 1A6 [43], whose contributions to glucuronidation of genistein or apigenin were negligible. This was because that UGT1A4 was not responsible for flavonoids metabolism and UGT1A6 was only able to metabolize flavonoids at a slower rate than UGT1A9. For endogenous UGT1A9, its expression was non-detectable in HeLa cells (Fig. 4A and B), which was also demonstrated by other investigators [43].

Furthermore, the UGT1A9 overexpressed in engineered HeLa cells either transiently or stably shared the same kinetics profile with human UGT1A9 Supersome^{TM} in metabolizing flavonoids to respective glucuronides (Fig. 6 and Fig. 7). For most flavonoids, the glucuronidation by UGT1A9 from both sources follows the Michaelis-Menten mechanism. The consistency of enzyme kinetics suggested that the active site of UGT1A9 was not easily affected by different sources. This was different from the findings of recombinant CYPs, whose kinetics might be changed due to the active site change from different sources [169]. Though it was not surprising to see the V_{max} values vary between sources, the different K_m values were not as our expectation. So far we could not provide a good explanation to this difference.

BCRP and MRPs were assumed to be responsible for the excretion of flavonoid glucuronides in engineered HeLa cells as efflux transporers. The further excretion study using LTC_4 and siRNA against MRP2 or MRP3 excluded the possible involvement of MRPs in the excretion of glucuronides (Fig. 9 and Fig. 10). Therefore, BCRP remained to be the main efflux transporter accounting for the excretion of glucuronides. This function assignment of each efflux transporter was consistent with its expression level in HeLa cells (Fig. 4C). The predominant expression of BCRP implied its main role in excretion of glucuronides in the engineered HeLa cells.

In summary, HeLa cells with stable transfection of *UGT1A9* were successfully established and well characterized. There was no essentially difference of glucuronidation mechanism between UGT1A9 predominantly expressed in the

engineered HeLa cells and the Supersome^{TM}, even though the kinetics parameters from both sources were different. On the other hand, BCRP, which was significantly expressed, seemed to be a main efflux transporter in the engineered HeLa cells that was responsible for the glucuronide excretion because no contribution of MRPs was demonstrated. Therefore, the interplay in the engineered HeLa cells should be between UGT1A9 and BCRP, which is the simplest interplay ever identified. Of course, the functional involvement of BCRP needs to be confirmed by using specific inhibitors. We expect that the ready-to-use engineered HeLa cells will provide us a great convenience in investigation of interplay mechanism.

CHAPTER 5: UGT1A9-OVEREXPRESSING HELA CELLS ARE AN APPROPRIATE TOOL TO DELINEATE THE KINETIC INTERPLAY BETWEEN UGT AND BCRP AND TO RAPIDLY IDENTIFY THE GLUCURONIDE SUBSTRATES OF BCRP

5.1. Abstract

The purpose of this study was to investigate the interplay mechanism between UGT1A9 and BCRP in the flavonoid disposition. Engineered HeLa cells were treated with selected flavonoids (e.g. genistein and apigenin) in the presence or absence of BCRP inhibitors or siRNA targeting UGT1A9. It indicated that siRNA-mediated UGT1A9 silence could result in a substantial reduction of glucuronide excretion and intracellular amounts of glucuronides (40-75%, $p<0.01$), as a result of expression inhibition of UGT1A9. On the other hand, a potent inhibitor of BCRP-Ko143 caused, in a dose-dependent manner, a substantial and marked reduction of the clearance (74%-94%, $p<0.01$), and a substantial increase in the intracellular glucuronide levels (4 to 8 folds, $p<0.01$), resulting in a moderate decrease in glucuronide excretion (19%-59%, $p<0.01$). In addition, a significant albeit moderate reduction in the fraction of genistein metabolized (or f_{met}) in the presence of Ko143 was observed. Similar results albeit to a less degree were observed when dipyridamole-a moderate inhibitor of both BCRP and glucuronidation was used. In addition, the microenvironment pH was proven to affect the interplay by modifying the function of each player. In conclusion, the engineered HeLa cells overexpressing UGT1A9 is an appropriate model to study the kinetic interplay between UGT1A9 and BCRP in the disposition of flavonoids. This simple cell model should also be very useful to rapidly identify if a phase II metabolite is the substrate of BCRP.

Keywords: UGT1A9, BCRP, MRP, HeLa cells, kinetic interplay

5.2. Introduction

Engineered HeLa cells, which are stably overexpressing UGT1A9, have been established and well characterized. In engineered HeLa cells, large amounts of flavonoid glucuronides metabolized by overexpressed UGT1A9, can be excreted via efflux transporters. According to our results (Chapter 4), BCRP, which is predominantly expressed in HeLa cells, is assumed to be mainly responsible for the excretion of flavonoid glucuronides. Thus, in the engineered HeLa cells, UGT1A9 and BCRP have the potential to be working coordinately in disposition of flavonoids.

It is well known that either UGT1A9 or BCRP plays an important role separately in disposition of various flavonoids and batches of clinical drugs. UGT1A9 is highly expressed in kidney and liver but not or less detected in intestine [39, 43]. Many clinical drugs such as SN-38 [159] and mycophenolic acid [176-177] are the substrates of UGT1A9. In addition, UGT1A9 can metabolize flavonoids with relatively high glucuronidation rates, compared with other UGT isoforms. BCRP, which is abundantly expressed in liver and intestine, on the other hand, can efflux a broad range of substances including flavonoids and their phase II metabolites (e.g. glucuronides and sulfates) [31, 98]

Previously, it was presumed that the interplay between UGTs and efflux transporters played an essential role in disposition of flavonoids and resulted in the low bioavailability of flavonoids [32]. However, there was no direct evidence to support this assumption. Inhibition of one player always accompanied with compensation of its function from the peers of the player. As a result, it is hard to

observe the obvious impacts from the inhibition of one player and to associate one player's function with another. For example, flavonoids were efficiently metabolized by UGT1A-deficient Gunn rats because of compensatory up-regulation of intestinal UGT2Bs and hepatic anion efflux transporters [178]. Therefore, a single cell model-the engineered HeLa cells with stable overexpression of UGT1A9 was developed, in which the compensation was least available.

It is a great advantage to use the well-characterized engineered HeLa cells as a simple model to study the interplay. First, it provides us an opportunity to determine the interdependence of two players-*UGT1A9 and BCRP.* In other words, the engineered HeLa cells can allow us to investigate how the efflux transporter like BCRP affects the glucuronidation activity of overexpressed UGT1A9 or vice versa. Second, it can allow us to control the intracellular level of glucuronides, which is very essential to the function of efflux transporters. Last but not least, it provides us an alternative approach to rapidly identify the glucuronide substrates of BCRP.

Therefore, the purpose of this research was to study the simplest interplay between UGT1A9 and an efflux transporter in control of glucuronidation of flavonoids and of excretion of their glucuronides. We believe that a better understanding of the factors that govern the metabolism of flavonoids holds the key to overcome their oral bioavailability barriers. Moreover, it is likely that the simplest interplay between an efflux transporter and a phase II enzyme will form the basis to understand and delineate the complex interplays between multiple

phase II enzymes and efflux transporters that determine the flavonoid bioavailability in vivo.

5.3. Materials and methods

5.3.1. Materials

HeLa cells stably transfected with *UGT1A9*, which were called engineered HeLa cells, were developed and characterized in our lab (Chapter 4). All the tested flavonoids were purchased from Indofine Chemical Company. UGT1A9 antibody was purchased from Abnova (Walnut, CA). siRNA of UGT1A9 and scrambled siRNA were purchased from Ambion (Austin, TX). Ko143 were purchased from Santa Cruz Biotechnology Inc (Santa Cruz, CA). Dipyridamole and dexamethasone were purchased from Sigma-Aldrich (St. Louis, MO). All other chemicals and solvents were of analytical grade or better.

5.3.2. Transfection of siRNA

The engineered HeLa cells were seeded at 0.5 $X10^5$ cells/well in a 12-well plate and maintained at 37ºC under 5% CO_2 in DMEM containing 10% FBS. On the next day, siRNA of UGT1A9 (sense: 5'-CGAAGUAUAUAUUUCUCUAUtt; antisense: 5'-AUAGAGAAUAUAUACUUCGta), scrambled siRNA (30pmole/well) or equal volume of water was introduced to the cells by using Lipofactamine™ 2000 (Invitrogen) following the manufacturer's protocol [168]. Cells were ready for experiment on the third day after transfection.

5.3.3. RT-PCR

Cells were collected and the RNA was extracted by using RNeasy Mini Kit (QIAGE, Valencia, CA). RT-PCR was run according to the manufacturer's protocol (OneStep RT-PCR Kit from QIAGEN). Briefly, a 50µl mixture containing 2pgtotal RNA, primers (final 0.6µM, sequences shown later), QIAGEN OneStep RT-PCR Enzyme Mix (2µl), dNTP mix (final 400µM of each dNTP) and QIAGEN OneStep RT-PCR Buffer as well as RNase-free water, was reversely transcribed at 50°C for 30min. Then the mixture was incubated continuously at 95°C for 15min followed by 25 cycles of expansion (94°C/0.5min, 55°C/0.5min, 72°C/1min), followed by the final extension at 72°C for 7min.The forward primer of p11 is 5'GTTGCCTATGGAATTTGA, and the reverse primer is 5' GGGTGACCAAGCAGAT [179]. The forward primer of β-actin is 5' GAGAAGATGACCCAGATCATGT, and the reverse primer is 5' TCGTCATACTCCTGCTTGCAG [168]. All these primers were shown to work previously and supplied by Sigma. After RT-PCR, agarose gel electrophoresis and UV visualization were used to determine the relative amounts of PCR products.

5.3.4. Preparation of cell lysates

The details were described in section 3.2.2, Chapter 3. Briefly, cells were washed and harvested in 50mM potassium phosphate buffer (KPI, pH7.4) after growing for 3-4 day. The collected cells were sonicated for 30 min in an ice-cold water bath (4°C) [150]. Then the cell lysates were centrifuged at 4°C (5min at 6000rpm).

The supernatant was taken to determine the protein concentration by BCA assay (Pierce Biotechnology, Rockford, IL) and to be used in the UGT activity assay or western blotting.

5.3.5. Western blotting

Cell lysates from engineered HeLa cells treated with or without UGT1A9 siRNA were boiled at 95^{o}C, and denatured protein was then run on a 10% SDS-PAGE gel to test the expression levels of UGTs. Following electrophoresis, the separated proteins on the gel were transferred to a PVDF membrane (Millipore) by a standard protocol. After blocking in 5% nonfat milk for one hour, the membrane was incubated with UGT1A9 antibody at 1:500 dilution in 3% milk at 4°C overnight. After washing for three times, the membrane was incubated with HRP-conjugated 2nd antibody (anti-rabbit) at 1:2000 dilution in 3% milk for one hour. Finally, the membrane was developed by enhanced chemiluminescence kit (Rockford, IL).The same membrane was stripped for detecting glyceraldehyde-3-phosphate dehydrogenase (GAPDH) as loading control.

5.3.6. Excretion experiments

The engineered HeLa cells (stably transfected with *UGT1A9*) were grown on 12-well plate (1 X10^{5} cells/ well) or on 6-well plate (2X10^{5} cells/ well) about 3-4 days. Before experiments were started, the engineered HeLa cells were washed twice with pre-warmed (37°C) HBSS buffer (Hank's balanced salt solution, pH=7.4). Then the cells were incubated with a HBSS buffer containing various flavonoids

with or without an inhibitor (defined as “loading solution”,1ml/well for 12-well plate and 2ml/well for 6-well plate) for a predetermined time interval (e.g. 40, 80 and 120min) at 37°C. In the loading solution, the proper concentration of flavonoids was diluted from 100X concentrated stock solutions in organic solvent (DMSO/Methanol=1:4), while the concentration of Ko143 (5 or 10μM) was diluted from 20mM stock solutions in DMSO. The concentration of dipyridamole (5 or 10μM) was diluted from 10mM stock solution in DMSO/Methanol=1:4. The sampling times were selected to ensure that the amounts excreted vs. time plots stay in the linear range. At each time point, 200l of incubating media from each well was collected and the same volume of loading solution was used to replenish each well. The collected incubating media were mixed with a “Stop Solution” consisted of 94%acetonitrile and 6% acetic acid containing 100uM testosterone as the internal standard. Supernatants were ready for UPLC analysis after centrifugation (15min at 15,000 rpm).

5.3.7. Determination of intracellular glucuronides in engineered HeLa cells

The details were described in section 3.2.4, Chapter 3. Briefly, cells were directly collected into 120ul or 200ul of HBSS buffer after excretion assay and broken by sonication (30min). The supernatant (100ul) was taken and mixed with 25ul of internal standard after centrifugation (15,500rpm/20min). The samples were processed by UPLC after another centrifugation.

5.3.8. UGT assay

The method was modified based on a previously published paper [151]. Briefly, we mixed cell lysates (final protein concentration from 0.026mg/ml or 0.053mg/ml), magnesium chloride (0.88mM), saccharolactone (4.4mM), and alamethicin (0.022 mg/ml), and 10µM of genistein, apigenin or wogonin in a 50 mM potassium phosphate (or KPI) solution (pH 7.4) diluted from 100X concentrated stock solutions in organic solvent (DMSO/Methanol=1:4). Uridine diphosphoglucuronic acid (3.5 mM) was added last to the previous mixture to the final volume of 170 µl, and the mixture was incubated at 37°C for 20min, 40min or 60min. At the end of the reaction, it was stopped by the addition of 50µl of 100µM testosterone solution (in 94% acetonitrile/6% glacial acetic acid) as the internal standard. Samples were ready for UPLC analysis after centrifugation (15min at 15,000 rpm).

5.3.9. Sample analysis by UPLC

The conditions for UPLC analysis of flavonoids and their glucuronides were described on details in section 3.3.1, Chapter 3.

5.3.10. Quantification of glucuronides

The conversion factors, representing the molar extinction coefficient ratio of glucuronides to aglycones, were used to quantify the amounts of flavonoids and their respective glucuronides. The details were referred to section 3.3.3, Chapter 3.

5.3.11. Calculation of f_{met} value and CL

Fraction metabolized or f_{met} value was defined as the fraction of dose metabolized (equation (1)). The f_{met} value was considered as the more appropriate parameter to reflect the extent of metabolism in the presence of a transporter-enzyme interplay [115].

$$f_{met} = \frac{\sum Metabolites}{\sum Metabolites + \sum Parent\ compound} \quad (1)$$

Clearance of efflux transporter (CL) was used here since intracellular concentrations could be very different from the extracellular concentrations of glucuronides.

$$CL = \frac{J}{Ci} = \frac{J_{max}}{K_m' + Ci} \quad (2)$$

where J_{max} is the excretion rates of glucuronides, K_m' is the Michaelis constant reflecting affinity of glucuronides to the efflux transporter BCRP, and C_i is the intracellular concentration of glucuronides. The J_{max} and K_m' were previously used as two parameters for transporters [131]. Assuming that the average volume of engineered HeLa cells was 4µl/mg protein [173], the intracellular concentrations of glucuronides were calculated after the total amounts of intracellular glucuronides were determined experimentally. Other investigators have estimated volume at a value that was a bit larger than 4µl/mg protein [174], so the intracellular concentrations might be slightly overestimated.

5.3.12. Statistical analysis

All the experiments were done in triplicates and data were analyzed by one-way ANOVA or student's t-test as appropriate and the level of significance was set at $p<0.05$ or $p<0.01$.

5.4. Results

5.4.1. Effects of siRNA-mediated UGT1A9 silencing on excretion of glucuronides

siRNA of UGT1A9 was introduced to the engineered HeLa cells to determine how changes in glucuronidation activity affected cellular glucuronide excretion, due to the unavailability of specific chemical inhibitor of UGT1A9. The appropriate dose and type of siRNA against UGT1A9, which caused the maximal inhibition of glucuronide excretion were determined for the later study (Appendix C). The negative control was the engineered HeLa cells transfected with water since there was no significant difference between the group transfected with water and with scrambled siRNA (Appendix D). For genistein group (Fig. 11), it revealed that siRNA-mediated UGT1A9 silencing inhibited the excretion of genistein by about 75% among all the loading concentrations. The intracellular glucuronides and f_{met} were reduced by 80-90% and 72-75%, respectively in the presence of UGT1A9 siRNA. However, the CL values of genistein glucuronide were not significantly changed with the UGT1A9 siRNA. For apigenin group (Fig. 12), the results indicated that the excretions of glucuronides were inhibited in the presence of UGT1A9 siRNA by 78%-87% with all the loading concentrations. Apigenin glucuronides accumulated inside cells and f_{met} were observed reducing by more than 94% and 70-87%, respectively due to the UGT1A9-mediated silencing. On the contrary to that of genistein group, the CL values of apigenin glucuronides were significantly affected by UGT1A9 siRNA. In particular, under

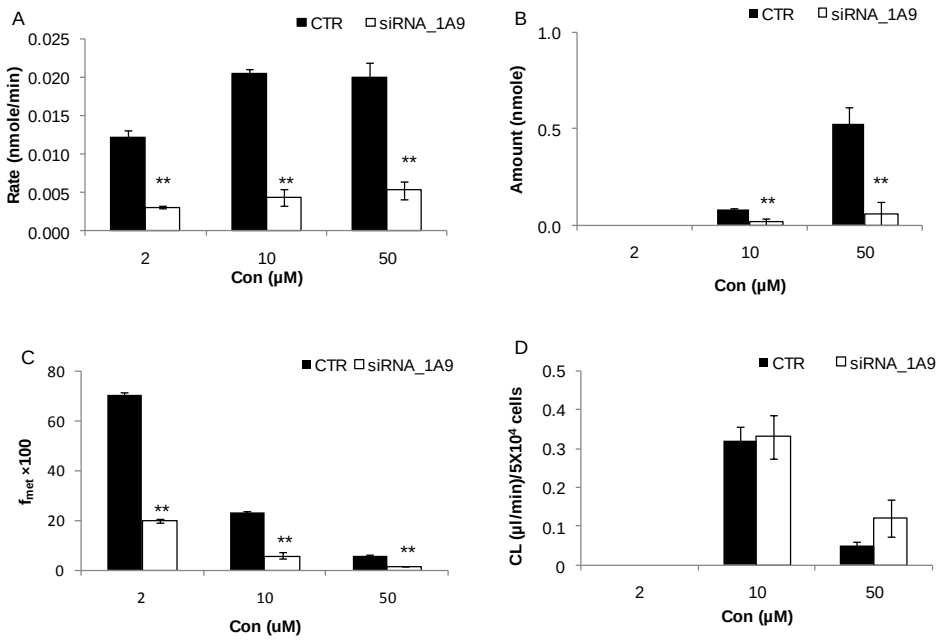

Fig. 11 Effects of siRNA-mediated UGT1A9 silencing on the excretion rates (A), intracellular amounts (B), fraction metabolized (f_{met}) (C), and clearance (CL) of genistein glucuronides (D). Engineered HeLa cells stably overexpressing UGT1A9 grown on 12-well plates were treated with 2, 10, 50μM genistein in the absence of siRNA (30μl water per well) or presence of 30pmole/well siRNA targeting UGT1A9. The intracellular amounts and f_{met} values were determined at 120min. Each data point was the average of three determinations (n=3). The error bar represents the standard deviation of the mean. p<0.05, *; p<0.01,.**

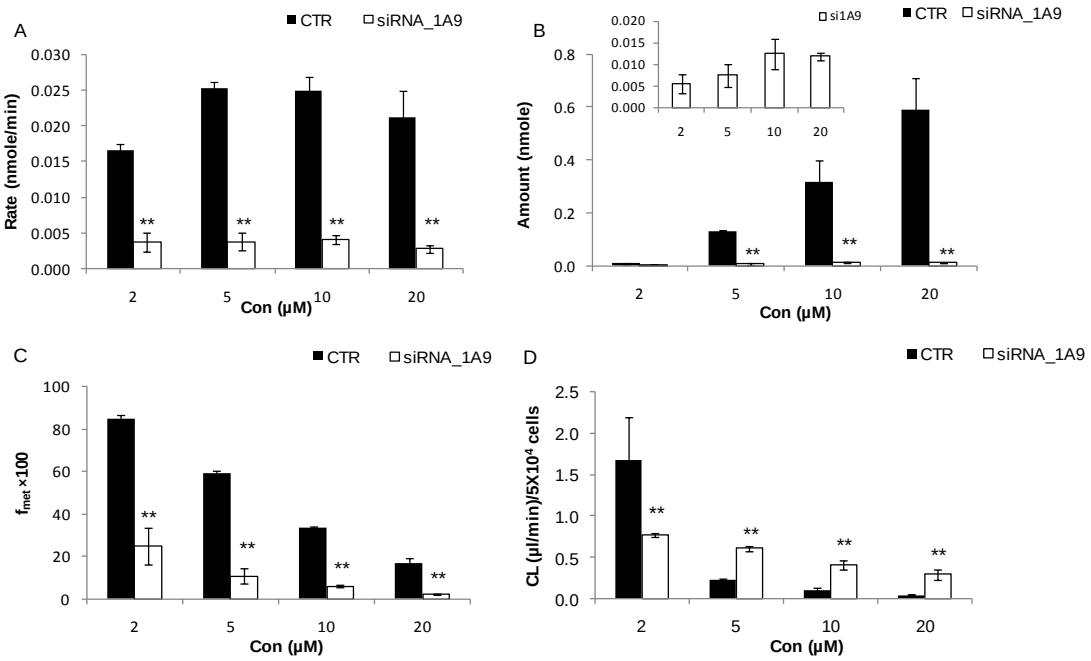

Fig. 12 Effects of siRNA-mediated UGT1A9 silencing on the excretion rates (A), intracellular amounts (B), fraction metabolized (f_{met}) (C), and clearance (CL) of apigenin glucuronides (D). Engineered HeLa cells stably overexpressing UGT1A9 grown on 12-well plates were treated with 2, 5, 10 and 20μM apigenin in the absence of siRNA (30μl water per well) or presence of 30pmole/well siRNA targeting UGT1A9. The intracellular amounts and f_{met} values were determined at 120min. Each data point was the average of three determinations (n=3). The error bar represents the standard deviation of the mean. p<0.05, *; p<0.01,. The small plot in B was the enlargement of intracellular glucuronides in the presence of siRNA**

loading concentrations of 5, 10 and 20μM, the CL of glucuronides were increased by 3 to 6 folds higher with siRNA treatment than those without siRNA treatment. For wogonin group Fig. 13, similar results to genistein group were observed: the glucuronide excretion (about 45%), the intracellular amounts of glucuronides (46%-56%) as well as f_{met} (38%-48%) were markedly inhibited in the presence of siRNA among all the loading concentrations; the CL values of wogonin glucuronide were not significantly changed.

These changes resulting from decreased glucuronidation activities (as demonstrated by a decrease in f_{met} in intact cells and by a reduction of glucuronidation rates in cell lysates Fig. 14A) were consistent with the decreases in expression levels of transfected UGT1A9 shown in the western blotting (Fig. 14B and C).

5.4.2. Effects of Ko143 on excretion of glucuronides

Next, the role of BCRP in excretion of glucuronides in engineered HeLa cells was determined, using a specific and potent chemical inhibitor Ko143 [101] (Fig. 15 and Fig. 16).The concentrations of Ko143 (5μM and 10μM) were selected based on references that showed this compound had a K_i value of less than 1 μM [102-103]. Our data showed that for genistein at 2μM, the excretion amounts of its glucuronides were reduced by 36% and 53% in the presence of 5μM and 10μM Ko143, respectively (Fig. 15A); for genistein at 10μM, the excretion amounts of glucuronides were decreased by 42% and 59% in the presence of 5μM and 10 μM Ko143, respectively (Fig. 15B). For apigenin at 2μM, on the other hand, the

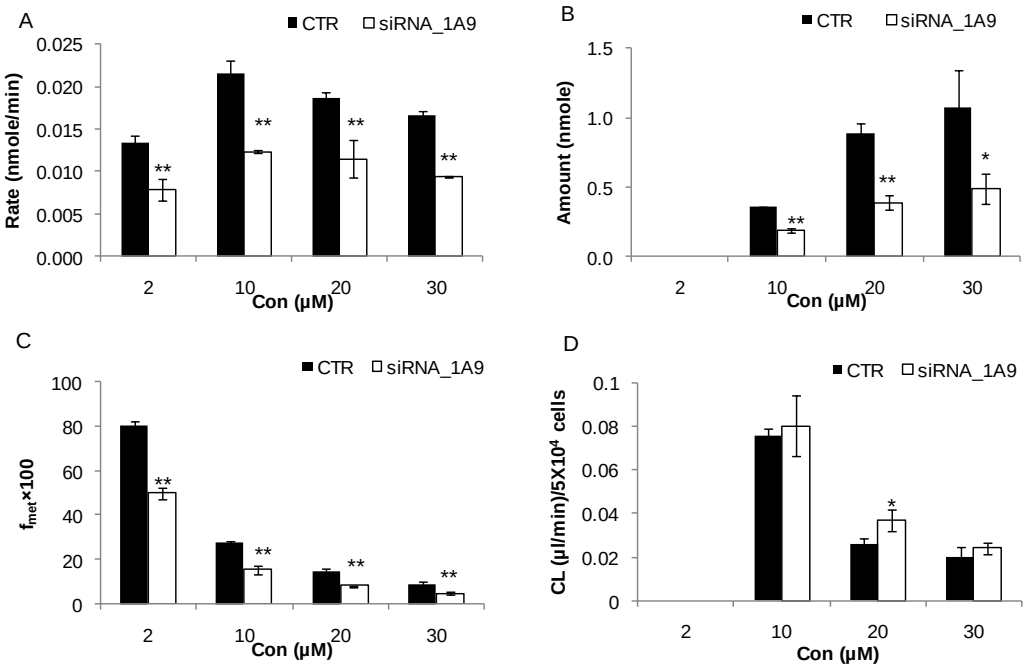

Fig. 13 Effects of siRNA-mediated UGT1A9 silencing on the excretion rates (A), intracellular amounts (B), fraction metabolized (f_{met}) (C), and clearance (CL) of wogonin glucuronides (D). Engineered HeLa cells stably overexpressing UGT1A9 grown on 12-well plates were treated with 2, 10, 20 and 30μM apigenin in the absence of siRNA (30μl water per well) or presence of 30pmole/well siRNA targeting UGT1A9. The intracellular amounts and f_{met} values were determined at 120min. Each data point was the average of three determinations (n=3). The error bar represents the standard deviation of the mean. p<0.05, *; p<0.01,.**

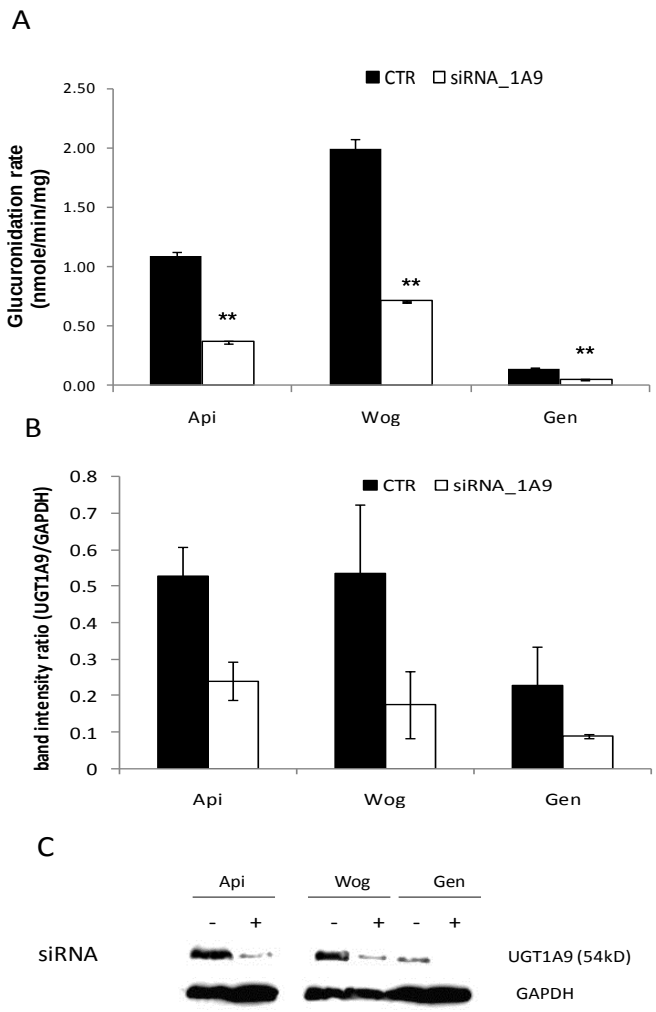

Fig. 14 Effects of siRNA-mediated UGT1A9 silencing on the glucuronidation rates (A) and expression of transfected UGT1A9 (B and C). siRNA of UGT1A9 (75pmole/well of a 6-well plate, corresponding 30pmole/well of a 12-well plate) was transfected to the engineered HeLa cells. Two days after transfection, cells were incubated with apigenin (Api), genistein (Gen) and wogonin (Wog) at 10μM for 40min to maximally mimic the condition of excretion assay. At the end of the experiments, the cells were collected and lysated for UGT activity assay (n=3) and western blotting (n=2), where 25μg of protein were loaded into each lane. The glucuronidation rates at 10μM from UGT activity assay were shown in (A); The band intensity ratio (UGT1A9 against GAPDH) (B) were originated from western blotting (C).

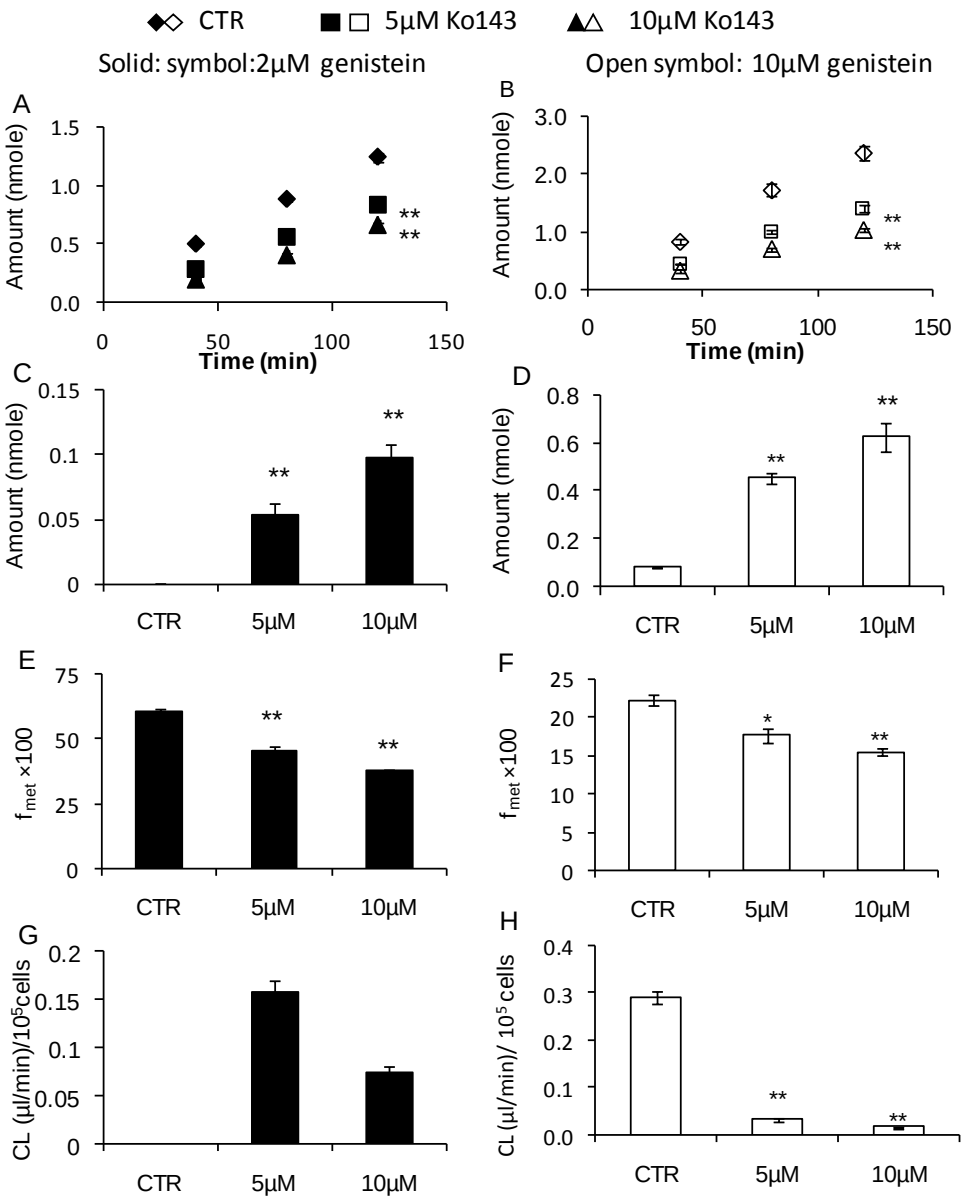

Fig. 15 Effects of BCRP-specific inhibitor Ko143 on the excretion, intracellular amounts, fraction metabolized (f_{met}), and clearance (CL) of genistein glucuronides. Engineered HeLa cells stably overexpressing UGT1A9 grown on 12-well plates were treated with 2 or 10μM genistein in the absence or presence of Ko143 at 5μM or 10μM. The amounts of excreted glucuronides as function of time was shown in the A and B and the intracellular amounts (determined at 120min) were shown in the C and D. The f_{met} values (determined at 120min) were shown in the E and F, and the CL values were given in the G and H. Each data point was the average of three determinations with error bar representing the standard deviation of the mean (n=3). $p<0.05$, *; $p<0.01$,.**

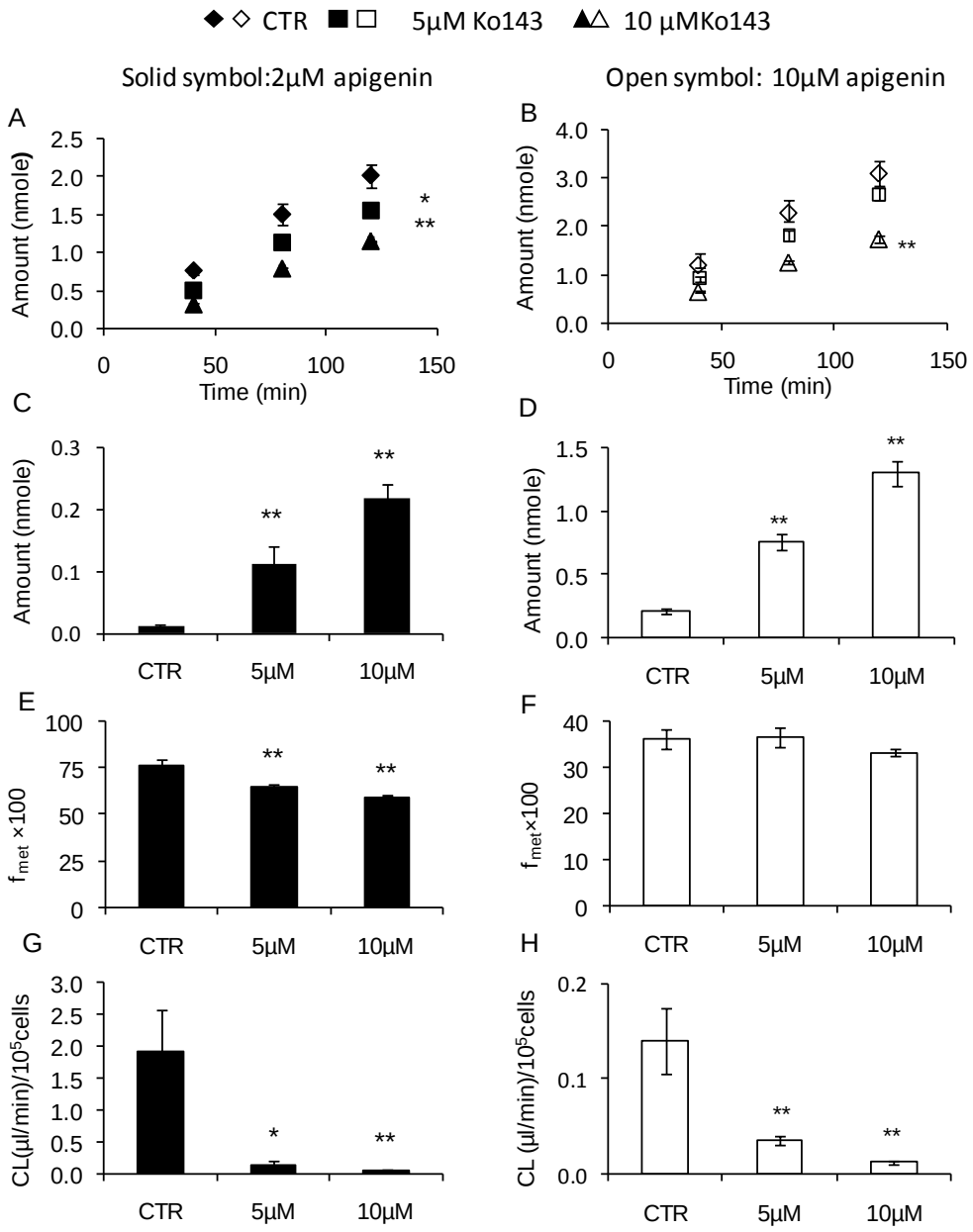

Fig. 16 Effects of BCRP-specific inhibitor Ko143 on the excretion, intracellular amounts, fraction metabolized (f_{met}), and clearance (CL) of apigenin glucuronides. Engineered HeLa cells stably overexpressing UGT1A9 grown on 12-well plates were treated with 2 or 10μM apigenin in the absence or presence of Ko143 at 5μM or 10μM. The amounts of excreted glucuronides as function of time was shown in the A and B and the intracellular amounts (determined at 120min) were shown in the C and D. The f_{met} values (determined at 120min) were shown in the E and F, and the CL values were given in the G and H. Each data point was the average of three determinations with error bar representing the standard deviation of the mean (n=3). p<0.05, *; p<0.01,.**

excretion amounts of its glucuronides were reduced by 28% and 50% with 5μM and 10μM Ko143, respectively (Fig. 16A); at 10μM apigenin, the excretion amounts of glucuronides were decreased by 19% and 44% with 5μM and 10μM Ko143, respectively (Fig. 16B). However, the amounts of genistein or apigenin glucuronides inside the cells showed the opposite trend. At 2μM genistein, the cellular glucuronides was not detected for control group, but increased a lot with 5μM or 10μM Ko143 (Fig. 15C); at 10μM genistien, the cellular glucuronides were increased by 6 (5μM Ko143) and 8 (10μM Ko143) folds when comparing to the control (Fig. 15D). Similarly, the amounts of apigenin glucuronides inside the cells were enhanced by 10 (5μM Ko143) and 20 (10μM Ko143) folds under 2μM apigenin, and augmented by 4 (5μM Ko143) and 6 (10μM Ko143) folds under 10μM apigenin when comparing to the control (Fig. 16C and D). Additional analysis of the results indicated that Ko143 had limited (or sometimes no) impact on the overall glucuronidation as represented by the f_{met} value, which was only moderately decreased. For f_{met} of genistein at 2μM, the decrease was about 25% (5μM Ko143) and 37% (10μM Ko143), whereas for f_{met} of genistein at 10μM, the decrease was about 21% (5μM Ko143) and 30% (10μM Ko143) (Fig. 15E and F). However, for f_{met} of apigenin at 2μM, the inhibition was 14% (5μM Ko143) and 22% (10μM Ko143); for apigenin at 10μM, the decrease of f_{met} was not statistically significant (Fig. 16E and F). Compared to limited reduction of f_{met}, cellular clearances (*or CL*) were inhibited drastically for both genistein and apigenin glucuronides by Ko143. In the presence of Ko143, CL of genistein glucuronide was reduced by 89% (5μM Ko143) and 94% (10μM Ko143),

respectively for 10μM genistein group (Fig. 15G and H). As for CL of apigenin glucuronide, the values were reduced by 92% (5μM Ko143) and 97% (10μM Ko143), respectively when incubating with 2μM apigenin; the CL were decreased by 74% (5μM Ko143) and 91% (10μM Ko143), respectively when incubating with 10μM apigenin (Fig. 16G and H).

Apart from genistein and apigenin, other flavonoids such as wogonin (wog), oroxylin A (Oro), 5,4'-dihydroxyflavone (5,4'diHF), 5,7-dihydroxyflavone (5,7diHF), 7-hydroxyflavone (7HF), 6-hydroxyflavone (6HF) and 3-hydroxyflavone (3HF) were all shown to be sensitive to Ko143 (5μM) to a different extent (Fig. 17). In general, Ko143 resulted in the moderate inhibition of glucuronide excretion rates (13%-36%); on the other hand, the intracellular glucuronides with Ko143 were enhanced by 2.3-6.3 folds higher than those in the control group. f_{met} values from various flavonoids were reduced in the presence of Ko143 in a compound-dependent manner. The maximal inhibition of f_{met} was observed for wogonin. Not surprisingly, the CL values of various flavonoid glucuronides were also considerably reduced with Ko143 (62%-87%), similar to CL of genistein or apigenin glucuronides.

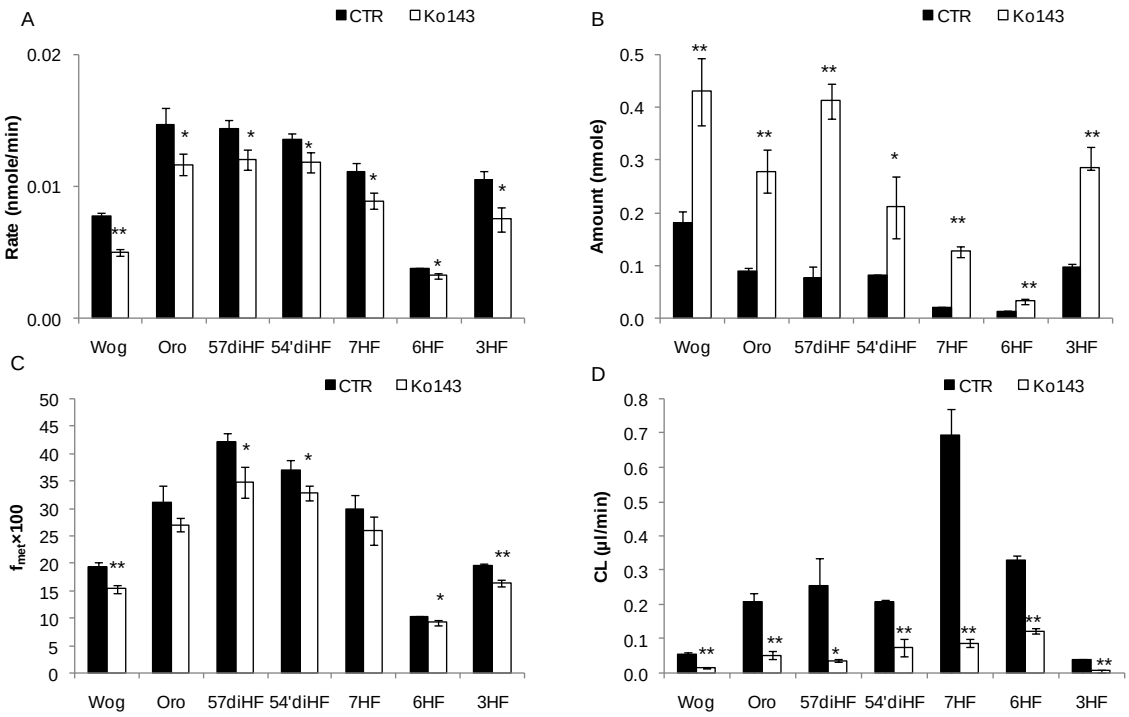

Fig. 17 Effects of BCRP-specific inhibitor Ko143 on the excretion rates (A), intracellular amounts (B), fraction metabolized (f_{met}) (C), and clearance (CL) of flavonoid glucuronides (D). Engineered HeLa cells stably overexpressing UGT1A9 grown on 12-well plates were treated with 10μM various of flavonoids in the absence or presence of Ko143 at 5μM. Each data point was the average of three determinations with error bar representing the standard deviation of the mean (n=3). p<0.05, *; p<0.01,.**

5.4.3. Effects of dipyridamole on excretion of glucuronides

Dipyridamole was reported as a chemical inhibitor of BCRP. Our unpublished data showed that it could also inhibit the glucuronidation reaction. Therefore, dipyridamole is a dual inhibitor of both BCRP and UGT1A9. Two lower doses (5μM and 10μM) of dipyridamole were selected (Fig. 18). As our expectation, the excretions of glucuronides were reduced in a dose-dependent manner. For genistein (Fig. 18A), 5μM and 10μM of dipyridamole could inhibit the excretion of glucuronides up to 36% and 52% respectively; for apigenin (Fig. 18B), the inhibition caused by dipyridamole could reach 21% at 5μM and 34% at 10μM, which were less than the effect on genistein. On the contrary trend to excretion, the intracellular levels of glucuronides were increased with increasing dose of dipyridamole. The genistein glucuronides inside the cells increased 2 to 3 folds (Fig. 18C). The apigenin glucuronides inside the cells increased about 2 folds (Fig. 18D). Furthemore, f_{met} value of genistein decreased from 29% (5μM) to 45% (10μM) of control. f_{met} value of apigenin dropped from 11% (5μM) to 21% (10μM) of control, though they were not statistically significant due to the lower dose of dipyridamole. Finally, CL values were found to decrease substantially in the presence of dipyridamole for both genistein and apigenin. In contrast to control, CL of genistein glucuronide were significantly inhibited by 75% (at 5μM) and 84% (at 10μM), respectively. Similarly, CL of apigenin glucuronide were significantly decreased by 59% (at 5μM) and 69% (at 10μM), respectively.

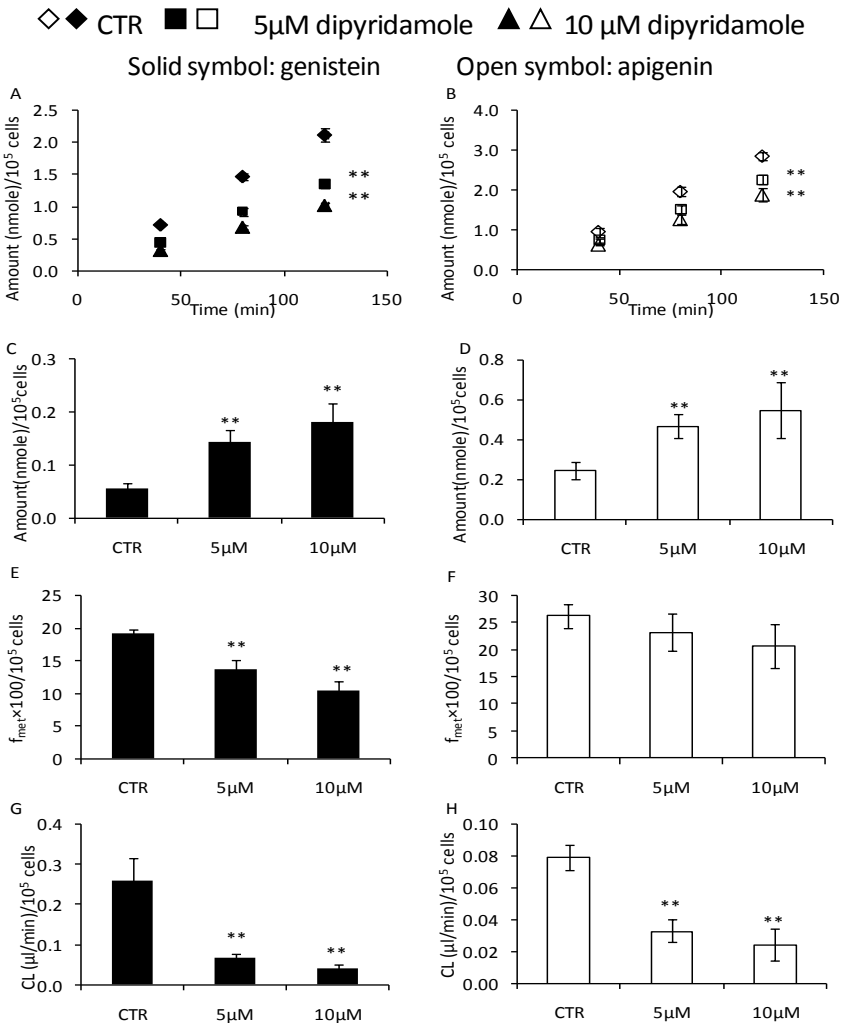

Fig. 18 Effects of BCRP and UGT1A9 inhibitor dipyridamole on the excretion rates, intracellular amounts, fraction metabolized (f_{met}) and clearance (CL) of glucuronides. Engineered HeLa cells stably overexpressing UGT1A9 were treated with 10μM genistein or apigenin in the absence or presence of dipyridamole at 5μM or 10μM. The excretion of glucuronides as a function of time was shown in the A and B and the intracellular amounts were shown in the C and D. The f_{met} values were shown in the E and F, and the CL values were given in the G and H. Each data point was the average of three determinations with error bar representing the standard deviation of the mean (n=3). P<0.05, *; P<0.01,.**

5.4.4. Effects of pH on excretion of glucuronides

It was reported that pH could affect glucuronidation reaction [180] and function of BCRP [181].To study the pH effects on the excretion of glucuronides, engineered HeLa cells were incubated with genistein or apigenin under three different pHs: pH6, pH7.4 and pH8, which represent acidic, physiological and basic microenviroment, respectively. It was found that pH had an impact on the excretion of glucuronides. In the case of apigenin (10μM) (Fig. 19), the excretion rate of glucuronides was reduced at pH6 by 30% while was unchanged at pH8 compared to pH7.4.The same trend was observed for f_{met}: 33% less at pH6 than that at pH7.4; no significant change between pH8 and pH7.4. Interestingly, intracellular amounts of apigenin glucuronides and apigenin were both decreased with increasing pH values, suggesting total cellular amounts of apigenin and its glucuronides were much dependent on pH. The cellular amounts of apigenin glucuronides and apigenin at pH7.4 were 24% and 83% less than those at pH6, respectively; at pH8, the cellular amounts of apigenin glucuronides and apigenin were 46% and 79% less than those at pH7.4, respectively. In contrast to intracellular amounts, the CL values of glucuronides were augmented from acidic pH to basic pH, though the difference was not significant due to large standard deviation at pH8.

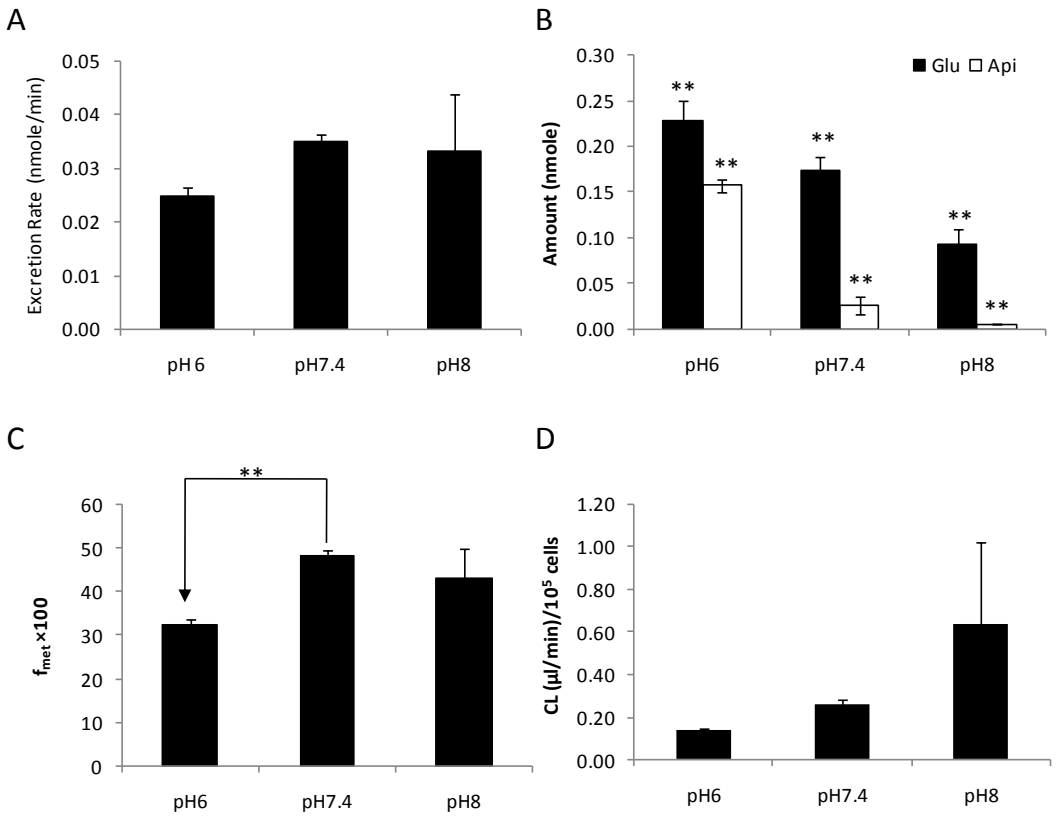

Fig. 19 Effects of pH on the excretion rates (A), intracellular amounts (B), fraction metabolized (f_{met}) (C) and clearance (CL) of apigenin glucuronides (D). Engineered HeLa cells stably overexpressing UGT1A9 grown on 12-well plates were treated with 10µM apigenin under pH6, pH7.4 and pH8. The intracellular amounts and f_{met} were determined at 120min. Each data point was the average of three determinations with error bar representing the standard deviation of the mean (n=3). P<0.05, *; P<0.01,. Glu was short for glucuronides whereas Api was short for apigenin.**

Consistently with apigenin group, pH had the similar effects on excretion of genistein glucuronides (Appendix E). At 10μM genistein, the excretion rate of glucuronides and f_{met} were inhibited by 32% and 36%, respectively at pH6 compared to pH7.4. The CL of genistein glucuronide mediated by BCRP was 55% lower at pH6 than that at pH7.4. However, the cellular genistein and its glucuronides at pH6 were 3.3 and 1.5 folds, respectively higher than those at pH7.4. At 20μM genistein, the excretion rate of glucuronide and f_{met} were not shown significant difference between pH7.4 and pH8. The CL of glucuronide at pH7.4 was 50% less than that at pH8. On the contrary, the cellular genistein and its glucuronides at pH7.4 were 3 and 2 folds, respectively higher than those at pH8. Moreover, the observed pH-dependent impacts for excretion rates, f_{met}, intracellular amounts and CL were not dependent on loading concentrations of genistein and apigenin since the similar results were found at concentration of 5μM under pH7.4 and pH8.

5.4.5. Effects of dexamethasone on excretion of glucuronides

Dexamethasone was used to induce the efflux transporters in engineered HeLa cells, since both BCRP and MRP2 could be induced in cells by dexamethasone at the concentration less than 1μM [182] . However, our results indicated that the excretions of apigenin glucuronides up to 8 hours in the engineered HeLa cells were not affected by 24-hour s' pretreatment of dexamethasone (from 200nM up to 50μM). The engineered HeLa cells were proved to be sensitive to dexamethasone since the mRNA level of p11 (a member of the S-100 family of

EF hand type Ca^{2+}-binding proteins) was induced by dexamethasone in a dose-dependent manner, consistent with previous observation [179]. Thus, the unchanged excretion of apigenin glucuronide in the presence of dexamethasone was due to other unidentified reasons. A part of the results were shown in Appendix F.

5.5. Discussion

The established and well-characterized engineered HeLa cells are an appropriate tool to study the simplest interplay between UGT1A9 and BCRP in disposition of flavonoids, which lays a foundation for future mechanism study on complex interplay. Both players-UGT1A9 and BCRP, which are kinetically interdependent to some extent, contribute essentially to the flavonoid disposition in the engineered HeLa cells. In particular, f_{met} was inhibited in the presence of Ko143 for some flavonoids, suggesting the glucuronidation activity of UGT1A9 in intact engineered HeLa cells could be inhibited with impaired function of BCRP (Fig. 15 and Fig. 17). Furthermore, microenvironment pH change can account for the disposition change of flavonoids by affecting the interplay (Fig. 19).

The glucuronidation of genistein, apigenin or wogonin by UGT1A9 overexpressed in the engineered HeLa cells was the rate-determining step in the interplay. The glucuronides were only detectable in the transfected but not in the wild type HeLa cells (Fig. 3, Chapter 4). Futhermore, the excretions of glucuronides and f_{met} were substantially decreased when siRNA of UGT1A9 was introduced (Fig. 11, Fig. 12 and Fig. 13). On the other hand, BCRP was found to be the dominant efflux transporter (i.e. gate-keeper) in the engineered HeLa cells since the intracellular levels of glucuronides were increased by several folds and the clearances of glucuronides by efflux transporter were inhibited by more than 90% in the presence of 10μM Ko143 (Fig. 15 and Fig. 16). However, the excretions of glucuronides with Ko143 did not decrease as much as the clearance, as one would have expected. This was due to the kinetic

compensation: i.e. the increasing levels of intracellular glucuronides compensated for the fact that function of efflux transporter was substantially inhibited by Ko143 (as demonstrated by large decreases in cellular CL). Taking consideration of least possibility for MRP2 and MRP3 contributing to the excretion of flavonoid glucuronides because neither the broad specific MRP inhibitor LTC4 nor the potent siRNAs against MRP2 and MRP3 was effective in inhibiting the glucuronide efflux, we are able to demonstrate that the observed interplay in the enginnered HeLa cells is mainly the result of the kinetic interplay between UGT1A9 and BCRP.

Interestingly and more importantly, it was the first time to demonstrate that the function of BCRP could affect the glucuronidation activity mediated by UGT1A9 overexpressed in engineered HeLa cells due to the evidence that f_{met} was observed decreasing when BCRP function was inhibited by Ko143 (Fig. 15, Fig. 16 and Fig. 17). Taken together with previous observation that CL of apigenin glucuronides was increased when glucuronidation activity was impaired by siRNA (Fig. 12D), the interdependence between UGT1A9 and BCRP in enginnered HeLa cells at kinetic level was obvious, though this phenomenon might not be ubiquitous for every flavonoid.

Furthermore, since more and more flavonoids are tested in the engineered HeLa cells, a classification system was proposed with 4 categories in terms of two criteria: glucuronidation (enzyme CL_{int}, obtained from glucuronidation assay using UGT1A9 supersome^{TM}) and excretion (transporter CL_{int}, obtained from excretion assay using engineered HeLa cells). So far due to the limiting tested

flavonoids, the exact number assigned to each CL_{int} might be bias. Therefore, we did not assigne any concrete number to classify groups in the (Fig. 20). For those flavonoids in the class with fast metabolism and slow excretion, the highest cellular glucuronides are expected. On the contrary, the lowest cellular glucuronides are expected for the flavonoids with slow metabolism and fast excretion. The glucuronides inside cells for other two categories are hard to tell. We surmise that the introduction of such a classification system for flavonoids will help us to identify those flavonoids, whose bioavailability has the greatest potentials to be improved in animal model. In other words, this classification for flavonoids could possibly provide us an opportunity to use engineered HeLa cells to predict bioavailability improvements in animal model.

Not surprisingly, microenvironment pH was shown to affect the interplay in the engineered HeLa cells. Compared to physiological pH7.4, acidic pH (pH6) was more likely to inhibit the glucuronidation activity (reducing f_{met}) (Fig. 19C) and function of BCRP (decreasing CL) (Fig. 19D). The decreasing function of BCRP at pH6 was contrary to the previous conclusion that BCRP transported substrate drugs more efficiently at low pH, independent of the dissociation status of the substrate [181]. So far the reason behind the controversy and the mechanism behind the pH effect on the function of BCRP in our case are unknown. On the contrary to acidic pH, basic pH seemed to only affect the BCRP-mediated glucuronides. As a result, the intracellular amounts of glucuronides were highest at pH6 and decreased with pH increasing. In addition, the cellular amounts of

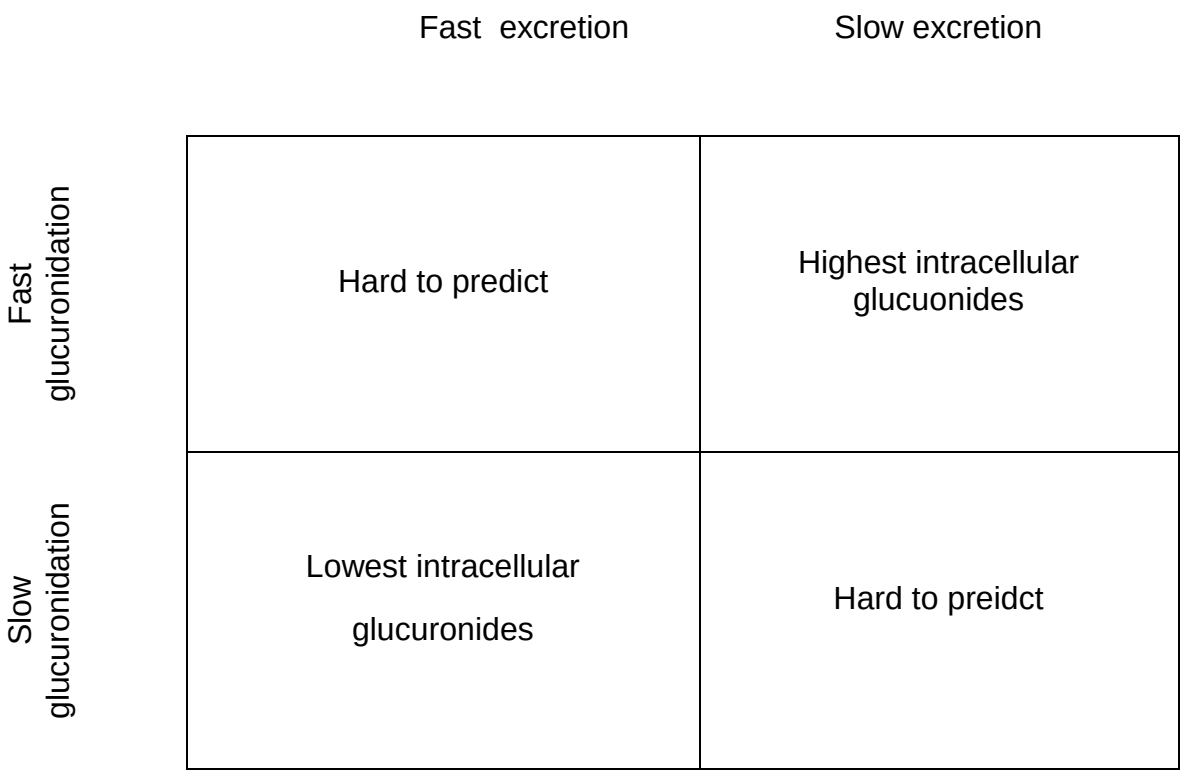

Fig. 20 Predicted intracellular glucuronides based on classification.

flavonoid aglycones were also decreased following the same trend as glucuronides. Therefore, the total flavonoid aglycones and their respective glucuronides contained in engineered HeLa cells were considerably hindered when microenvironment pH increased. Another reason leading to this observation might be that the total flavonoid aglycones passively diffusing into cells were much more at pH6 than at pH7.4 followed by pH8. On the basis of the pKa values of genistein (7.2, 10.0 and 13.1) [183] and apgienin (6.6 and 9.3) [184], both flavonoid aglycones without any charge are more easily enter the cells by passive diffusion under pH6; they are relatively hard to get into cells via passive diffusion when they gradually carry charges arising from the increasing environmental pH. Thus, microenvironment pH change can not only affect two players in the interplay, but also have an influence on the passive diffusion process, which is regarded as the predominant process for flavonoid aglycones to enter cells.

In addition to application of engineered HeLa cells to understanding kinetic interplay between UGT1A9 and BCRP, the newly engineered HeLa cells are useful for determining if a glucuronide (e.g., apigenin glucuronide) is a substrate of BCRP. This could not be routinely done previously since one would have to use purified glucuronides together with membrane vesicles that overexpress BCRP to positively identify if a glucuronide is the substrate of BCRP, a tedious and time- and resource- consuming process. As a consequence, very few glucuronides have been positively identified as a substrate of BCRP [185]. Of course, our simple model also has some additional limitations. For example, the

capability of BCRP may be exaggerated. The substrates may prefer other efflux transporters, if other options are available. But here they have to depend on BCRP to get out of the cells because BCRP is the most available efflux transporter in the model. Another limitation is that the compound must be the substrate of UGT1A9, which can be alleviated by using the same approach to build additional HeLa cell models.

In conclusion, the engineered HeLa cells are very suitable to study the kinetic interplay between UGT1A9 and BCRP in disposition of flavonoids due to several advantages: first, the interplay in this built cell system was extremely simple and exclusively between one UGT isoform (UGT1A9) and one efflux transporter (BCRP); second, it is relatively easy for us to manipulate each player in the interplay without interference; last but not the least, cellular change of glucuronides is readily to be observed, which is never possibly detected in other cellular systems. With assistance of the engineered HeLa cells, we were able to experimentally demonstrate the interdependence between UGT1A9 and BCRP at kinetic level for the first time. On the one hand, the impaired function of BCRP could inhibit the glucuronidation activity by UGT1A9, which provided the strong support to our hypothesis that the function of efflux transporters could affect the glucuronidation activity; on the other hand, the reducing activity of UGT1A9 by siRNA could result in increasing function of BCRP for some flavonoids (e.g. apigenin). In addition, pH was proved to have an effect on either UGT1A9 or BCRP in the engineered HeLa cells as our expectation. We believe that the present and future studies on the interplay between phase II conjugating

enzymes and efflux transporters in the engineered HeLa cells may provide us with the insight necessary to manipulate the oral bioavailability of flavonoids and other therapeutically relevant phenolics.

CHAPTER 6: COMPARISON OF ROLE OF INTERPLAY IN FLAVONOID DISPSOITION AMONG DIFFERENT CELL AND MOUSE MODELS

6.1. Abstract

The purpose of this research was to compare the flavonoid disposition mediated by interplay in the engineered HeLa cells to that in other *in vitro* cellular models (e.g. Caco-2 cells and engineered MDCKII-BCRP or MDCKII-MRP2 cells), and the mouse model *in vivo*. Genistein, apigenin or wogonin at 10μM was incubated with Caco-2 cells at apical side in the presence or absence of potent BCRP inhibitor Ko143 (5μM). In particular, wogonin was selected to incubate with the engineered MDCKII-BCRP and MDCKII-MRP2 cells transiently overexpressing UGT1A9. Wogonon was also orally administered to Bcrp (-/-) mice at dose of 20mg/kg. In Caco-2 cells, the results showed that for all the tested favonoids, inhibition of BCRP by Ko143 caused a decrease (50%) in the apical but an increase (2 folds) in the basolateral excretion of sulfates. In contrast, Ko143 (5μM) had no effects on glucuronide excretion from the either side. Furthermore, unlike what was obserbved in engineered HeLa cells, the f_{met} for phase II metabolism and the intracellular levels of flavonoid conjugates in the presence of Ko143 remained the same as control. All these results suggested that inhibition of BCRP in Caco-2 cells could only significantly affect the distribution of flavonoid sulfates but not the activities of phase II enzymes. In MDCKII cells transiently overexpressing UGT1A9, glucuronide excretions, cellular glucuronide levels and f_{met} were increased in MDCKII-BCRP or MDCKII –MRP2 cells but not in MDCKII-WT cells. This result also supported our hypothesis that the glucuronidation activity is linked with the function of efflux transporters. Finally, AUC of wogonin

and its phase II metabolites were improved by approximately 10 folds in Bcrp (-/-) mice, implying that bioavailability of flavonoids could be experimentally improved by disrupting the main player involved in the interplay between an efflux transporter and relevant conjugating enzymes.

Keywords: engineered HeLa cells, Caco-2, MDCKII, genistein, apigenin, wogonin, BCRP, UGT1A9, MRP2, bioavailability, interplay

6.2. Introduction

Flavonoids have been reported to have multifaceted “claimed” beneficial effects in humans, including chemoprevention, cardiovascular disease prevention and depression alleviation [20, 164, 186]. However, low bioavailability of flavonoids has limited their contribution to improve human health. It was well known that extensive phase II metabolism and efflux of phase II metabolites significantly contributed to the low bioavailability of flavonoids. Previously, investigators had proposed that phase II enzymes (e.g. UGTs and SULTs) and efflux transporters from ABC transporter family (e.g. BCRP and MRPs) might not work separately but coordinately to limit the bioavailability of flavonoids on the basis of idea that CYPs and P-gp cooperate to limit the bioavailability of clinical drugs, which was originally proposed 15 years ago [32, 111]. Accordingly, it was hypothesized that it was the interplay between phase II enzymes and efflux transporters that led to the low bioavailability of flavonoids.

Unlike the interplay between CYPs and P-gp which has been widely accepted and well demonstrated in both cell and animal models, the idea of interplay between phase II enzymes and efflux transporters is at its infancy. The big challenge for scientists to study the interplay between phase II enzymes and efflux transporters in flavonoid dispositon is the occurrence of many compensatory mechanisms that occur in current cell and animal models. This is because all these models contain multiple interplays, which roughly can be classified into two types: interplay between UGTs and efflux transporters and the interplay between SULTs and efflux transporters. If one type of interplay is

disrupted, the other type can take the place. Additionally, if the function of only one enzyme or efflux transporter in in the interplay is adversely affected, the other can compensate. As a result, it is very hard to study the mechanism of either type of interplay.

To find a way leading to improve the bioavailability of flavonoids, it is necessary for us to begin with the mechanism study on the simplest interplay which consists of only one phase II enzyme and one efflux transporter in order to prevent the potential compensations. Therefore, engineered HeLa cells were established and characterized. It was found that UGT1A9 and BCRP were predominantly expressed and functional in the engineered HeLa cells. Based on this cell line model, we are able to demonstrate the kinetic interplay between UGT1A9 and BCRP in disposition of flavonoids and the kinetic interdependence of these two players for the first time (Chapter 5). The activity of one player is associated with other player's function. In particular, the weakened function of BCRP could inhibit the glucuronidation activity toward flavonoids mediated by UGT1A9 overexpressed in engineered HeLa cells. Therefore, we are assuming that it is possible for us to reduce the glucuronidation activity via inhibition of BCRP in more complex system, which finally lead to improvement of flavonoid bioavailability in vivo.

It is very advantageous for us to use the engineered HeLa cells to study the mechanism of interplay in flavonoid disposition. However, the conclusions obtained from this simple cell model might be challenged since the model is too simple to mimic the real physiological conditions. Consequently, the conclusions

about flavonoid disposition based on the interplay in the engineered HeLa cells may be biased. To make our conclusions from the engineered HeLa cells more convincing, Caco-2 cells, BCRP-overexpressing MDCKII cells (MDCKII-BCRP cells), MRP2-overexpressing MDCKII cells (MDCKII-MRP2) and FVB mice with disruption of Abcg2 gene (Bcrp (-/-)) were used to study the impact of disrupting the interplay on flavonoid disposition.

In the consideration of accumulating data from genistein and apigenin as model flavonoids in the engineered HeLa cells, we will continue to use these two model flavonoids in the Caco-2 cells. In addition, the specific flavonoid will be selected to study the interplay in the engineered MDCKII-BCRP and –MRP2 cells (the cells with transient transfection of *UGT1A9*) and Bcrp (-/-) mice according to the following criteria: first, it has faster glucuronidation rates and slower sulfation rates; second, it is most sensitive to the inhibition of BCRP; third, its glucuronide excretion is relatively slower.

Therefore, the purpose of this paper was to study and compare the interplay between UGTs and BCRP in the flavonoid disposition among different cell and mouse models. A successful comparative study of different interplays among these models will provide us a reasonable way to project the results from the engineered HeLa cells and eventually establish a link between results in the engineered HeLa cells and that from more complex system containing multiple pairs of interplays. We hypothesized that the established and well-characterized engineered HeLa cells can be used to predict the interplay in the flavonoid disposition in vivo under certain conditions.

6.3. Materials and methods

6.3.1 Materials

Engineered HeLa cells were established and characterized (Chapter 4). Cloned Caco-2 TC7 cells were a kind gift from Dr. Moniqué Rousset of INSERM U178 (Villejuit, France). Madin Darby canine kidney (MDCK) series cells: MDCKII overexpressing BCRP (MDCKII-BCRP) cells and MDCKII wild type (MDCKII-WT) cells were purchased from the Netherlands Cancer Institute (Amsterdam, the Netherlands). Apigenin, genistein, wogonin and other flavonoids were purchased from Indofine Chemical Company. Ko143 were purchased from Santa Cruz Biotechnology Inc (Santa Cruz, CA). Dipyridamole, 3'-phosphoadenosine 5'-phosphosulfate (PAPS), uridine diphosphoglucuronic acid (UDPGA), alamethicin, D-saccharic-1,4-lactone monohydrate, magnesium chloride, and Hanks' balanced salt solution (HBSS, powder form) were purchased from Sigma-Aldrich (St Louis, MO). All other chemicals and solvents were of analytical grade or better.

6.3.2. Cell cultures

The details were on section 3.2.1, Chapter 3. Briefly, Caco-2 TC-7 cells were seeded on the monolayer at density of 100,000cells/ cm^2, and maintainedat 37ºC under 5% CO_2 in DMEM supplemented with 10% FBS. Media were changed every other day. The cells on the monaolayers were ready for transport experiments from day 19 to 22 since seeding. For engineered HeLa cells and

MDCKII series cells, they are regularly maintained in the same condition as Caco-2 cells and split every three or four days. These two cell lines are only grown on the plates with multiple wells but not on the monolayers.

6.3.3. Transient transfection of UGT1A9 in MDCKII-BCRP, MDCKII-MRP2 and MDCKII-WT cells

The MDCKII-BCRP (MDCKII cells overexpressing BCRP), MDCKII-MRP2 (MDCKII cells overexpressing MRP2) and MDCKII-WT (MDCKII cells wild type) cells were seeded at $1X10^5$ cells/well in a 6-well plate and maintained at 37ºC under 5% CO_2 in DMEM containing 10% FBS. The UGT1A9 plasmids (4µg/well) prepared by Maxi prep kit (QIAGEN) were introduced to the cells by using Lipofactamine^{TM} 2000 (Invitrogen) following the manufacturer's protocol. Cells were ready for excretion assay on the third day after transfection. These cells with transient transfection of *UGT1A9* are called engineered MDCK II series cells.

6.3.4. Transport study on Caco-2 monolayers

The protocol was modified according to previously published papers [63]. Briefly, cells on monolayers were washed three times with pre-warmed HBSS buffer (37°C pH7.4). The transeptithelial electrical resistance were measured to guarantee the quality of the monolayers (>420ohmscm^2). Then the cells were incubated with blank HBSS buffer for one hour followed by addition of 2.5ml loading solutions (HBSS buffer containing 10µM of genistein, apigenin or

wogonin with or without Ko143 (5μM)) at the apical side and addition of 2.5ml of HBSS buffer at basolateral side. Samples (500μl) from apical side or basolateral side were collected at 40, 80, 120 and 180min. After collection at each time point, same volume of loading solutions and HBSS buffer were added back to the apical and the basolateral side, respectively. Then, 200μl of collected samples was mixed with 50μl of 100μM testosterone dissolved in the solution of 94% acetonitrile and 6% glacial acetic acid. After centrifugation at 15,500rpm for 15min, the supernatant was taken and ready for UPLC analysis.

6.3.5. Determination of phase II metabolites in Caco-2 cells

The details were described in section 3.2.4, Chapter 3. Briefly, Caco-2 cells were collected in 1ml of acetonitrile and broken by sonication (30min) after transport study. The supernatant was taken after centrifugation (15,000rpm/20min). Subsequently, the supernatant was evaporated to dryness under air, the residue was reconstituted into 200ul of HBSS buffer with 50ul of internal standard. The samples were ready for UPLC analysis after centrifugation (15,000rpm/20min).

6.3.6. Preparation of mouse liver s9 fractions

The mouse liver s9 fractions are regularly prepared in our lab. It can be used to do both glucuronidation and sulfation study since it is enriched with both Ugts and Sults. The purpose for us to use mouse liver s9 fractions is to find a proper flavonoid, which has a relatively fast glucuronidation rate but a slow sulfation

rate. Briefly, mouse livers were harvested and blood in livers were removed by ice-cold solution A (8mM KH_2PO_4, 5.6mM Na_2HPO_4, 1.5mM KCl, 96mM NaCl and 0.04mg/ml PMSF) followed by solution B (8mM KH_2PO_4, 5.6mM Na_2HPO_4, 1.5mM EDTA, and 0.5mM dithiothreitol and 0.04mg/ml PMSF). Then livers were cut into small pieces and suspended in 100ml homogenization buffer (10mM KH_2PO_4, 250mM sucrose, 1mM EDTA, and 0.04mg/ml PMSF, pH7.4) followed by homogenization with a motorized Teflon/glass homogenizer. After centrifugation at 9,000Xg for 15min, the fat layer and pellets were discarded. The supernatant were aliquoted as mouse liver s9 fractions and stored in -80°C until further use. The protein concentrations were determined using a protein assay kit with bovine serum albumin serving as a standard. All the procedures including centrifugation are operated at 4°C to prevent the activity loss.

6.3.7. UGT activity assay

The method was modified based on a previously published paper [151]. Briefly, we mixed human UGT1A9 Supersome™ (final protein concentration from 0.013mg/ml to 0.026mg/ml) or mouse liver s9 fraction (final protein concentration from 0.23mg/ml to 0.46mg/ml) , magnesium chloride (0.88mM), saccharolactone (4.4mM), and alamethicin (0.022mg/ml), and different concentrations of genistein or apigenin in a 50 mM potassium phosphate (or KPI) solution (pH7.4). Uridine diphosphoglucuronic acid (3.5mM) was added last to the previous mixture to the final volume of 170 µl, and the mixture was incubated at 37°C for different time intervals, which were pre-determined to make sure the metabolites produced

were less than 30% and the glucuronidation rates were within linear range. At the end of the reaction, it was stopped by the addition of 50µl solution consisting of 94% acetonitrile/6% glacial acetic acid and the specific internal standard. Samples were ready for UPLC analysis after centrifugation (15,000 rpm/15min).

6.3.8. Sulfation of flavonoids using liver s9 fractions

The method for sulfation was described previously [31]. Briefly, liver s9 fractions produced from FVB mice (diluted from stock solutions, 1mg/ml) were mixed with 10µM of flavonoids in 50mM potassium phosphate buffer (KPI, pH7.4) diluted from 1mM stock solution in 80% of MeOH and 20% of DMSO. A 0.1mM 3'-phosphoadenosine 5'-phosphosulfate (PAPS) solution was finally added to the above reaction mixture (total volume 200 µl). Incubate the mixture in the water bath (37°C) for different time intervals, which were pre-determined to make sure the metabolites produced were less than 30% and the sulfation rates were within linear range. The reaction was terminated by addition of 50µl solution consisting of 94% acetonitrile/6% glacial acetic acid and the specific internal standard. Samples were ready for UPLC analysis after centrifugation (15min at 15,000 rpm).

6.3.9. Excretion experiments for engineered HeLa or MDCKII series cells

Before experiments were started, the engineered HeLa cells or engineered MDCKII series cells were washed twice with pre-warmed (37°C) HBSS buffer

(Hank's balanced salt solution, pH=7.4). Then the cells were incubated with a HBSS buffer containing the testing flavonoid with or without Ko143 (5μM) (defined as "loading solution",1ml/well for 12-well plates, 2ml/well for 6-well plates) for a predetermined time interval (e.g. 60, 120, 180, 240min) at 37°C. In the loading solution, 10μM flavonoids (e.g. apigenin) was diluted from 100X concentrated stock solutions in organic solvent (DMSO/Methanol=1:4).The sampling times were selected to ensure that the amounts excreted vs. time plots stay in the linear range. At each time point, 200l of incubating media from each well was collected and the same volume of loading solution was used to replenish each well. The collected incubating media were mixed with a "Stop Solution" consisted of 94%acetonitrile and 6% acetic acid and the specific internal standard. Supernatants were ready for UPLC analysis after centrifugation (15min at 15,000 rpm).

6.3.10. Determination of intracellular glucuronides in engineered HeLa cells or engineered MDCKII series cells

The details were described in Section 3.2.4, Chapter 3. Briefly, cells were directly collected into 120ul or 200ul of HBSS buffer after excretion assay and broken by sonication (30min). The supernatant (100ul) was taken and mixed with 25ul of internal standard after centrifugation (15,500rpm/20min). The samples were processed by UPLC after another centrifugation.

6.3.11. Sample analysis by UPLC

The conditions for UPLC analysis of flavonoids and their glucuronides were described on details in Section 3.3.1, Chapter 3.

6.3.12. Quantification of glucuronides

The conversion factors, representing the molar extinction coefficient ratio of glucuronides to aglycones, were used to quantify the amounts of flavonoids and their respective glucuronides. The details were referred to Section 3.3.3, Chapter 3.

6.3.13. Pharmacokinetic experiment on mice

Male wild type FVB mice and Bcrp (-/-) mice (22-27g, 8-10 weeks old) were purchased from Harlan Laboratory (Indianapolis, IN) and kept for at least 1 week in an environmentally controlled room (temperature: 25 $\pm$ 2°C, humidity: 50$\pm$5%, 12h dark-light cycle) before the experiments. To avoid the flavonoid interference from food, the mice were fed with non-soy food (AIN 76A) for at least one week before the pharmacokinetic study [152].

The protocols used in the pharmacokinetic study were approved by the University of Houston's Institutional Animal Care and Uses Committee. Mice were fasted for about 12 hours with free access to water prior to experiment. Wogonin was dispersed in oral suspension vehicle and then given orally to two groups of mice (FVB and Bcrp (-/-), each group consisting of 4 mice, n=4) by

gavage at dose of 20mg/kg [152]. After mice were anesthetized with isoflurane gas, blood samples (40µl) were collected in heparinized tubes from the tip of the tail with snipping at 15, 30, 60, 120, 240 and 480min after oral administration. Samples were stored in -20°C until further analysis by UPLC-MS.

6.3.14. Blood sample analysis by UPLC-MS/MS

The UPLC method was modified based on previously published papers [31], and the mobile phase A was changed from ammonium acetate (2.5mM, pH7.4) under negative ion mode to formic acid (0.1%, v/v) under positive ion mode. The gradient was, 0-2.0min, 10-35% B, 2.0-2.5min, 35-70%B, 2.5-3.0min 70-100%B; 3.0-3.9min, 100-10%B. For MS/MS analysis, an API3200-Qtrap triple quadruplole mass spectrometer (Applied Biosystem/MDS SCIEX, Foster City, CA) equipped with a TurboIOnSprayTM source was operated at the positive ion mode for wogonin and its glucuronides, whereas at the negative ion mode for wogonin sulfates. The formononetin used as internal standards were detected at both positive and negative ion modes. The concentrations of wogonin and its glucuronides and sulfates in mice blood were determined by multiple reaction monitoring (MRM) method. The compound-dependent and instrument-dependent parameters were summarized in Table 2. Analyte concentrations were determined using the software Analyst 1.4.2.

Table 2a Compound-dependent parameters of wogonin and its glucuronides (Wog-Glu) and sulfates (Wog-Sult) as well as formononetin in MRM mode in UPLC-MS/MS method

Compounds	Mode	Dwell time (ms)	Q1 (m/z)	Q3 (m/z)	DP (v)	CE (v)	EP (V)	CXP (V)
Wogonin	+	100	285	270	64	34	2	4
Wog-Glu	+	100	461	285	30	30	7	4
Wog-Sult	-	100	363	283	-24	-22	-5	-3
Formononetin	+	100	269	197	10	49	10	3
	-	100	267	252	-54	-28	-10	-2

DP: declustering potential; CEP: collision cell entrance potential; CE: collision energy; CXP: collision cell exit potential

Table 2b Instrument-dependent parameters for positive and negative modes in analysis of wogonin and its glucuronides and sulfates using MRM in UPLC-MS/MS method

Mode	CAD	CUR (psi)	Ion-spray voltage (kv)	TEM (°C)	Gas1 (psi)	Gas2 (psi)
+	High	20	5500	650	40	60
-	Medium	30	-4500	600	60	60

CAD: collision gas; CUR: curtain gas; TEM: ion source temperature

6.3.15. Biosynthesis of standards of wogonin sulfates

30μM of wogonin was mixed with mouse liver s9 fractions and PAPS in KPI buffer (pH7.4) for overnight to produce wogonin sulfates, following the protocol shown in “sulfation of flavonoids”. The reaction mixture was then applied to C8 column for solid phase extraction. After washing out the salts by water, 3ml of methanol was used to elute the wogonin sulfates. The eluted fraction of methanol was collected and evaporated to dryness under air. The residue was reconstituted into 1ml of 15% acetonitrile aqueous solution and stored into -80°C until further analysis. The standard of wogonin glucuronides was commercially available from China.

6.3.16. Blood sample preparation

The blood sample (40μl) was spiked with (formononetin in acetonitrile 1μM). The mixture was vigorously vortexed for 1min. After centrifuging at 15,500rpm for 20min, the supernatant was transferred to a new tube and evaporated to dryness under a stream of air. The residue was reconstituted in 100μL of 15% acetonitrile acqueous solution followed by centrifugation at 15,500rpm for 15min [152]. The supernatant was ready to inject into the UPLC-MS/MS system.

6.3.17. Calculation of f_{met} and CL

Fraction metabolized or f_{met} value was defined as the fraction of dose metabolized (equation (1)). The f_{met} value is considered as the more appropriate

parameter to reflect the extent of metabolism in the presence of a transporter-enzyme interplay [115].

$$f_{met}=\frac{\sum Metabolites}{\sum Metabolites+\sum Parent\ compound} \quad (1)$$

Clearance of efflux transporter (CL) was used here since intracellular concentration could be very different from the extracellular concentration of glucuronides.

$$CL=\frac{J}{Ci}=\frac{J_{max}}{K_m'+Ci} \quad (2)$$

where J_{max} is the excretion rates of glucuronides, K_m' is the Michaelis constant reflecting affinity of glucuronides to the efflux transporter BCRP, and C_i is the intracellular concentration of glucuronides. The J_{max} and K_m' were previously used as two parameters for transporters [131]. Assuming that the average volume of engineered HeLa cells is 4µl/mg protein [173], the intracellular concentrations of glucuronides were calculated after the total amounts of intracellular glucuronides were determined experimentally. Other investigators have estimated volume at a value that is a bit larger than 4µl/mg protein [174], so the intracellular concentrations might be slightly overestimated.

6.3.18. Statistical analysis

All the experiments were done in duplicates or triplicates and data were analyzed by one-way ANOVA or student's t-test as appropriate and the level of significance was set at $p<0.05$ or $p<0.01$.

6.4. Results

6.4.1. Effects of Ko143 on excretions of phase II metabolites of flavonoids in Caco-2 cells

Ko143, a potent chemical inhibitor of BCRP, was proved to have an effect on the glucuronide excretion, cellular glucuronides and glucuronidation activity for multiple flavonoids in the engineered HeLa cells. This suggested that inhibition of BCRP could affect the simplest interplay between UGT1A9 and BCRP, which finally led to disposition change of tested flavonoids in the engineered HeLa cells. To see Ko143 effects in other cell models and compare with our engineered HeLa cells, Caco-2 cells, a traditional cell model used to study drug metabolism and transport, were incubated with genistein, apigenin and wogonin at 10μM. For genistein (Fig. 21), the excretions of glucuronides at both apical and basolateral sides were not affected by Ko143; however, the excretion of sulfates were inhibited by 43% at apical side and increased by 1.4 folds at basolateral side ($p<0.01$). The cellular amounts of both phase II metabolites and activity of phase II metabolism did not show any significant change in the presence of Ko143. Consistently, Ko143 had no effects on the glucuronide excretion of apigenin (Fig. 22) or wogonin (Fig. 23) at both sides; whereas the sulfate excretions were reduced by 57% and 49% at apical side, and were enhanced by 1.2 and 1.8 folds at basolateral side for apigenin and wogonin, respectively ($p<0.01$). No statistical significance was observed for phase II metabolites of apigenin or wogonin inside cells and for the activity of glucuronidation or sulfation.

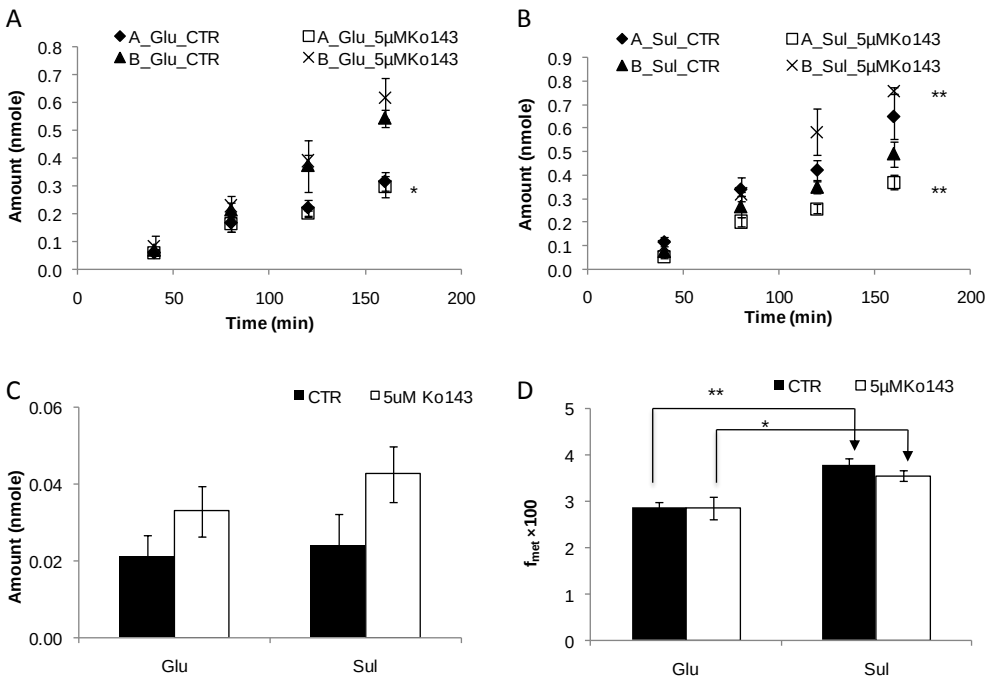

Fig. 21 Effects of Ko143 on transport study in Caco-2 cells model. 10uM genistein was loaded on the apical side together with or without Ko143 (5uM). Samples (500ul) were taken at 40, 80, 120 and 160min from both apical and basolateral sides. The same volumes of loading solutions and HBSS buffer were added back to apical and basolateral sides, respectively. Each symbol represents the average of three determinations (n=3).The error bar is the standard deviation of the mean. Glu was short for glucuronides, Sul was short for sulfates, CTR was short for control.

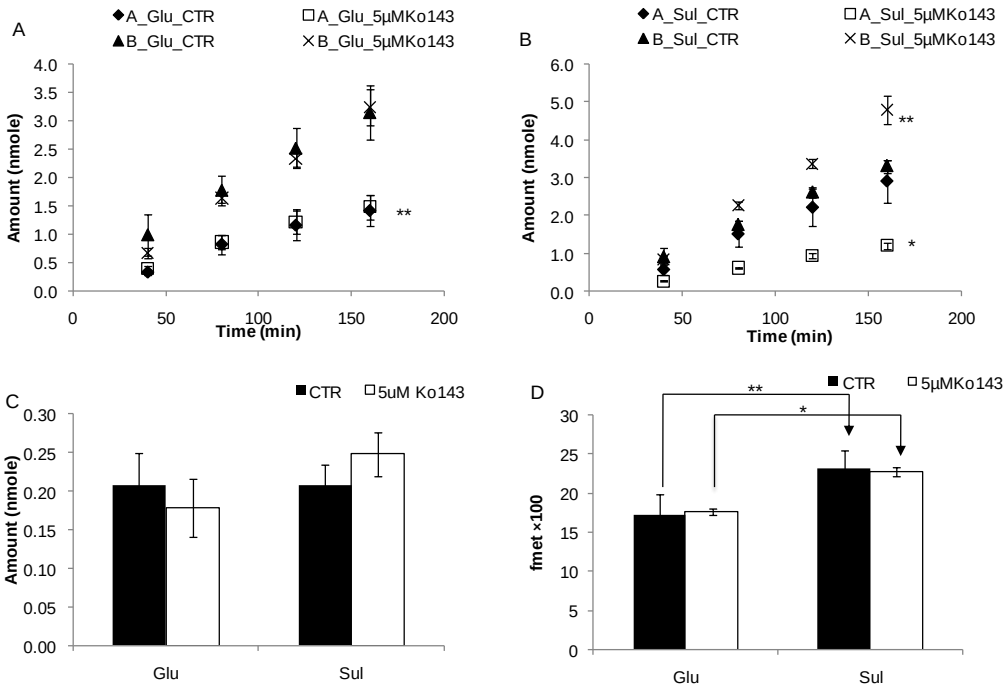

Fig. 22 Effects of Ko143 on transport study in Caco-2 cells model. 10uM apigenin was loaded on the apical side together with or without Ko143 (5uM). Samples (500ul) were taken at 40, 80, 120 and 160min from both apical and basolateral sides. The same volumes of loading solutions and HBSS buffer were added back to apical and basolateral sides, respectively. Each symbol represents the average of three determinations (n=3). The error bar is the standard deviation of the mean. Glu was short for glucuronides, Sul was short for sulfates, CTR was short for control.

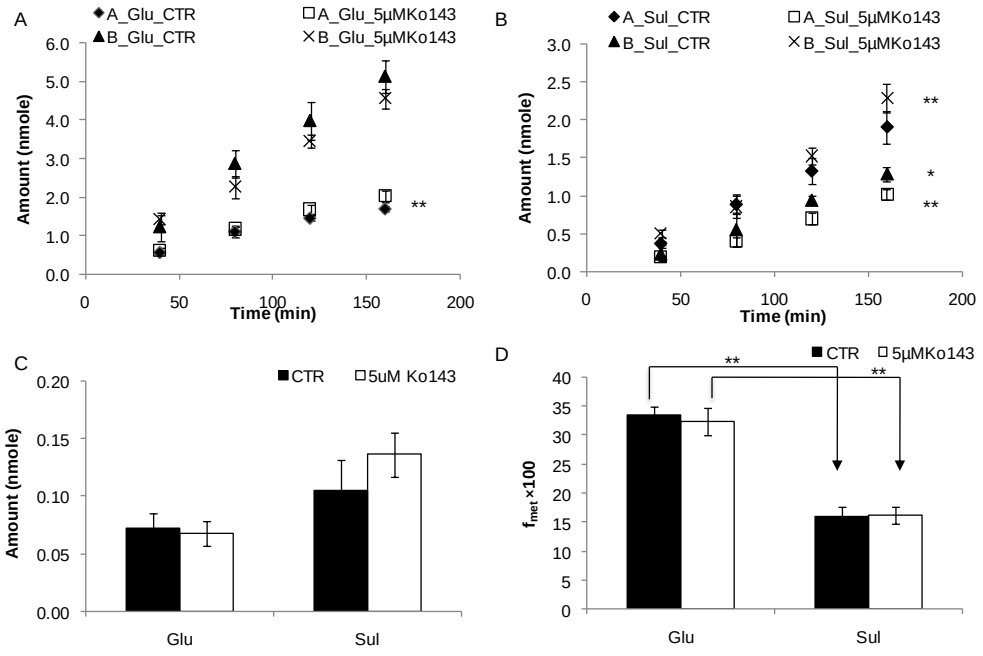

Fig. 23 Effects of Ko143 on transport study in Caco-2 cells model. 10uM wogonin was loaded on the apical side together with or without Ko143 (5uM). Samples (500ul) were taken at 40, 80, 120 and 160min from both apical and basolateral sides. The same volumes of loading solutions and HBSS buffer were added back to apical and basolateral sides, respectively. Each symbol represents the average of three determinations (n=3). The error bar is the standard deviation of the mean. Glu was short for glucuronides, Sul was short for sulfates, CTR was short for control.

6.4.2. Excretions of wogonin glucuronides in engineered MDCKII-BCRP and –MRP2 cells

The hypothesis that the two players in the interplay worked interdependently was supported by the evidence that the inhibition of BCRP could cause less glucuronidation activity of UGT1A9 for some flavonoids in the engineered HeLa cells. To lend more support to above hypothesis, MDCKII cells overexpressing either BCRP or MRP2 with transient transfection of *UGT1A9* were used instead of the engineered HeLa cells with transient transfection of *BCRP or MRP2* due to the unsuccessful establishment of the latter cell line. In the two engineered MDCKII series cells, we may investigate the interplay between UGT1A9 and one efflux transporter (either BCRP or MRP2) under the condition that the efflux transporter was overexpressed. Wogonin was selected exclusively to treat the engineered MDCKII series cells, since these cells had negligible phase II metabolism without transfection with *UGT1A9*. The results (Fig. 24) showed that compared to engineered MDCKII-WT cells, the excretion rates of wogonin glucuronides were increased by 2.2 and 1.3 folds in the engineered MDCKII-MRP2 and –BCRP cells, respectively. The same trend was observed for accumulating glucuronides inside cells and f_{met}. The cellular glucuronides in engineered MDCKII-MRP2 and –BCRP cells were 2.9 and 2.1 folds, respectively higher than that in engineered MDCKII-WT cells used as control. The values of f_{met} in the engineered MDCKII-MRP2 and –BCRP cells were raised by 2.2 and 1.2 folds, respectively higher than that of control. As for CL of glucuronides, it was not amplified significantly in the engineered MDCKII-BCRP cells but

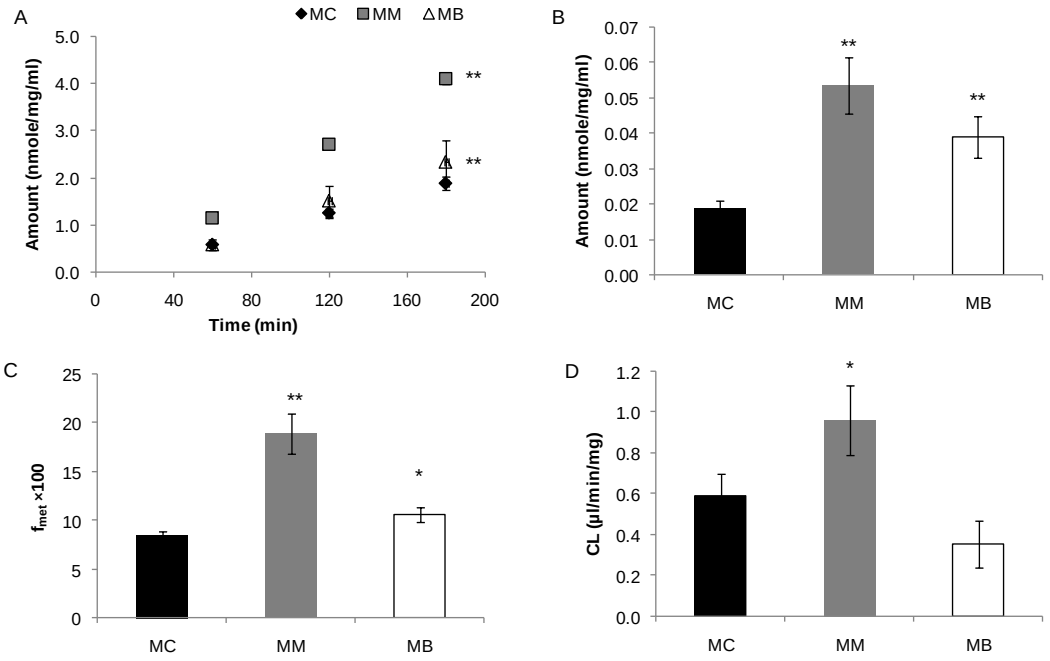

Fig. 24 Excretion of wogonin glucuronide in engineered MDCKII series cells. MDCKII-BCRP, MDCKII-MRP2 and MDCKII-WT cells (control) were transiently transfected with *UGT1A9* to form corresponding engineered cells called MB, MM and MC, respectively. These cells were incubated with wogonin (10uM). Samples (200ul) were taken at 60, 120 and 180min and the same volumes of loading solutions were added back. Each symbol represents the average of three determinations (n=3). The error bar is the standard deviation of the mean.

increased by 1.6 folds in the engineered MDCKII-MRP2 cells.

6.4.3. Selection of the specific flavonoid for pharmacokinetic study in mouse model

Accumulating data from various flavonoids suggested that engineered HeLa cells were an ideal model to study the interplay mechanism. Next, we want to see whether the conclusion reached in the engineered HeLa cell model can be confirmed in mouse model. Therefore, several criteria are used to select an appropriate flavonoid for the further interplay study in mice since it is not practical to use multiple flavonoids to do the pharmacokinetic experiment. First, the flavonoid should have a relatively faster glucuronidation rate but a slower sulfation rate; second, the flavonoid is supposed to have a slower excretion rate of glucuronide; third, the expecting flavonoid is sensitive to the inhibition of BCRP. Multiple flavonoids were screened according to above criteria (Table 3). Among all the tested flavonoids, wogonin had a faster glucuronidation rates mediated by both UGT1A9 and mouse liver s9 fraction. On the contrary, the sulfation rate of wogonin by mouse liver s9 fraction was slower than others. The excretion rate of wogonin glucuronides determined in the engineered HeLa cells was rapid and reduced to a higher extent in the presence of BCRP inhibitor.Taken together, wogonin was finally selected for the pharmacokinetic study.

Table 3 Flavonoid selection for pharmacokinetic experiment in mouse model

Flavonoids	5,7-dihydroxy	Apigenin	7-Hydroxy	Oroxylin A	Wogonin	5,4'-dihydroxy
Glucuronidation rate_1A9 (nmole/min/mg)	3.52±0.062	2.42±0.11	2.25±0.095	1.88±0.046	1.32±0.011	0.64±0.014
Glucuronidation rate_MLS9 (nmole/min/mg)	9.66±0.074	7.74±0.31	10.61±0.44	4.99±0.146	2.24±0.058	3.68±0.013
Sulfation rate_MLS9 (nmole/min/mg)	0.66±0.011	0.38±0.014	1.47±0.030	0.11±0.001	0.05±0.002	1.05±0.023
Excretion Rate (nmole/min/mg)	0. 37±0. 03	0. 26±0.00	0. 35±0. 02	0. 29±0. 02	0. 17±0. 00	0. 46±0. 06
BCRP inhibition (%)	16	20	20	24	35	21
$f_{met} \times 100$	42.24	36.2	29.88	31.13	19.39	36.98

Notes: 1A9 represents UGT1A9; MLS9 represents mouse liver s9 fraction; the excretion rate was obtained from engineered HeLa cells; BCRP inhibition was resulting from Ko143 (5μM).

6.4.4. Mass chromatograms and spectrums of wogonin and its phase II metabolites

A specific method to determine the blood concentrations of wogonin and its phase II metabolites (glucuronides and sulfates) was established. To achieve the highest sensitivity, wogonin and its glucuronides were detected at positive ion mode whereas sulfates were detected at negative ion mode. The typical mass chromatograms of wogonin and its phase II metabolites in mouse blood samples were shown in Fig. 25. The formononetin was used as internal standards (I.S.) because of its high sensitivity under both positive and negative ion modes.

Wogonin and its phase II metabolites were then confirmed by mass spectrums shown in Fig. 26. , which included both single-stage and MS2 full scans. It indicated that wogonin had the ion $[M-H]^+$ at m/z 285, which subsequently split into $[M-H]^+$ at m/z 270. Wogonin glucuronides had the pseudomolecular ion $[M-H]^+$at m/z 461, which was 176Da higher (characteristic of the addition of glucuronic acid) than that of wogonin under positive mode, whose pseudomolecular ion was at m/z 285. Similarly, wogonin sulfates had the psedomolecular ion $[M-H]^-$ at m/z 383, which was 80Da higher (characteristic of the addition of a sulfate) than that of wogonin under negative mode, whose pseudomolecular ion was at m/z 283.

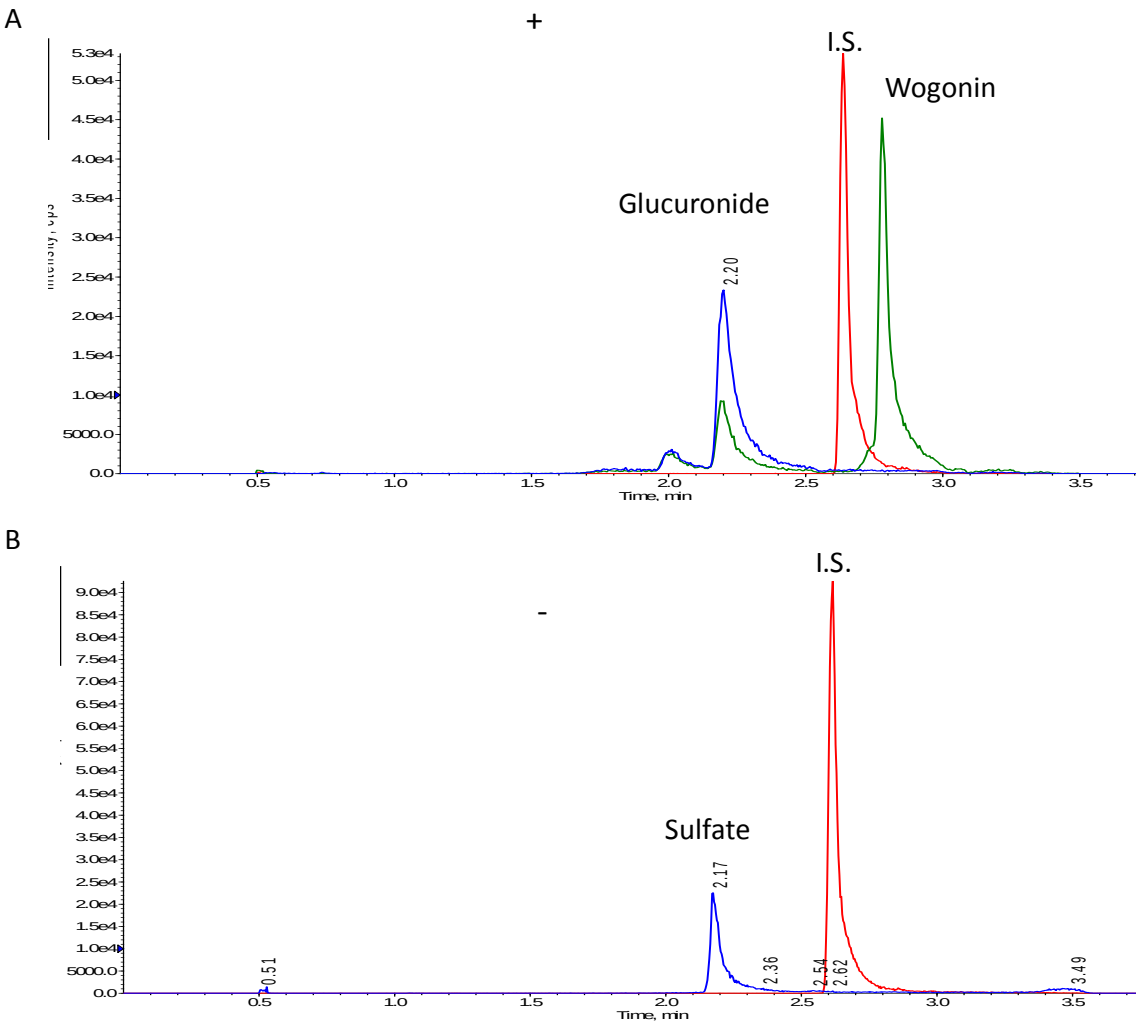

Fig. 25 UPLC-MS/MS chromatograms of wogonin and its phase II metabolites. Panel A was the chromatograms of wogonin and its glucuronides under positive mode; while Panel B was the chromatograms of wognin sulfate under negative mode. The I.S. was short for internal standard.

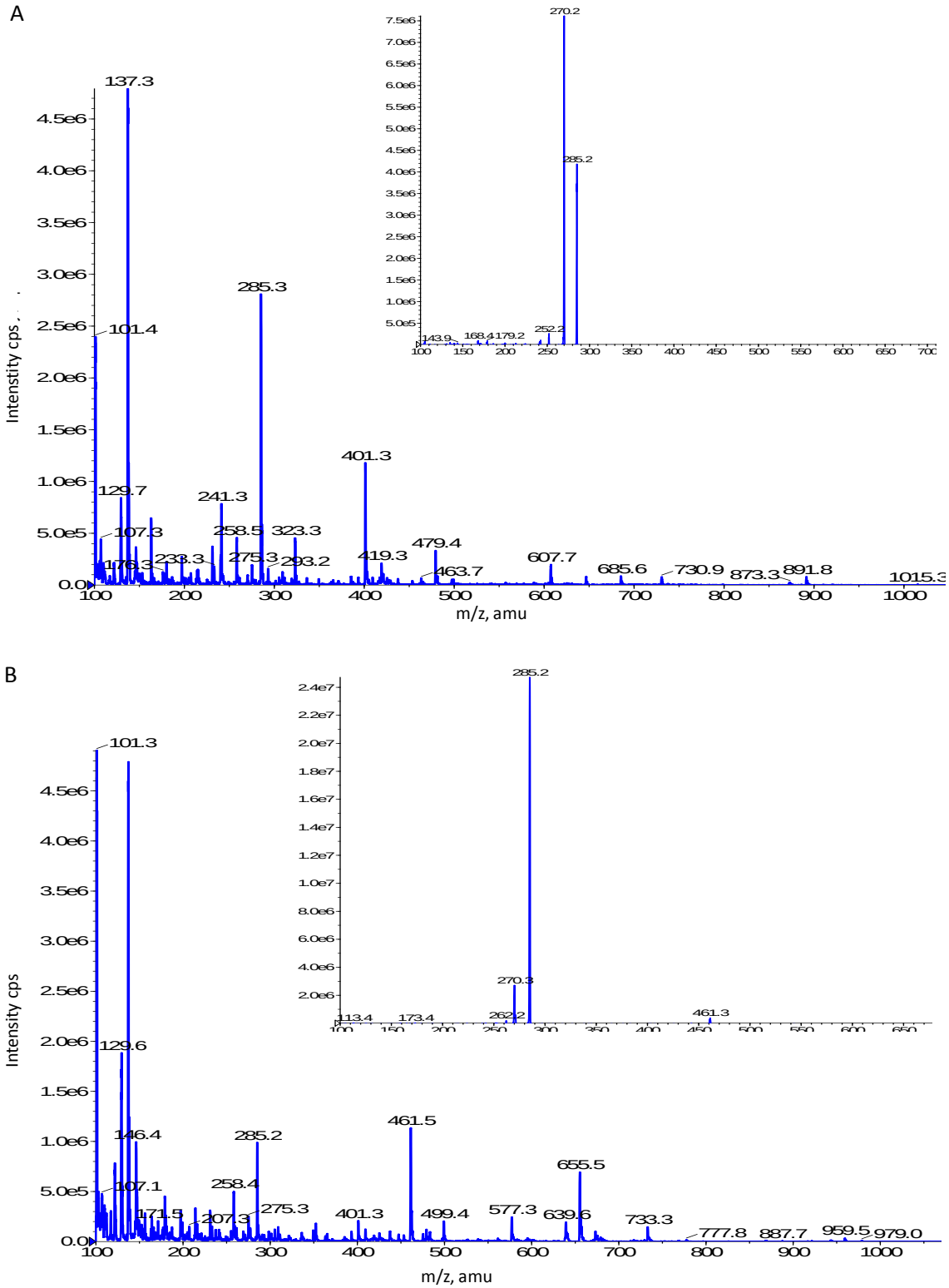
A
Intenstity cps
m/z, amu
137.3
101.4
285.3
401.3
129.7
241.3
107.3
258.5
323.3
479.4
419.3
607.7
685.6
730.9
873.3
891.8
1015.3
270.2
285.2
B
Intensity cps
m/z, amu
101.3
129.6
146.4
285.2
461.5
107.1
258.4
655.5
275.3
401.3
499.4
577.3
639.6
733.3
777.8
887.7
959.5
979.0
270.3
461.3

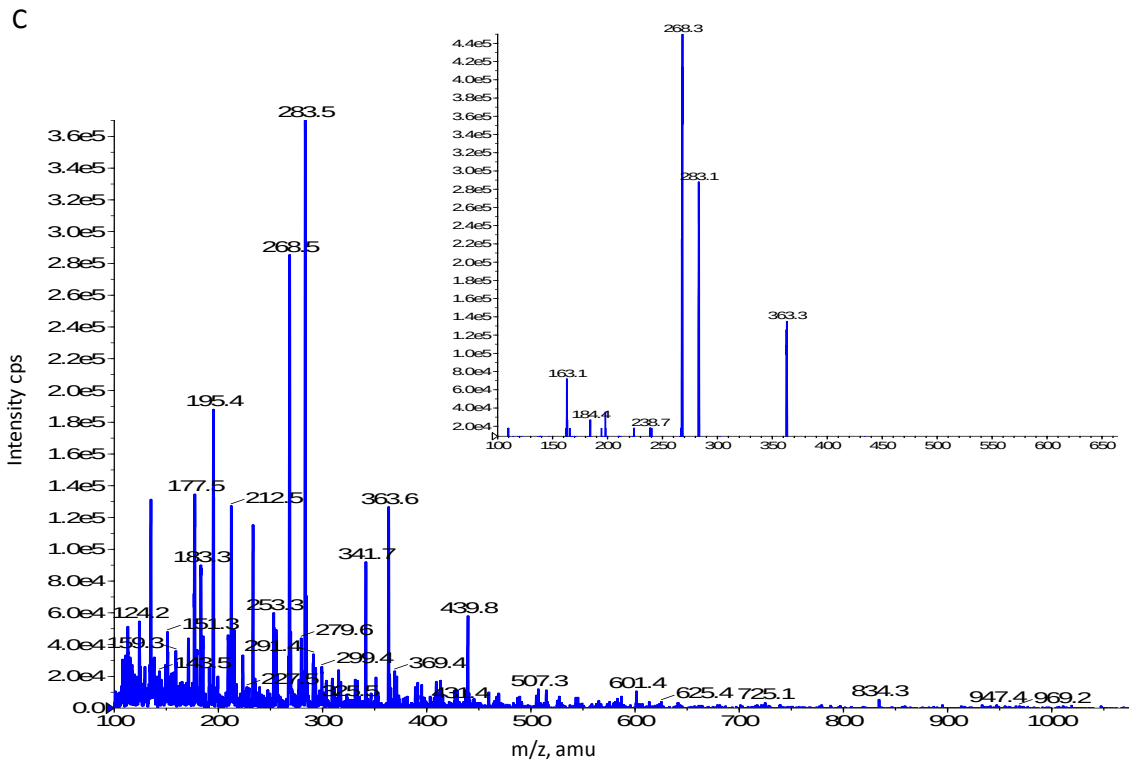

Fig. 26 Mass spectra of wogonin and its phase II metabolites. Panel A was the full scan spectra of wogonin; Panel B and C were the full scan spectra of wogonin glucuronide and sulfate, respectively. The big window was the Q1 scan and the small window was the MS2 scan.

6.4.5. Role of Bcrp in disposition of wogonin in mice

To finally test our hypothesis that the bioavailability of flavonoids can be improved experimentally by disrupting the main players in the interplay between UGTs and BCRP, Bcrp (-/-) mice, which totally lost the function of Bcrp by gene disruption, and wild type FVB mice were given wogonin at dose of 20mg/kg by oral administration. It was found that the blood concentrations of wogonin and its phase II metabolites were all considerably increased in the Bcrp (-/-) mice (Fig. 27). The concentration ratio of phase II metabolites over wogonin was slightly increased in the Bcrp (-/-) mice. Further analysis indicated that the $AUC_{0\text{-}480min}$ of wogonin was 10 folds higher in Bcrp (-/-) mice than that in wild type mice. The $AUC_{0\text{-}480min}$ of glucuronides and sulfates were all improved by similar folds in Bcrp (-/-) mice. The significant improvement of wogonin AUC in *Bcrp* gene knockout mice suggested that the bioavailability of flavonoids could be improved experimentally by maximally impairing the function of BCRP as one main player in the interplay.

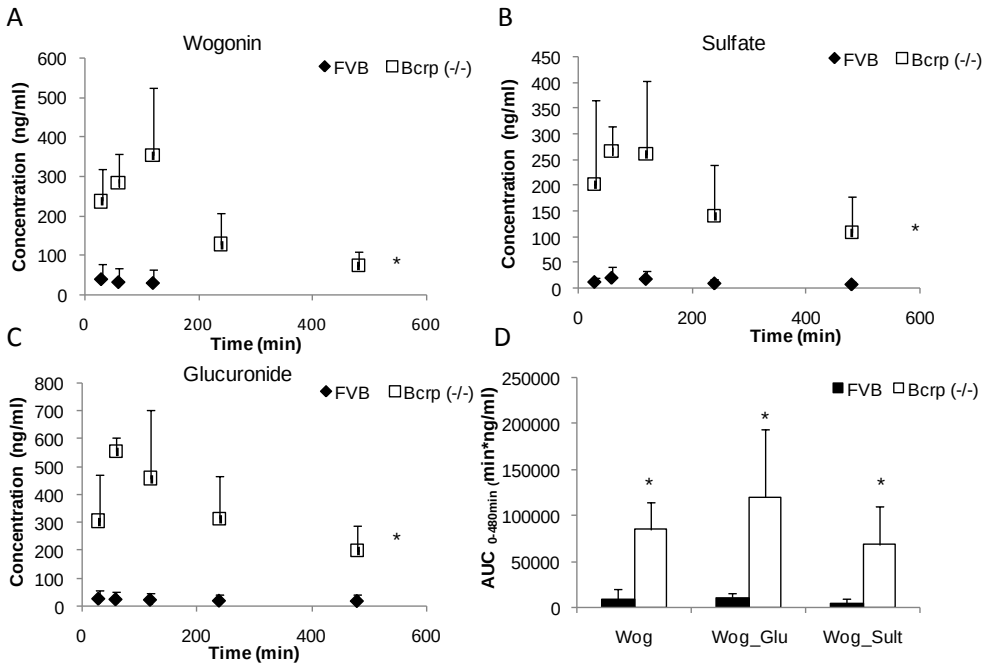

Fig. 27 Blood concentrations and $AUC_{0\text{-}480min}$ of wogonin and its phase II metabolites in FVB and Bcrp (-/-) mice. Each symbol represents the average of four determinations (n=4). The error bar is the standard deviation of the mean. P<0.05, *.

6.5. Discussion

Engineered HeLa cells are an appropriate model to study the mechanism of simplest interplay between UGT1A9 and BCRP in disposition of flavonoids. The hypothesis that the function of efflux transporters can control the glucuronidation activity was supported not only in the enginnered HeLa cells, but also in the engineered MDCKII series cells (Fig. 24). However, it was not the case in the Caco-2 cells model, where the inhibition of BCRP could only affect the distribution of sulfates between apical and basolateral side but not affect the phase II metabolism (Fig. 21,Fig. 22 and Fig. 23). In addition to cell models, it is very important for us to show the considerable wogonin AUC improvement in Bcrp(-/-) mice (Fig. 27). This finding might be attributed to the reduction of phase II metabolism of wogonin arising from the complete inhibition of Bcrp.

It appeared that efflux transporters worked cooperatively with UGT1A9 in the disposition of wogonin. In the engineered HeLa cells, the impaired functional BCRP (decreasing CL attributed to Ko143) caused overexpressed UGT1A9 to metabolize less wogonin (decreasing f_{met} in the presence of Ko143); on the other hand, in the engineered MDCKII series cells (Fig. 24), the increasing functional efflux transporters due to overexpression contributed to the boost of glucuronidation activity of UGT1A9 (increasing f_{met} in the engineered MDCKII-BCRP and –MRP2 cells). It should be emphasized that such an interdependence between two players is observed only for the simplest interplay consisting of one predominant efflux transporter and one predominant UGT isoform (e.g. UGT1A9).

On the contrary to the results in the engineered HeLa cells, the dysfunctional BCRP did not have any impact on glucuronidation or sulfation of flavonoids, but changed the distribution of sulfates in Caco-2 cells due to the fact that more sulfates were excreted from basolateral side and less from apical side in the presence of Ko143 (Fig. 21, Fig. 22 and Fig. 23). Interestingly, the excreted glucuronides at both sides were not affected by the dysfunctional BCRP. Taken together, it seems that BCRP is mainly responsible for the sulfate excretion to apical side, while MRPs are mainly responsible for the glucuronide excretion. Once the function of BCRP is impaired, sulfates have to be excreted via another efflux transporter. According to the increasing sulfates at basolateral side, the efflux transporter mainly involved in compensation of sulfate transport medicated by BCRP is speculated at basolateral side. MRP2, which is located to the apical membrane of Caco-2 cells, is not believed to have enough capacity to compensate the sulfate transport. It is the first time to define such a redistribution of sulfates in the Caco-2 cells with inhibition of BCRP.

Caco-2 cells is a well-accepted cell model to study drug absorption and metabolism. As a popular model, it has several advantages: first, this cell line can be used to study vectorial transport of drug due to its polarity; second, it contains plenty of phase II enzymes and various transporters, which is close to the physiological condition in human. However, there is one weakness of this cell model: the expression ratio of BCRP to MRP2 is reversely to that in the heptocytes and enterocytes [93-94]. Normally, BCRP is expressed more than MRP2 in liver and intestines. Therefore, the contribution of BCRP may be under-

evaluated in Caco-2 cells. In comparison, the predominant expression of BCRP in engineered HeLa cells makes it more mimic the expression pattern in liver and intestines. Hence, the engineered HeLa cells have another advantage over Caco-2 cells for investigation of interplay between UGTs and BCRP in disposition of flavonoids.

It was very exciting to see the substantial improvement of AUC of wogonin in Bcrp (-/-) mice. This lent the strongest support to our hypothesis that the bioavailability of flavonoids could be improved experimentally by disrupting the main players in the interplay between UGTs and BCRP. Furthermore, this result was consistent with the findings in the engineered HeLa cells that f_{met} value, which was an indicator of glucuronidation activity, was reduced with the inhibition of BCRP. From interplay point of view, we assumed that the reduction of phase II metabolism resulting from complete loss of Bcrp was one of the reasons that accounted for the AUC improvement of wogonin. Interestingly, the AUC of wogonin glucuronides or sulfates was also increased to a similar degree to wogonin. It seemed that blocking function of Bcrp on the apical membrane, the phase II metabolites were more likely to enter the blood circulation via other transporters on the basolateral membrane. Therefore, the preferring distribution of phase II metabolites in circulation system may explain their AUC improvements. In fact, it was not the first time to see such AUC improvements for both parent compound and phase II metabolites. Previous study on genistein in Bcrp (-/-) mice also indicated the similar results. However, the AUC improvement for genistein (about 5 folds) was not as much as that for wogonin (10 folds).

Since wogonin, compared to genistein, has a rapid glucuronidation rate and a slow excretion rate, we speculate that the bioavailabioity of those flavonoids belonging to the same category as wogonin according to our classification system, would be more readily improved via BCRP inhibition.

In conclusion, the kinetic intperlay in flavonoid disposition observed in engineered HeLa cells was confirmed in the engineered MDCKII series cells.In addition, the results that impaired BCRP caused reducing glucuornidation activity from engineered HeLa cells were consistent with the AUC improvement of wogonin in Bcrp knockout mice. However, inhibition of BCRP could only cause the redistribution of flavonoid sulfates in Caco-2 cells. We believe that the usage of engineered HeLa cells in studying kinetic interplay will assist us to predict the AUC improvement of flavonoids in vivo.

CHAPTER 7: ENGINEERED HELA CELLS ARE A NOVEL TOOL TO DETERMINE THE KINETICS PARAMETERS OF GLUCURONIDES EFFLUX BY BCRP

7.1. Abstract

The purpose of this study was to broaden the applications of the engineered HeLa cells to determine the kinetics parameters of glucuronide efflux by BCRP. Selected substrates (e.g. mono-hydroxyflavones and wogonin) at a series of loading concentrations were incubated with engineered HeLa cells stably overexpressing UGT1A9. The glucuronide excretion rates were calculated as slopes of amounts excreted v.s. time curves. The intracellular glucuronides were also determined to calculate the cellular concentrations of glucuronides. Kinetic profiles (intracellular concentrations v.s. excretion rates) were analyzed and fitted to various kinetics models to identify the best fit model and to determine the kinetics parameters (e.g. K_m and V_{max}). The kinetics parameters were then compared with those obtained by using BCRP-overexpressing vesicles originated from insect cell membranes. Results indicated that in the engineered HeLa cells, glucuronides of mono-hydroxyflavones were transported by BCRP following a classical Michaelis-Menten profile; whereas wogonin glucuronides were transported by BCRP following a substrate inhibition profile. Futhermore, the K_m' values of glucuronides mediated by BCRP obtained in the engineered HeLa cells had a relatively good correlation with those obtained using the vesicles. However, the correlations of V_{max} and CL_{int} ($=V_{max}/K_m$) were not as good as K_m', mostly likely due to different expression levels of the BCRP in these two models. Using the good correlation in K_m' values as the criterion, engineered

HeLa cells appear to be a novel tool to determine the kinetics parameters of glucuronides transported by BCRP. This proposed method has an advantage over the traditional method (of using membrane) vesicles in that the preparation of purified glucuronides is no longer necessary, which substantially reduce the time and effort necessary to carry out such studies.

Keywords: engineered HeLa cells, BCRP, efflux, kinetics parameters, glucuronides, mono-hydroxflavone

7.2. Introduction

BCRP, also called ABCG2, is a member of ATP-binding cassette (ABC) transporter. As an efflux transporter, BCRP is able to move the cellular substrates out of the cells with the expenditure of ATP. It is expressed in the apical membrane of the polarized cells and widely distributed in both normal and tumor tissues in humans [92]. A growing body of xenobiotics and their metabolites were reported to be the substrates of BCRP, including flavonoids and their phase II metabolites (glucuronides and sulfates) [31, 98]. More and more evidence revealed that the drug resistance mediated by BCRP is one of the leading reasons that cause the low bioavailability of clinical drugs [187-189], which is further translated to the lack of therapeutic efficacy. Therefore, it is very important to identify critical structural features that will make the substrates less likely to be excreted by BCRP.

To characterize the substrate interactions with BCRP, the efflux kinetics of substrates is the focus. Currently, the popular method to determine the kinetics parameters of a substrate transported by the specific efflux transporter is dependent on the vesicles, which is prepared from insect membrane and carries a particular efflux transporter. For easily obtained substrates of BCRP, this vesicle-dependent method is acceptable. However, if the substrate of BCRP is hard to obtain (e.g. glucuronides of xenobiotics), using the traditional vesicle to determine the kinetics will be extremely time and labor-consuming. As a matter of fact, few papers reported the efflux kinetics of glucuronides mediated by BCRP [185].

Engineered HeLa cells, which were stably transfected with *UGT1A9*, were developed and characterized in order to study the mechanism of interplay between UGTs and efflux transporters in the flavonoid disposition. In the engineered HeLa cells, BCRP was predominantly expressed and primarily facilitated the excretion of glucuronides metabolized by overexpressed UGT1A9. In other words, loading flavonoids can passively diffuse into the engineered HeLa cells and converted to corresponding glucuronides, which are subsequently excreted by BCRP. This promoted us to use the engineered HeLa cells as a novel tool to determine the kinetics of glucuronides mediated by BCRP without preparation of glucuronides, since the intracullar glucuronides could be adjusted by different loading concentrations of parent compounds.

Several model flavonoids, primarily consisting of all the commercially available mono-hydroxyflavones, were selected to try the novel method, since they can be converted by UGT1A9 to one predominant glucuronide at specific position in the engineered HeLa cells. In addition, the kinetics data obtained from vesicles were also available for the glucuronides of those flavonoids. Hence, it is ready to compare the kinetics parameters of glucuronides from engineered HeLa cells to those from vesicles, and finally set up the correlations of kinetics parameters from different methods.

In a word, the purpose of the present study was to apply the engineered HeLa cells, which were originally developed to study interplay mechanism in disposition of flavonoids, to determine the kinetics parameters of flavonoid glucuronides effluxed by BCRP. From this standpoint, the selected flavonoids at different

concentrations will be incubated with the engineered HeLa cells to get the different concentrations of intracellular glucuronides. The kinetics parameters will be calculated according to the excretion rates and cellular concentration of glucuronides. Compared to the kinetics data from vesicle method, the correlation can be established to help us find an appropriate kinetics parameter, which is more reliable to use in the engineered HeLa cells. It is expected that engineered HeLa cells will provide us a rapid and easy way to determine the kinetics parameters of glucuronides transported by BCRP.

7.3. Materials and methods

7.3.1. Materials

Engineered HeLa cells were established and characterized (Chapter 4). All the tested flavonoids were purchased from Indofine Chemical Company. All other chemicals and solvents were of analytical grade or better.

7.3.2. Cell cultures

Briefly, engineered HeLa cells were seeded on the 6-well plates at the density of 20,000 cells/well, and maintained at 37ºC under 5% CO_2 in DMEM supplemented with 10% FBS. Cells are ready for experiment on the third day after seeding.

7.3.3. Excretion experiments

Before experiments were started, the engineered HeLa cells were washed twice with pre-warmed (37°C) HBSS buffer (Hank's balanced salt solution, pH=7.4). Then the cells were incubated with a HBSS buffer containing each selected flavonoid (defined as "loading solution", 2ml/well for 6-well plates) for a predetermined time interval (40, 80 and 120min) at 37°C. In the loading solution, the proper concentration of each flavonoid (e.g. from lowest 0.625up to 25μM) diluted from 100X concentrated stock solutions in organic solvent (DMSO/Methanol=1:4).The sampling times were selected to ensure that the amounts excreted vs. time plots stay in the linear range. At each time point, 200μl of incubating media from each well was collected and the same volume of

loading solution was used to replenish each well. The collected incubating media were mixed with a “Stop Solution” consisted of 94%acetonitrile and 6% acetic acid. Supernatants were ready for UPLC analysis after centrifugation (15min at 15,000 rpm).

7.3.4. Determination of intracellular glucuronides in engineered HeLa cells

The details were described in section 3.2.4, Chapter 3.

7.3.5. Sample analysis by UPLC

The conditions for UPLC analysis of flavonoids and their glucuronides were described in section 3.3., Chapter 3. The detection wavelength for each mono-hydroxyflavone and its glucuronide was shown in Table 4.

7.3.6. Quantification of glucuronides

The conversion factors, representing the molar extinction coefficient ratio of glucuronides to aglycones, were used to quantify the amounts of flavonoids and flavonoid glucuronides as described in section 3.3.3, Chapter 3. The conversion factors were shown in Table 4

Table 4 The conversion factors (K) of molar extinction coefficients of glucuronides to their corresponding aglycone.

	2'HF	3HF	3'HF	4'HF	5HF	6HF	7HF
λmax (nm)	308	300	300	317	269	304	307
K	1.21±0.041	1.62±0.077	1.23±0.020	1.07±0.0331	1.04±0.0249	1.25±0.023	1.37±0.0634

7.3.7. Determination of whole protein concentrations

After excretion experiments, engineered HeLa cells were washed with ice-cold HBSS buffer twice and dissolved into 0.1N NaOH solution containing 0.1% Triton for overnight. The next day, the whole protein concentration was determined by BCA assay (Pierce Biotechnology, Rockford, IL).

7.3.8. Kinetics study of BCRP-mediated glucuronide transportation

Excretion rates of glucuronides were expressed as amounts of glucuronides excreted/min/mg protein (nmole/min/mg). If the Eadie-Hofstee plot was linear, excretion rates (J) of flavonoid glucuronides at various cellular concentrations of glucuronides (C_i) were fit to the standard Michaelis-Menten equation:

$$J = \frac{J_{max} C_i}{K_m' + C_i} \quad (1)$$

where K_m' represents the Michaelis constant of BCRP and J_{max} represents the maximum excretion rate of glucuronides. If Eadie-Hofstee plots showed characteristic profiles of atypical kinetics such as substrate inhibition,

autoactivation and biphasic kinetics [169-170], the data were fit to other corresponding equations using Excel program [171]. The best-fit model was determined based on Akaike's information criterion (AIC) [172] and the rule of parsimony was applied.

7.3.9. Statistical analysis

All the experiments were done in duplicates or triplicates and data were analyzed by one-way ANOVA or student's t-test as appropriate and the level of significance was set at $p<0.05$ or $p<0.01$.

7.4. Results and discussion

7.4.1. Chromatograms comparison of glucuronide excretion in wild and engineered HeLa cells

All commercially available mono-hydroxyflavones (MHF) (structures shown in Fig. 28), including 2'-hydroxyflavone (2'-HF), 3-hydroxyflavone (3HF), 3'-hydroxyflavone (3'-HF), 4'-hydroxyflavone (4'HF), 5-hydroxyflavone (5HF), 6-hydroxyflavone (6HF) and 7-hydroxyflavone (7HF) were incubated with engineered or wild type HeLa cells at low (2.5μM), middle (5μM) and high (20μM) concentrations for up to 2 hours. The typical chromatograms at 5μM were shown in Fig. 29. The predominant glucuronide of each mono-hydroxyflavone was observed only when incubating with engineered HeLa cells but not with wild type HeLa cells. The authenticity of the glucuronides was demonstrated using UPLC-MS/MS.

7.4.2. Determination of kinetics parameters in engineered HeLa cells

The kinetics profiles of BCRP-transported glucuronides were determined by using engineered HeLa cells (Fig. 30). The corresponding kinetics parameters were summarized in Table 5A. It seemed that all the MHF-glucuronides (MHF-Glu) transported by BCRP followed the Michaelis-Menten profile, which was the same as that from vesicles overexpressing BCRP, though the goodness of fit for each MHF-Glu was different. It appeared that 3'HF-Glu, 4'HF-Glu and 5-Glu did not fit the model as well as others. Unlike MHF-Glu, BCRP-transported

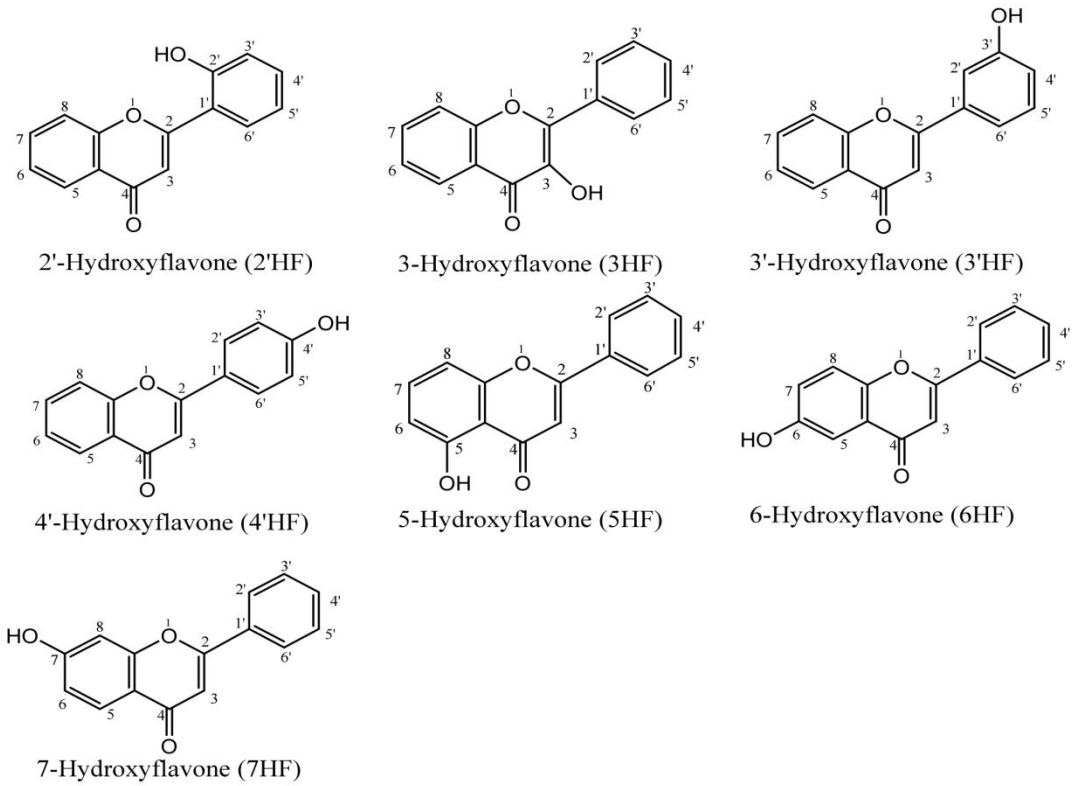

Fig. 28 Chemical structures of mono-hydroxyflavones (MHF)

A

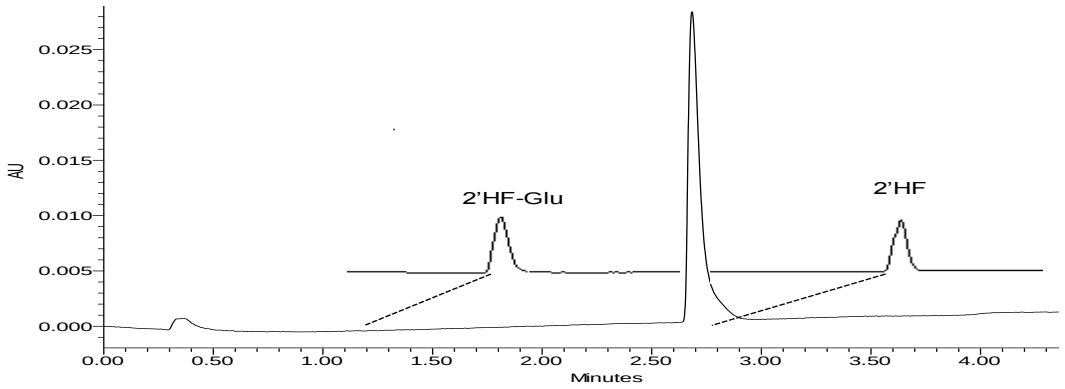
AU
0.025
0.020
0.015
0.010
0.005
0.000
2'HF-Glu
2'HF
0.00
0.50
1.00
1.50
2.00
2.50
3.00
3.50
4.00
Minutes

B

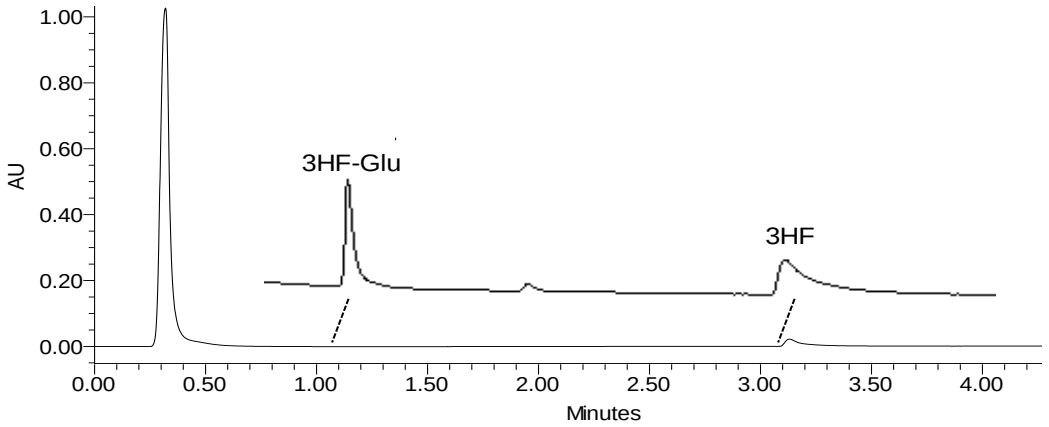
AU
1.00
0.80
0.60
0.40
0.20
0.00
3HF-Glu
3HF
0.00
0.50
1.00
1.50
2.00
2.50
3.00
3.50
4.00
Minutes

C

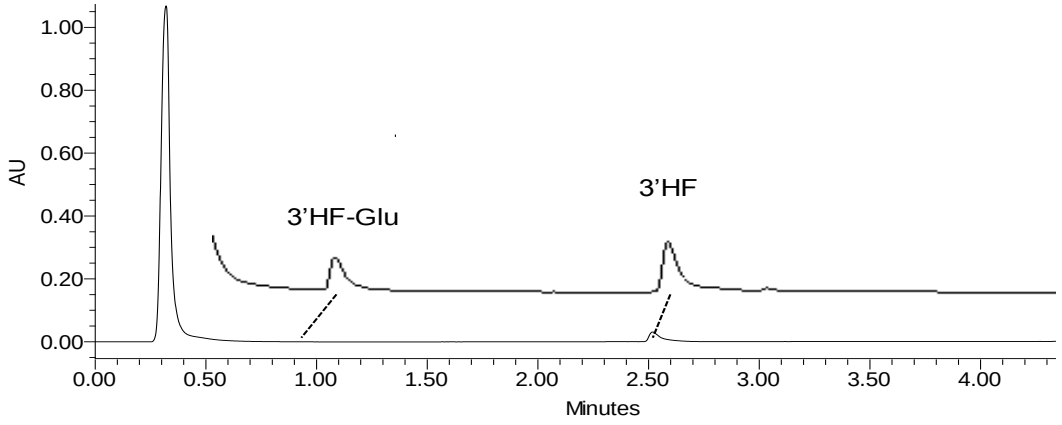
AU
1.00
0.80
0.60
0.40
0.20
0.00
3'HF-Glu
3'HF
0.00
0.50
1.00
1.50
2.00
2.50
3.00
3.50
4.00
Minutes

D

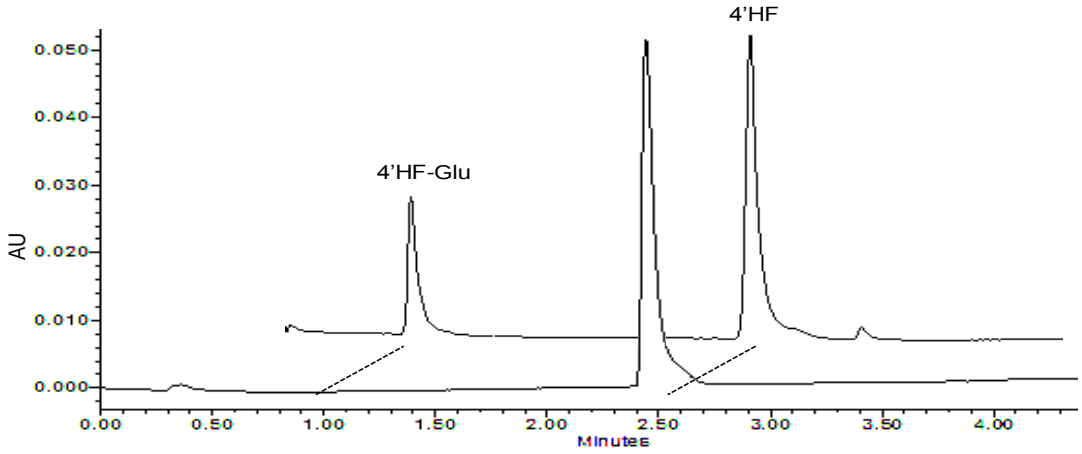
4'HF
4'HF-Glu
AU
0.050
0.040
0.030
0.020
0.010
0.000
0.00
0.50
1.00
1.50
2.00
2.50
3.00
3.50
4.00
Minutes

E

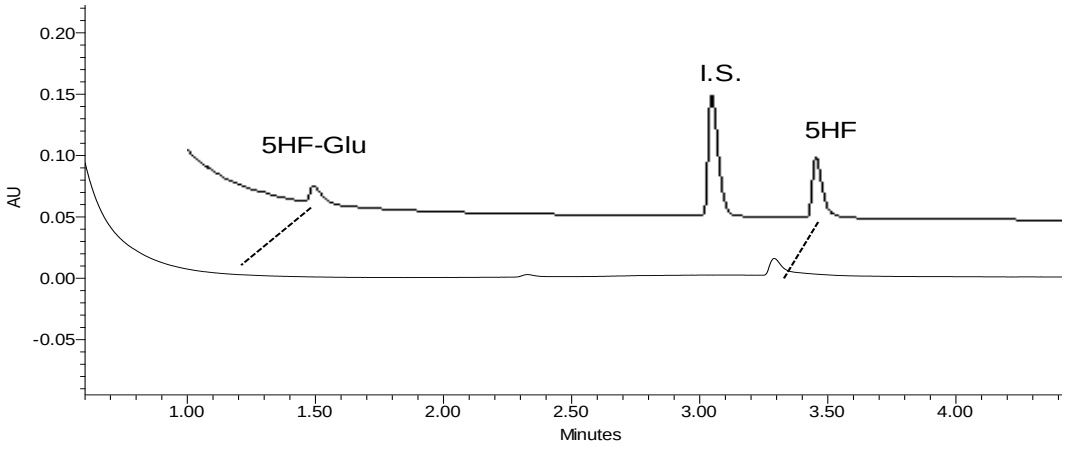
I.S.
5HF
5HF-Glu
AU
0.20
0.15
0.10
0.05
0.00
-0.05
1.00
1.50
2.00
2.50
3.00
3.50
4.00
Minutes

F

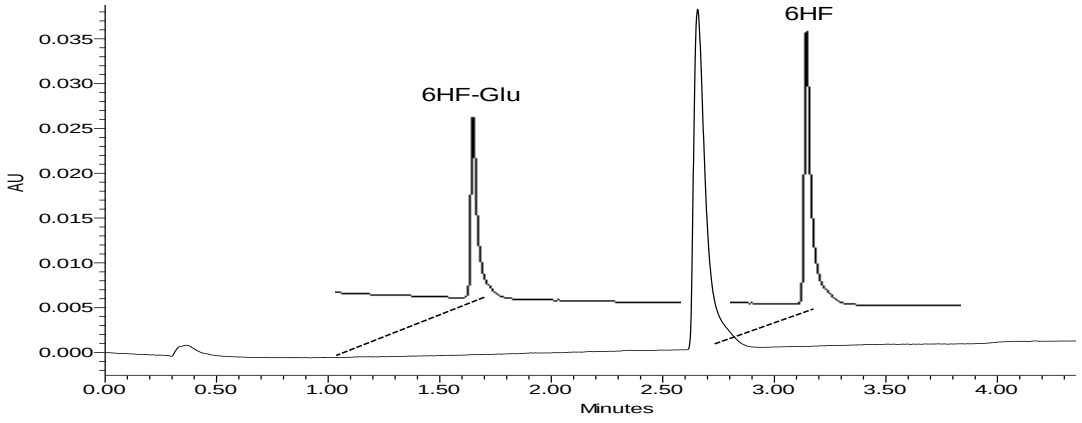
6HF
6HF-Glu
AU
0.035
0.030
0.025
0.020
0.015
0.010
0.005
0.000
0.00
0.50
1.00
1.50
2.00
2.50
3.00
3.50
4.00
Minutes

G

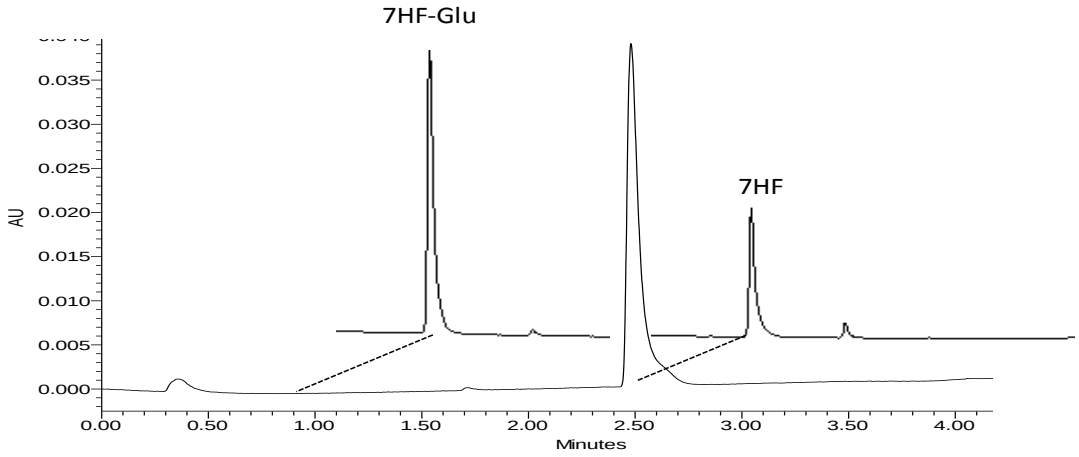

Fig. 29 UPLC chromatograms of mono-hydroxyflavones (MHF) and their respective glucuronides (A-G). Wild type or engineered HeLa cells were incubated with each MHF at 5μM for 2 hours. The profile witout the glucuronide was derived from the wild type HeLa cells whereas the profile with the glucuronide was from the engineered HeLa cells. Glu was short for glucuronide. n=2. I.S. was short for internal standard.

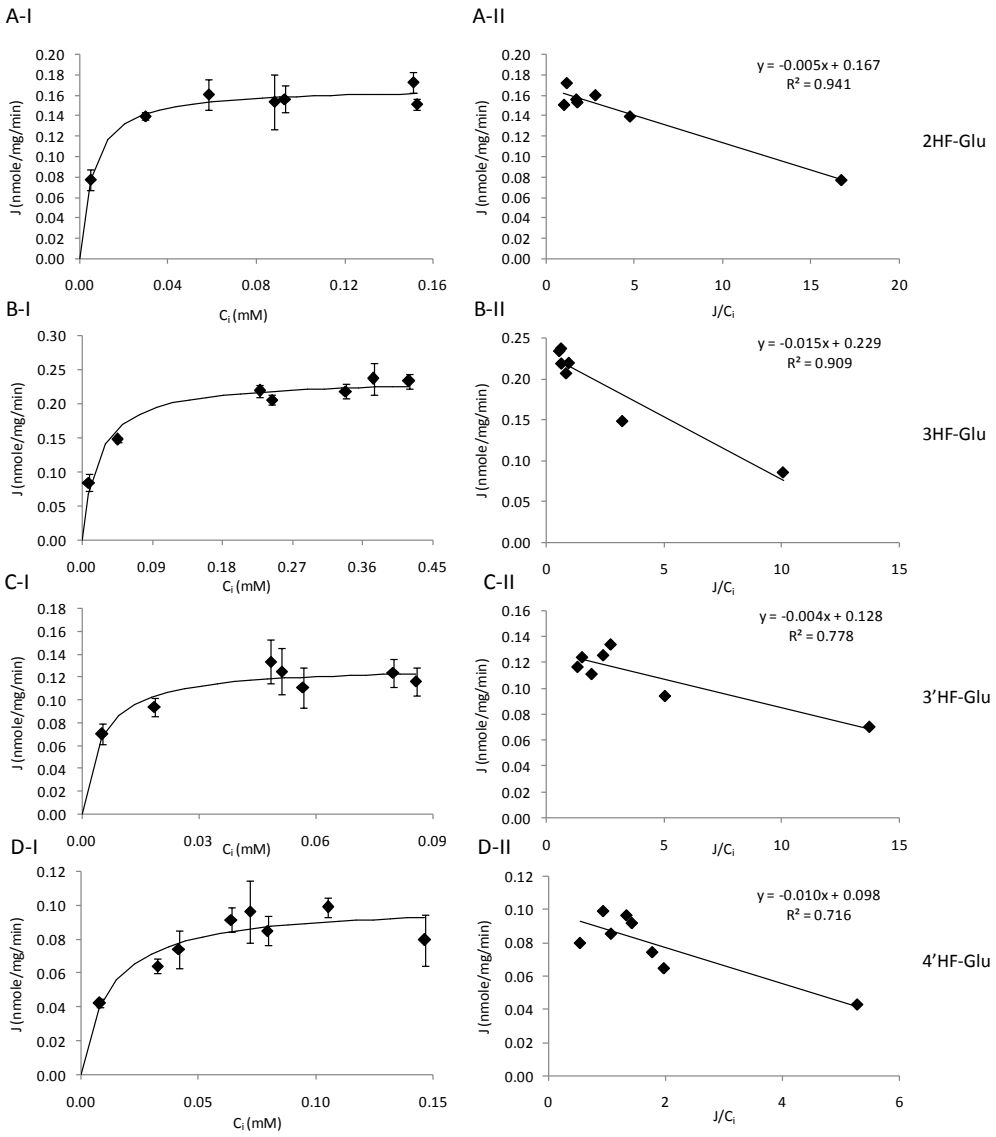
A-I
A-II
y = -0.005x + 0.167
R² = 0.941
2HF-Glu
B-I
B-II
y = -0.015x + 0.229
R² = 0.909
3HF-Glu
C-I
C-II
y = -0.004x + 0.128
R² = 0.778
3'HF-Glu
D-I
D-II
y = -0.010x + 0.098
R² = 0.716
4'HF-Glu
J (nmole/mg/min)
Ci (mM)
J/Ci

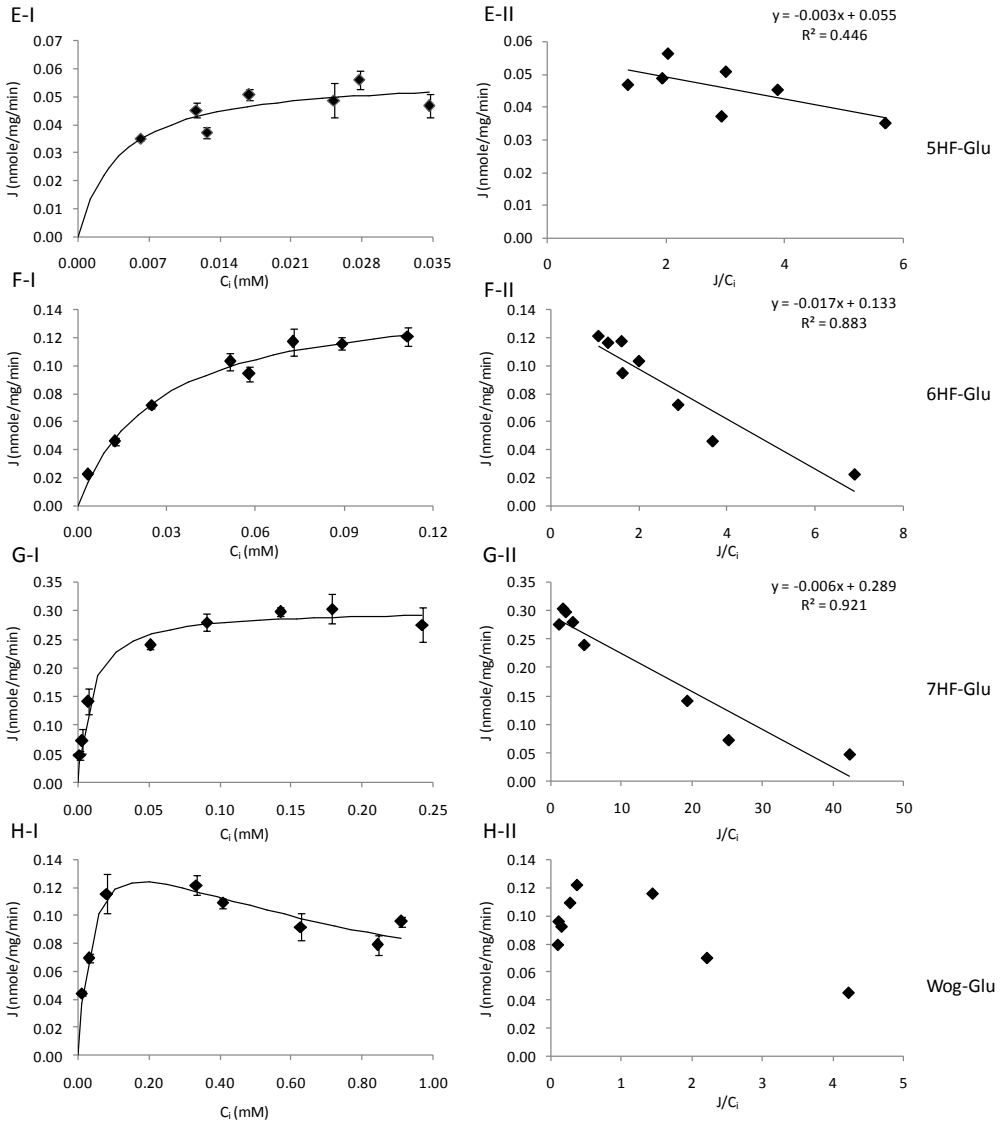

Fig. 30 Determination of kinetics parameters of glucuronides (Glu) in the engineered HeLa cells. The kinetics of each MHF-glucuronide was shown in panel I (A, 2'HF-Glu; B, 3HF-Glu; C, 3'HF-Glu; D, 4'HF-Glu; E, 5HF-Glu; F, 6HF-Glu; G, 7HF-Glu; H, Wogonin-Glu), whereas the related Eadie-Hofstee plot was shown in panel II. In Panel I, the X-axis was the intracellular concentration of glucuronides (symbolized as C_i); the Y-axis was the glucuronide excretion rates (symbolized as J). In Panel II, the X-axis was the ratio of glucuronide excretion rate over cellular concentration of glucuronides. Each data point was the average of three determinations (n=3) with error bars representing the standard deviation of the mean.

Table 5a Apparent kinetics parameters of glucuronides efflux by BCRP in engineered HeLa cells

Substrates	K_m' (μM)	J_{max} (nmole/min/mg)	CL_{int} (μl/min/mg)	K_s (μM)	AIC	R^2
2'HF-Glu	5.37	0.168	31.2	-	-52.57	0.95
3HF-Glu	20.6	0.237	11.5	-	-45.19	0.95
3'HF-Glu	4.75	0.130	27.4	-	-49.20	0.82
4'HF-Glu	12.2	0.100	8.20	-	-56.64	0.79
5HF-Glu	4.04	0.058	14.3	-	-58.86	0.62
6HF-Glu	26.9	0.151	5.61	-	-65.06	0.98
7HF-Glu	8.60	0.302	35.1	-	-49.90	0.98
Wog-Glu	39.4	0.177	4.49	837	-56.49	0.91
4MU-Glu*	27.0	0.104	3.85	-	-	-

Table 5b Apparent kinetics parameters of glucuronides efflux by BCRP in vesicles *

Substrates	K_m' (μM)	J_{max} (nmole/min/mg)	CL_{int} (μl/min/mg)
2'HF-Glu	5.00	1.16	233
3HF-Glu	29.0	4.02	139
3'HF-Glu	18.0	4.80	263
4'HF-Glu	16.0	4.04	257
5HF-Glu	2.80	1.58	562
6HF-Glu	5.60	1.78	313
7HF-Glu	12.0	1.74	144
Wog-Glu	75.0	3.72	49.6
4MU-Glu	24.0	0.79	33.0

Note: CL equals J_{max} over K_m'; the data marked with * were obtained from Baojian; 4MU-Glu was short for 4-methylumbelliferone glucuronides; wog-Glu was short for wogonin glucuronides, HF-Glu was short for glucuronides of hydroxyflavone.

glucuronides of wogonin followed substrate inhibition profile. This was different from kinetics profile (Michaelis-Menten) obtained by using vesicles.

Moreover, 3HF-Glu, 6HF-Glu, 4'-Glu and 7-Glu had relatively higher K_m' values (Table 5A) than the other mono-hydroxyflavone glucuronides, clearly suggesting glucuronides at 3, 6, 4' and 7 position had a weaker affinity to BCRP. Oppositely, 5HF-Glu appeared to have the strongest affinity to BCRP since it had the lowest K_m' value among all the glucuronides.Therefore, BCRP had a structural preference for glucuronides at different positions. We speculate that glucuronide (the hydrophilic group) was most favored by BCRP at 5 position and least favored at 6, 3 and 4' position. This structural preference of BCRP for glucuronides was consistent with the structural preference of BCRP for flavonoids. It suggested that the presence of a 2, 3-double bond in ring C, ring B attached at position 2, hydroxylation at position 5, lack of hydroxylation at position 3 and hydrophobic substitution at positions 6, 7, 8 or 4', were important structural properties for potent flavonoid–BCRP interaction [98]. This is for the first time to directly prove the glucuronide structural preference of BCRP.

7.4.3. Correlation of kinetics parameters obtained from different method

Three kinetics parameters (K_m', J_{max} and CL_{int}) derived from engineered HeLa cells were correlated with those from vesicles (Fig. 31). It seemed that K_m' had a better correlation than the other two parameters. For correlation of J_{max} or CL_{int}, the one from vesicles was always higher than that from the engineered HeLa

cells with inconsistently large folds. It was not uncommon to see such a big difference of J_{max} or CL_{int} when they were compared from different sources. The different membrane composition and various expression levels of BCRP from mammalian and insect cells could contribute to the discrepancy. As a result, according to the better correlation, the K_m' appeared to be a reliable kinetics parameter which could be determined in engineered HeLa cells instead of in vesicles.

7.5. Conclusion

Engineered HeLa cells are a promisingly novel tool to determine the kinetics parameter- K_m' of glucuronides transported by BCRP. In addition, this novel tool might also help us to determine the structural preference of BCRP.

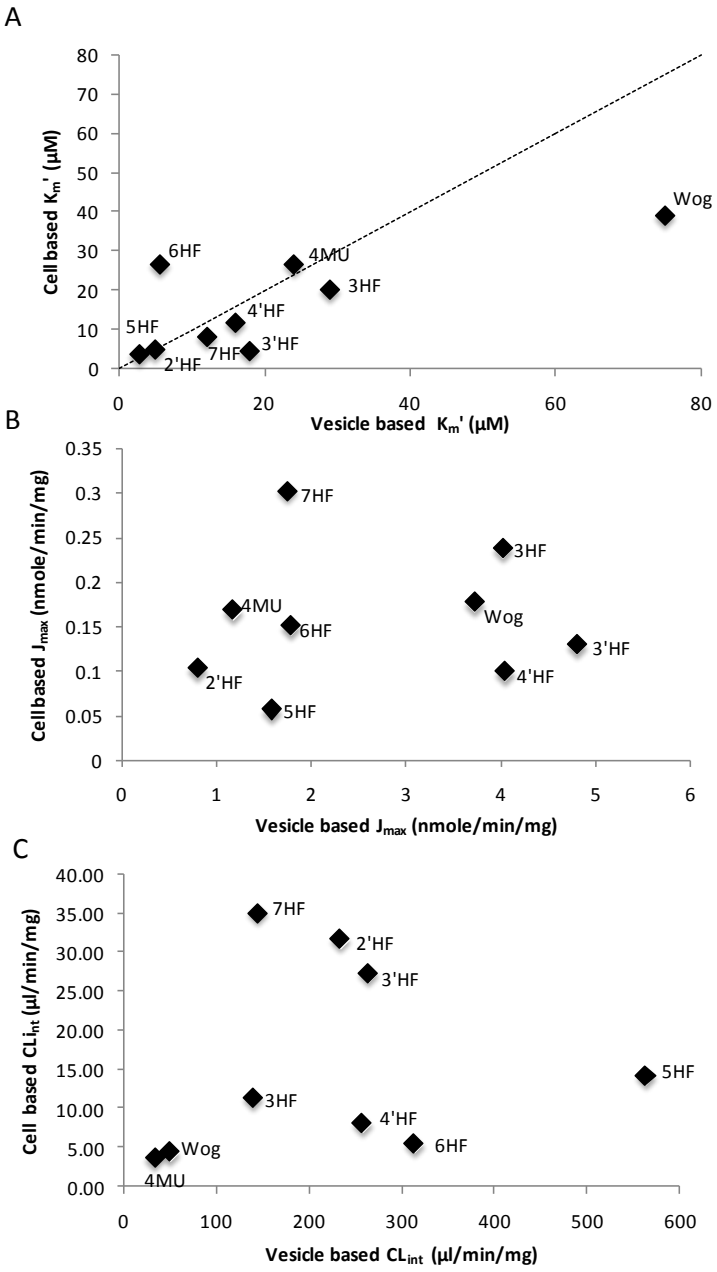

Fig. 31 The correlations of kinetics parameters of glucuronides efflux by BCRP. The kinetics parameters obtained by using vesicles were correlated with those obtained by using engineered HeLa cells, as shown in Panel A (K_m'), Panel B (J_{max}) and Panel C (CL_{int}). The symbols representing glucuronides were named simply by their respective aglycones. 4MU was short for 4-methylumbelliferone, wog was short for wogonin, HF was short for hydroxyflavone. The dotted line has a slope of 1.

CHAPTER 8: SUMMARY

The purpose of this project was to investigate the mechanisms of interplay between UGTs and efflux transporters in flavonoid disposition. Current available models contain multiple phase II enzymes (e.g. UGTs and SULTs) and various efflux transporters (e.g. MRP2 and BCRP), therefore, it is very hard to prove the interplay, as potential functional compensations usually impede the determination of the mechanism of interplay. To maximally avoid the functional compensation, we established a cell model by introduction of *UGT1A9* gene to HeLa cells, which was called engineered HeLa cells. After stably transfected cells were established and well characterized, the engineered HeLa cells were shown to express predominantly UGT1A9 and BCRP, and these two players were further demonstrated to work coordinately in the disposition of flavonoids. Thus, for the first time we have shown that there is a kinetic interplay between UGT1A9 and BCRP in flavonoid disposition in the engineered HeLa cells: the inhibition of BCRP by Ko143 could result in the reduction of glucuronidation activity of UGT1A9; on the other hand, the inhibition of glucuronidation activity toward flavonoids by siRNA could sometimes affect the function of BCRP. Furthermore, we also demonstrated that pH played a critical role in the interplay by adjusting the function of each player for the first time. Accordingly, the engineered HeLa cells are an appropriate model to study the interplay between UGT1A9 and BCRP in the disposition of flavonoids.

In addition, the flavonoid disposition mediated by the kinetic interplay was not only observed in the engineered HeLa cells but also in the engineered MDCKII-

BCRP and –MRP2 cells (the MDCKII-BCRP and MDCKII-MRP2 cells transiently transfected with *UGT1A9*). In the engineered MDCKII series cells, the highly expressed MRP2 or BCRP was linked with the higher activity of glucuronidations and intracellular glucuronides. This evidence also supported the hypothesis that efflux transporters can control the glucuronidation activity towards flavonoids. On the contrary, in the Caco-2 cells, the inhibition of BCRP by Ko143 could not lead to the reduction of phase II metabolism or to the intracellular change of phase II metabolites. The only thing affected was the distribution of flavonoid sulfates, which was excreted increasingly at basolateral side but decreasingly at apical side in the presence of Ko143.

Most importantly, results from pharmacokinetic study revealed that the AUC of wogonin was improved by 10 folds in the Bcrp (-/-) mice. It provided the evidence to support the hypothesis that the bioavailability of flavonoids could be experimentally improved by disrupting one player in the interplay. Wogonin is selected because it has a faster glucuronidation rate and slower sulfation rate as well as high sensitivity to BCRP inhibition. Therefore, it was regarded as a good model flavonoid to study the interplay between UGTs and Bcrp in the mouse model. The substantial improvement of AUC for wogonin might be explained by the reduction of glucuronidation activity in Bcrp (-/-) mice. This was consistent with the conclusion obtained from the engineered HeLa cells that the reducing glucuronidation activity of wogonin was attributed to the inhibition of BCRP. Of course, this might not be the only reason for the increase in wogonin AUC. Surprisingly, not only the AUC of wogonin was increased, but also the AUC of its

phase II metabolites including glucuronides and sulfates were improved in Bcrp (-/-) mice. The redistribution of phase II metabolites to blood circulation might be a reason to explain these phenomena.

Finally, we expanded the application of the engineered HeLa cells to determine the kinetics parameters of glucuronide efflux by BCRP. Our newly developed method of determining kinetics parameters of glucuronide efflux by BCRP has an advantage over the traditional method (that uses membrane vesicles) since the preparation of glucuronides as substrates of BCRP is no longer necessary.

Taken together, we have demonstrated the kinetic interplay between UGT1A9 and BCRP and the mechanism of their interplay on the flavonoid disposition in the engineered HeLa cells stably overexpressing UGT1A9, which might also be an appropriate tool for the determination of kinetics parameters of glucuronide efflux by BCRP. The conclusion of the kinetic interplay in the disposition of wogonin was further confirmed in the engineered MDCKII-BCRP and –MRP2 cells and Bcrp (-/-) mice. The consistent results assured us that the bioavailability of flavonoids could be improved experimentally by disrupting the main player in the interplay.

Our studies have shown that flavonoids like wogonin, which belong to the class with fast glucuronidation and slow efflux, could have improved bioavailability as long as we are able to maximally disrupting the functions of BCRP. Whereas these studies are promising, we need to identify the practical means (i.e., clinically relevant to humans) to increase the bioavailabilities of these

compounds. We also need to further validate these observations by using more compounds to determine the classification of flavonoids because a predictive model capable of determining how improvement of bioavailability could be best achieved would serve the field well.

Furthermore, the conceptual framework established from our work can be applied to future studies on other similar interplay and determine if additional future cell models that incorporate additional enzymes and/or efflux transporters can also be used as the screening tools. For example, other UGT isoforms can be introduced into HeLa cells to study different simple interplay between one UGT isoform and BCRP. The substrates could be expanded to clinical drugs such as SN-38 or mycophenolic acid. We believe that a better understanding of the kinetic interplay between UGTs and efflux transporters on the basis of our study will provide an insight for the future study on the other types of interplay and ultimately lead to the improvement of oral bioavailability of wide variety of drugs and dietary chemicals.

Besides, since our focus was on the kinetic interplay between UGTs and efflux transporters, the mechanism of interplay from molecular level was not investigated. In other words, the coregulation of UGTs and efflux transporters by the same nuclear receptors (e.g. CAR or PXR, both of which were reported to regulate UGTs and efflux transporters [112]) has not been covered yet. Considering the fact that the cells were incubated with flavonoids for short intervals (usually less than 240min), the regulation of UGTs or efflux transporters at expression levels by nuclear receptors might not be obvious because the

expression change under control of nuclear receptors usually takes a longer incubation time. Therefore, the molecular interplay via nuclear receptors in flavonoid disposition might not be as important as kinetic interplay within short time. However, in the long run, it will be meaningful and worthwhile to study the interplay at molecular level in flavonoid disposition. We believe the deeper investigation on the interplay between UGTs and efflux transporters at both kinetic and molecular levels will provide a more complete perspective to understand mechanisms of interplay.

REFERENCE

1. Busby, M.G., et al., *Clinical characteristics and pharmacokinetics of purified soy isoflavones: single-dose administration to healthy men.* Am J Clin Nutr, 2002. **75**(1): p. 126-36.
2. Bloedon, L.T., et al., *Safety and pharmacokinetics of purified soy isoflavones: single-dose administration to postmenopausal women.* Am J Clin Nutr, 2002. **76**(5): p. 1126-37.
3. Meyer, H., et al., *Bioavailability of apigenin from apiin-rich parsley in humans.* Ann Nutr Metab, 2006. **50**(3): p. 167-72.
4. Hollman, P.C., et al., *Bioavailability of the dietary antioxidant flavonol quercetin in man.* Cancer Lett, 1997. **114**(1-2): p. 139-40.
5. Chun, O.K., S.J. Chung, and W.O. Song, *Estimated dietary flavonoid intake and major food sources of U.S. adults.* J Nutr, 2007. **137**(5): p. 1244-52.
6. de Vries, J.H., et al., *Consumption of quercetin and kaempferol in free-living subjects eating a variety of diets.* Cancer Lett, 1997. **114**(1-2): p. 141-4.
7. Hertog, M.G., et al., *Intake of potentially anticarcinogenic flavonoids and their determinants in adults in The Netherlands.* Nutr Cancer, 1993. **20**(1): p. 21-9.
8. Narayana, K.R., et al., *Bioflavonoids classification, pharmacological, biochemical effects and therapeutic potential.* Indian J Pharmacol, 2001. **33**: p. 2-16.
9. Schroder, G., et al., *Flavonoid methylation: a novel 4'-O-methyltransferase from Catharanthus roseus, and evidence that partially methylated flavanones are substrates of four different flavonoid dioxygenases.* Phytochemistry, 2004. **65**(8): p. 1085-94.
10. Wong, Y.C., et al., *Structure-activity relationships of the glucuronidation of flavonoids by human glucuronosyltransferases.* Expert Opin Drug Metab Toxicol, 2009. **5**(11): p. 1399-419.
11. Chu, Y.F., et al., *Antioxidant and antiproliferative activities of common vegetables.* J Agric Food Chem, 2002. **50**(23): p. 6910-6.
12. Somerset, S.M. and L. Johannot, *Dietary flavonoid sources in Australian adults.* Nutr Cancer, 2008. **60**(4): p. 442-9.
13. Kuti, J.O. and H.B. Konuru, *Antioxidant capacity and phenolic content in leaf extracts of tree spinach (Cnidoscolus spp.).* J Agric Food Chem, 2004. **52**(1): p. 117-21.
14. Slimestad, R., T. Fossen, and I.M. Vagen, *Onions: a source of unique dietary flavonoids.* J Agric Food Chem, 2007. **55**(25): p. 10067-80.
15. Vinson, J.A., et al., *Phenol antioxidant quantity and quality in foods: fruits.* J Agric Food Chem, 2001. **49**(11): p. 5315-21.
16. Astill, C., et al., *Factors affecting the caffeine and polyphenol contents of black and green tea infusions.* J Agric Food Chem, 2001. **49**(11): p. 5340-7.

17. Harapu, C.D., et al., *[Flavonoids--bioactive compounds in fruits juice].* Rev Med Chir Soc Med Nat Iasi, 2010. **114**(4): p. 1209-14.
18. Actis-Goretta, L., et al., *Comparative study on the antioxidant capacity of wines and other plant-derived beverages.* Ann N Y Acad Sci, 2002. **957**: p. 279-83.
19. Bosetti, C., et al., *Flavonoids and breast cancer risk in Italy.* Cancer Epidemiol Biomarkers Prev, 2005. **14**(4): p. 805-8.
20. Grassi, D., et al., *Flavonoids, vascular function and cardiovascular protection.* Curr Pharm Des, 2009. **15**(10): p. 1072-84.
21. Ames, B.N., M.K. Shigenaga, and T.M. Hagen, *Oxidants, antioxidants, and the degenerative diseases of aging.* Proc Natl Acad Sci U S A, 1993. **90**(17): p. 7915-22.
22. Koga, T. and M. Meydani, *Effect of plasma metabolites of (+)-catechin and quercetin on monocyte adhesion to human aortic endothelial cells.* Am J Clin Nutr, 2001. **73**(5): p. 941-8.
23. Walle, T., *Absorption and metabolism of flavonoids.* Free Radic Biol Med, 2004. **36**(7): p. 829-37.
24. Walgren, R.A., et al., *Cellular uptake of dietary flavonoid quercetin 4'-beta-glucoside by sodium-dependent glucose transporter SGLT1.* J Pharmacol Exp Ther, 2000. **294**(3): p. 837-43.
25. Walle, T., et al., *Quercetin glucosides are completely hydrolyzed in ileostomy patients before absorption.* J Nutr, 2000. **130**(11): p. 2658-61.
26. Day, A.J., et al., *Dietary flavonoid and isoflavone glycosides are hydrolysed by the lactase site of lactase phlorizin hydrolase.* FEBS Lett, 2000. **468**(2-3): p. 166-70.
27. Day, A.J., et al., *Deglycosylation of flavonoid and isoflavonoid glycosides by human small intestine and liver beta-glucosidase activity.* FEBS Lett, 1998. **436**(1): p. 71-5.
28. Gradolatto, A., et al., *Metabolism of apigenin by rat liver phase I and phase ii enzymes and by isolated perfused rat liver.* Drug Metab Dispos, 2004. **32**(1): p. 58-65.
29. Manach, C. and J.L. Donovan, *Pharmacokinetics and metabolism of dietary flavonoids in humans.* Free Radic Res, 2004. **38**(8): p. 771-85.
30. Miranda, S.R., et al., *Hepatic metabolism and biliary excretion of silymarin flavonolignans in isolated perfused rat livers: role of multidrug resistance-associated protein 2 (Abcc2).* Drug Metab Dispos, 2008. **36**(11): p. 2219-26.
31. Zhu, W., et al., *Breast cancer resistance protein (BCRP) and sulfotransferases contribute significantly to the disposition of genistein in mouse intestine.* AAPS J, 2010. **12**(4): p. 525-36.
32. Liu, Z. and M. Hu, *Natural polyphenol disposition via coupled metabolic pathways.* Expert Opin Drug Metab Toxicol, 2007. **3**(3): p. 389-406.
33. Guengerich, F.P., ed. *Cytochrome P450: structure, mechanism, and biochemistry, Chapter 14*. second ed., ed. P.R.O.d. Montellano. 1995, Plenum Press,: New York.

34. Nebert, D.W., R.A. McKinnon, and A. Puga, *Human drug-metabolizing enzyme polymorphisms: effects on risk of toxicity and cancer.* DNA Cell Biol, 1996. **15**(4): p. 273-80.
35. Nelson, D.R., *Cytochrome P450 and the individuality of species.* Arch Biochem Biophys, 1999. **369**(1): p. 1-10.
36. Otake, Y. and T. Walle, *Oxidation of the flavonoids galangin and kaempferide by human liver microsomes and CYP1A1, CYP1A2, and CYP2C9.* Drug Metab Dispos, 2002. **30**(2): p. 103-5.
37. Walle, U.K. and T. Walle, *Bioavailable flavonoids: cytochrome P450-mediated metabolism of methoxyflavones.* Drug Metab Dispos, 2007. **35**(11): p. 1985-9.
38. Miley, M.J., et al., *Crystal structure of the cofactor-binding domain of the human phase II drug-metabolism enzyme UDP-glucuronosyltransferase 2B7.* J Mol Biol, 2007. **369**(2): p. 498-511.
39. Tukey, R.H. and C.P. Strassburg, *Human UDP-glucuronosyltransferases: metabolism, expression, and disease.* Annu Rev Pharmacol Toxicol, 2000. **40**: p. 581-616.
40. Mackenzie, P.I., *Expression of chimeric cDNAs in cell culture defines a region of UDP glucuronosyltransferase involved in substrate selection.* J Biol Chem, 1990. **265**(6): p. 3432-5.
41. Mackenzie, P.I., et al., *Nomenclature update for the mammalian UDP glycosyltransferase (UGT) gene superfamily.* Pharmacogenet Genomics, 2005. **15**(10): p. 677-85.
42. Burchell, B., *Genetic variation of human UDP-glucuronosyltransferase: implications in disease and drug glucuronidation.* Am J Pharmacogenomics, 2003. **3**(1): p. 37-52.
43. Nakamura, A., et al., *Expression of UGT1A and UGT2B mRNA in human normal tissues and various cell lines.* Drug Metab Dispos, 2008. **36**(8): p. 1461-4.
44. Bosio, A., et al., *The human gene CGT encoding the UDP-galactose ceramide galactosyl transferase (cerebroside synthase): cloning, characterization, and assignment to human chromosome 4, band q26.* Genomics, 1996. **34**(1): p. 69-75.
45. Mackenzie, P.I., et al., *Identification of UDP glycosyltransferase 3A1 as a UDP N-acetylglucosaminyltransferase.* J Biol Chem, 2008. **283**(52): p. 36205-10.
46. Tang, L., et al., *Structure and concentration changes affect characterization of UGT isoform-specific metabolism of isoflavones.* Mol Pharm, 2009. **6**(5): p. 1466-82.
47. Cheng, Z., A. Radominska-Pandya, and T.R. Tephly, *Studies on the substrate specificity of human intestinal UDP- lucuronosyltransferases 1A8 and 1A10.* Drug Metab Dispos, 1999. **27**(10): p. 1165-70.
48. Chen, Y., et al., *Glucuronidation of flavonoids by recombinant UGT1A3 and UGT1A9.* Biochem Pharmacol, 2008. **76**(3): p. 416-25.

49. Boersma, M.G., et al., *Regioselectivity of phase II metabolism of luteolin and quercetin by UDP-glucuronosyl transferases.* Chem Res Toxicol, 2002. **15**(5): p. 662-70.
50. Lee, H.S., et al., *In vitro metabolism of eupatilin by multiple cytochrome P450 and UDP-glucuronosyltransferase enzymes.* Xenobiotica, 2007. **37**(8): p. 803-17.
51. Turgeon, D., et al., *Glucuronidation activity of the UGT2B17 enzyme toward xenobiotics.* Drug Metab Dispos, 2003. **31**(5): p. 670-6.
52. Xie, S., L. You, and S. Zeng, *Studies on the flavonoid substrates of human UDP-glucuronosyl transferase (UGT) 2B7.* Pharmazie, 2007. **62**(8): p. 625-9.
53. Williams, J.A., et al., *Drug-drug interactions for UDP-glucuronosyltransferase substrates: a pharmacokinetic explanation for typically observed low exposure (AUCi/AUC) ratios.* Drug Metab Dispos, 2004. **32**(11): p. 1201-8.
54. Miners, J.O., R.A. McKinnon, and P.I. Mackenzie, *Genetic polymorphisms of UDP-glucuronosyltransferases and their functional significance.* Toxicology, 2002. **181-182**: p. 453-6.
55. Levesque, E., et al., *The impact of UGT1A8, UGT1A9, and UGT2B7 genetic polymorphisms on the pharmacokinetic profile of mycophenolic acid after a single oral dose in healthy volunteers.* Clin Pharmacol Ther, 2007. **81**(3): p. 392-400.
56. Johnson, L.A., et al., *Pharmacogenetic effect of the UGT polymorphisms on mycophenolate is modified by calcineurin inhibitors.* Eur J Clin Pharmacol, 2008. **64**(11): p. 1047-56.
57. Gamage, N., et al., *Human sulfotransferases and their role in chemical metabolism.* Toxicol Sci, 2006. **90**(1): p. 5-22.
58. Nagata, K. and Y. Yamazoe, *Pharmacogenetics of sulfotransferase.* Annu Rev Pharmacol Toxicol, 2000. **40**: p. 159-76.
59. Ung, D. and S. Nagar, *Variable sulfation of dietary polyphenols by recombinant human sulfotransferase (SULT) 1A1 genetic variants and SULT1E1.* Drug Metab Dispos, 2007. **35**(5): p. 740-6.
60. Vaidyanathan, J.B. and T. Walle, *Glucuronidation and sulfation of the tea flavonoid (-)-epicatechin by the human and rat enzymes.* Drug Metab Dispos, 2002. **30**(8): p. 897-903.
61. Huang, C., et al., *Sulfation of dietary flavonoids by human sulfotransferases.* Xenobiotica, 2009. **39**(4): p. 312-22.
62. Otake, Y., F. Hsieh, and T. Walle, *Glucuronidation versus oxidation of the flavonoid galangin by human liver microsomes and hepatocytes.* Drug Metab Dispos, 2002. **30**(5): p. 576-81.
63. Hu, M., J. Chen, and H. Lin, *Metabolism of flavonoids via enteric recycling: mechanistic studies of disposition of apigenin in the Caco-2 cell culture model.* J Pharmacol Exp Ther, 2003. **307**(1): p. 314-21.
64. Sun, H., et al., *A catenary model to study transport and conjugation of baicalein, a bioactive flavonoid, in the Caco-2 cell monolayer:*

demonstration of substrate inhibition. J Pharmacol Exp Ther, 2008. **326**(1): p. 117-26.
65. Meinl, W., et al., *Sulfotransferase forms expressed in human intestinal Caco-2 and TC7 cells at varying stages of differentiation and role in benzo[a]pyrene metabolism.* Drug Metab Dispos, 2008. **36**(2): p. 276-83.
66. Linton, K.J., *Structure and function of ABC transporters.* Physiology (Bethesda), 2007. **22**: p. 122-30.
67. Dean, M., *The human ATP-binding cassette (ABC) transporter superfamily*. 2002: National center for biotechnology information.
68. Riordan, J.R. and V. Ling, *Purification of P-glycoprotein from plasma membrane vesicles of Chinese hamster ovary cell mutants with reduced colchicine permeability.* J Biol Chem, 1979. **254**(24): p. 12701-5.
69. Germann, U.A., I. Pastan, and M.M. Gottesman, *P-glycoproteins: mediators of multidrug resistance.* Semin Cell Biol, 1993. **4**(1): p. 63-76.
70. Cascorbi, I., *P-glycoprotein: tissue distribution, substrates, and functional consequences of genetic variations.* Handb Exp Pharmacol, 2011(201): p. 261-83.
71. Kruh, G.D., et al., *MRP subfamily transporters and resistance to anticancer agents.* J Bioenerg Biomembr, 2001. **33**(6): p. 493-501.
72. Buchler, M., et al., *cDNA cloning of the hepatocyte canalicular isoform of the multidrug resistance protein, cMrp, reveals a novel conjugate export pump deficient in hyperbilirubinemic mutant rats.* J Biol Chem, 1996. **271**(25): p. 15091-8.
73. Ito, K., et al., *Molecular cloning of canalicular multispecific organic anion transporter defective in EHBR.* Am J Physiol, 1997. **272**(1 Pt 1): p. G16-22.
74. Paulusma, C.C., et al., *Congenital jaundice in rats with a mutation in a multidrug resistance-associated protein gene.* Science, 1996. **271**(5252): p. 1126-8.
75. Taniguchi, K., et al., *A human canalicular multispecific organic anion transporter (cMOAT) gene is overexpressed in cisplatin-resistant human cancer cell lines with decreased drug accumulation.* Cancer Res, 1996. **56**(18): p. 4124-9.
76. van Kuijck, M.A., et al., *Assignment of the canalicular multispecific organic anion transporter gene (CMOAT) to human chromosome 10q24 and mouse chromosome 19D2 by fluorescent in situ hybridization.* Cytogenet Cell Genet, 1997. **77**(3-4): p. 285-7.
77. Deeley, R.G., C. Westlake, and S.P. Cole, *Transmembrane transport of endo- and xenobiotics by mammalian ATP-binding cassette multidrug resistance proteins.* Physiol Rev, 2006. **86**(3): p. 849-99.
78. Zimmermann, C., et al., *Mapping of multidrug resistance gene 1 and multidrug resistance-associated protein isoform 1 to 5 mRNA expression along the human intestinal tract.* Drug Metab Dispos, 2005. **33**(2): p. 219-24.

79. Koike, K., et al., *A canalicular multispecific organic anion transporter (cMOAT) antisense cDNA enhances drug sensitivity in human hepatic cancer cells.* Cancer Res, 1997. **57**(24): p. 5475-9.
80. Kawabe, T., et al., *Enhanced transport of anticancer agents and leukotriene C4 by the human canalicular multispecific organic anion transporter (cMOAT/MRP2).* FEBS Lett, 1999. **456**(2): p. 327-31.
81. Sasabe, H., A. Tsuji, and Y. Sugiyama, *Carrier-mediated mechanism for the biliary excretion of the quinolone antibiotic grepafloxacin and its glucuronide in rats.* J Pharmacol Exp Ther, 1998. **284**(3): p. 1033-9.
82. Ahmed, S., et al., *Involvement of Mrp2 (Abcc2) in biliary excretion of moxifloxacin and its metabolites in the isolated perfused rat liver.* J Pharm Pharmacol, 2008. **60**(1): p. 55-62.
83. Jedlitschky, G., et al., *ATP-dependent transport of bilirubin glucuronides by the multidrug resistance protein MRP1 and its hepatocyte canalicular isoform MRP2.* Biochem J, 1997. **327 (Pt 1)**: p. 305-10.
84. Ho, R.H. and R.B. Kim, *Transporters and drug therapy: implications for drug disposition and disease.* Clin Pharmacol Ther, 2005. **78**(3): p. 260-77.
85. Belinsky, M.G., et al., *Characterization of MOAT-C and MOAT-D, new members of the MRP/cMOAT subfamily of transporter proteins.* J Natl Cancer Inst, 1998. **90**(22): p. 1735-41.
86. Donner, M.G. and D. Keppler, *Up-regulation of basolateral multidrug resistance protein 3 (Mrp3) in cholestatic rat liver.* Hepatology, 2001. **34**(2): p. 351-9.
87. Rodriguez-Garay, E.A., *Cholestasis: human disease and experimental animal models.* Ann Hepatol, 2003. **2**(4): p. 150-8.
88. Doyle, L.A., et al., *A multidrug resistance transporter from human MCF-7 breast cancer cells.* Proc Natl Acad Sci U S A, 1998. **95**(26): p. 15665-70.
89. Allikmets, R., et al., *A human placenta-specific ATP-binding cassette gene (ABCP) on chromosome 4q22 that is involved in multidrug resistance.* Cancer Res, 1998. **58**(23): p. 5337-9.
90. Ozvegy, C., et al., *Functional characterization of the human multidrug transporter, ABCG2, expressed in insect cells.* Biochem Biophys Res Commun, 2001. **285**(1): p. 111-7.
91. Giacomini, K.M., et al., *Membrane transporters in drug development.* Nat Rev Drug Discov, 2010. **9**(3): p. 215-36.
92. Robey, R.W., et al., *ABCG2: a perspective.* Adv Drug Deliv Rev, 2009. **61**(1): p. 3-13.
93. Englund, G., et al., *Regional levels of drug transporters along the human intestinal tract: co-expression of ABC and SLC transporters and comparison with Caco-2 cells.* Eur J Pharm Sci, 2006. **29**(3-4): p. 269-77.
94. Albermann, N., et al., *Expression of the drug transporters MDR1/ABCB1, MRP1/ABCC1, MRP2/ABCC2, BCRP/ABCG2, and PXR in peripheral blood mononuclear cells and their relationship with the expression in intestine and liver.* Biochem Pharmacol, 2005. **70**(6): p. 949-58.

95. Polgar, O., R.W. Robey, and S.E. Bates, *ABCG2: structure, function and role in drug response.* Expert Opin Drug Metab Toxicol, 2008. **4**(1): p. 1-15.
96. van Herwaarden, A.E., et al., *Multidrug transporter ABCG2/breast cancer resistance protein secretes riboflavin (vitamin B2) into milk.* Mol Cell Biol, 2007. **27**(4): p. 1247-53.
97. van Herwaarden, A.E. and A.H. Schinkel, *The function of breast cancer resistance protein in epithelial barriers, stem cells and milk secretion of drugs and xenotoxins.* Trends Pharmacol Sci, 2006. **27**(1): p. 10-6.
98. Zhang, S., et al., *Structure activity relationships and quantitative structure activity relationships for the flavonoid-mediated inhibition of breast cancer resistance protein.* Biochem Pharmacol, 2005. **70**(4): p. 627-39.
99. Rabindran, S.K., et al., *Fumitremorgin C reverses multidrug resistance in cells transfected with the breast cancer resistance protein.* Cancer Res, 2000. **60**(1): p. 47-50.
100. Zhang, Y., et al., *BCRP transports dipyridamole and is inhibited by calcium channel blockers.* Pharm Res, 2005. **22**(12): p. 2023-34.
101. Pick, A., W. Klinkhammer, and M. Wiese, *Specific inhibitors of the breast cancer resistance protein (BCRP).* ChemMedChem, 2010. **5**(9): p. 1498-505.
102. Brand, W., et al., *Metabolism and transport of the citrus flavonoid hesperetin in Caco-2 cell monolayers.* Drug Metab Dispos, 2008. **36**(9): p. 1794-802.
103. Cooray, H.C., et al., *Interaction of the breast cancer resistance protein with plant polyphenols.* Biochem Biophys Res Commun, 2004. **317**(1): p. 269-75.
104. Tamura, A., et al., *In vitro evaluation of photosensitivity risk related to genetic polymorphisms of human ABC transporter ABCG2 and inhibition by drugs.* Drug Metab Pharmacokinet, 2007. **22**(6): p. 428-40.
105. Sparreboom, A., et al., *Effect of ABCG2 genotype on the oral bioavailability of topotecan.* Cancer Biol Ther, 2005. **4**(6): p. 650-8.
106. Sparreboom, A., et al., *Diflomotecan pharmacokinetics in relation to ABCG2 421C>A genotype.* Clin Pharmacol Ther, 2004. **76**(1): p. 38-44.
107. Zamboni, W.C., et al., *Disposition of 9-nitrocamptothecin and its 9-aminocamptothecin metabolite in relation to ABC transporter genotypes.* Invest New Drugs, 2006. **24**(5): p. 393-401.
108. Lepper, E.R., et al., *Mechanisms of resistance to anticancer drugs: the role of the polymorphic ABC transporters ABCB1 and ABCG2.* Pharmacogenomics, 2005. **6**(2): p. 115-38.
109. Itoda, M., et al., *Eight novel single nucleotide polymorphisms in ABCG2/BCRP in Japanese cancer patients administered irinotacan.* Drug Metab Pharmacokinet, 2003. **18**(3): p. 212-7.
110. Zhang, Y. and L.Z. Benet, *The gut as a barrier to drug absorption: combined role of cytochrome P450 3A and P-glycoprotein.* Clin Pharmacokinet, 2001. **40**(3): p. 159-68.

111. Wacher, V.J., C.Y. Wu, and L.Z. Benet, *Overlapping substrate specificities and tissue distribution of cytochrome P450 3A and P-glycoprotein: implications for drug delivery and activity in cancer chemotherapy.* Mol Carcinog, 1995. **13**(3): p. 129-34.
112. Urquhart, B.L., R.G. Tirona, and R.B. Kim, *Nuclear receptors and the regulation of drug-metabolizing enzymes and drug transporters: implications for interindividual variability in response to drugs.* J Clin Pharmacol, 2007. **47**(5): p. 566-78.
113. Nies, A.T., M. Schwab, and D. Keppler, *Interplay of conjugating enzymes with OATP uptake transporters and ABCC/MRP efflux pumps in the elimination of drugs.* Expert Opin Drug Metab Toxicol, 2008. **4**(5): p. 545-68.
114. Salphati, L., *Transport-metabolism interplay.* Mol Pharm, 2009. **6**(6): p. 1629-30.
115. Pang, K.S., H.J. Maeng, and J. Fan, *Interplay of transporters and enzymes in drug and metabolite processing.* Mol Pharm, 2009. **6**(6): p. 1734-55.
116. Endres, C.J., M.G. Endres, and J.D. Unadkat, *Interplay of drug metabolism and transport: a real phenomenon or an artifact of the site of measurement?* Mol Pharm, 2009. **6**(6): p. 1756-65.
117. Thummel, K.E. and G.R. Wilkinson, *In vitro and in vivo drug interactions involving human CYP3A.* Annu Rev Pharmacol Toxicol, 1998. **38**: p. 389-430.
118. Schuetz, E.G., W.T. Beck, and J.D. Schuetz, *Modulators and substrates of P-glycoprotein and cytochrome P4503A coordinately up-regulate these proteins in human colon carcinoma cells.* Mol Pharmacol, 1996. **49**(2): p. 311-8.
119. Matheny, C.J., et al., *Effect of prototypical inducing agents on P-glycoprotein and CYP3A expression in mouse tissues.* Drug Metab Dispos, 2004. **32**(9): p. 1008-14.
120. Benet, L.Z., *The drug transporter-metabolism alliance: uncovering and defining the interplay.* Mol Pharm, 2009. **6**(6): p. 1631-43.
121. Cummins, C.L., et al., *In vivo modulation of intestinal CYP3A metabolism by P-glycoprotein: studies using the rat single-pass intestinal perfusion model.* J Pharmacol Exp Ther, 2003. **305**(1): p. 306-14.
122. van Waterschoot, R.A., et al., *Absence of both cytochrome P450 3A and P-glycoprotein dramatically increases docetaxel oral bioavailability and risk of intestinal toxicity.* Cancer Res, 2009. **69**(23): p. 8996-9002.
123. Fisher, J.M., et al., *First-pass midazolam metabolism catalyzed by 1alpha,25-dihydroxy vitamin D3-modified Caco-2 cell monolayers.* J Pharmacol Exp Ther, 1999. **289**(2): p. 1134-42.
124. Hochman, J.H., et al., *Influence of P-glycoprotein on the transport and metabolism of indinavir in Caco-2 cells expressing cytochrome P-450 3A4.* J Pharmacol Exp Ther, 2000. **292**(1): p. 310-8.

125. Cummins, C.L., W. Jacobsen, and L.Z. Benet, *Unmasking the dynamic interplay between intestinal P-glycoprotein and CYP3A4.* J Pharmacol Exp Ther, 2002. **300**(3): p. 1036-45.
126. Cummins, C.L., et al., *CYP3A4-transfected Caco-2 cells as a tool for understanding biochemical absorption barriers: studies with sirolimus and midazolam.* J Pharmacol Exp Ther, 2004. **308**(1): p. 143-55.
127. Benet, L.Z., C.L. Cummins, and C.Y. Wu, *Unmasking the dynamic interplay between efflux transporters and metabolic enzymes.* Int J Pharm, 2004. **277**(1-2): p. 3-9.
128. Chan, L.M., et al., *P-glycoprotein potentiates CYP3A4-mediated drug disappearance during Caco-2 intestinal secretory detoxification.* J Drug Target, 2004. **12**(7): p. 405-13.
129. Christians, U., V. Schmitz, and M. Haschke, *Functional interactions between P-glycoprotein and CYP3A in drug metabolism.* Expert Opin Drug Metab Toxicol, 2005. **1**(4): p. 641-54.
130. Mouly, S.J., M.F. Paine, and P.B. Watkins, *Contributions of CYP3A4, P-glycoprotein, and serum protein binding to the intestinal first-pass extraction of saquinavir.* J Pharmacol Exp Ther, 2004. **308**(3): p. 941-8.
131. Sun, H. and K.S. Pang, *Permeability, transport, and metabolism of solutes in Caco-2 cell monolayers: a theoretical study.* Drug Metab Dispos, 2008. **36**(1): p. 102-23.
132. Tam, D., H. Sun, and K.S. Pang, *Influence of P-glycoprotein, transfer clearances, and drug binding on intestinal metabolism in Caco-2 cell monolayers or membrane preparations: a theoretical analysis.* Drug Metab Dispos, 2003. **31**(10): p. 1214-26.
133. Sun, H., et al., *The Caco-2 cell monolayer: usefulness and limitations.* Expert Opin Drug Metab Toxicol, 2008. **4**(4): p. 395-411.
134. Jia, X., et al., *Disposition of flavonoids via enteric recycling: enzyme-transporter coupling affects metabolism of biochanin A and formononetin and excretion of their phase II conjugates.* J Pharmacol Exp Ther, 2004. **310**(3): p. 1103-13.
135. van de Wetering, K., et al., *Targeted metabolomics identifies glucuronides of dietary phytoestrogens as a major class of MRP3 substrates in vivo.* Gastroenterology, 2009. **137**(5): p. 1725-35.
136. Sun, H., Y.Y. Zeng, and K.S. Pang, *Interplay of phase II enzymes and transporters in futile cycling: influence of multidrug resistance-associated protein 2-mediated excretion of estradiol 17beta-D-glucuronide and its 3-sulfate metabolite on net sulfation in perfused TR(-) and Wistar rat liver preparations.* Drug Metab Dispos, 2010. **38**(5): p. 769-80.
137. Hagenbuch, B. and P.J. Meier, *Organic anion transporting polypeptides of the OATP/ SLC21 family: phylogenetic classification as OATP/ SLCO superfamily, new nomenclature and molecular/functional properties.* Pflugers Arch, 2004. **447**(5): p. 653-65.
138. Abe, T., et al., *Identification of a novel gene family encoding human liver-specific organic anion transporter LST-1.* J Biol Chem, 1999. **274**(24): p. 17159-63.

139. Hsiang, B., et al., *A novel human hepatic organic anion transporting polypeptide (OATP2). Identification of a liver-specific human organic anion transporting polypeptide and identification of rat and human hydroxymethylglutaryl-CoA reductase inhibitor transporters.* J Biol Chem, 1999. **274**(52): p. 37161-8.
140. Konig, J., et al., *A novel human organic anion transporting polypeptide localized to the basolateral hepatocyte membrane.* Am J Physiol Gastrointest Liver Physiol, 2000. **278**(1): p. G156-64.
141. Tamai, I., et al., *Molecular identification and characterization of novel members of the human organic anion transporter (OATP) family.* Biochem Biophys Res Commun, 2000. **273**(1): p. 251-60.
142. Kullak-Ublick, G.A., et al., *Organic anion-transporting polypeptide B (OATP-B) and its functional comparison with three other OATPs of human liver.* Gastroenterology, 2001. **120**(2): p. 525-33.
143. Hagenbuch, B. and P.J. Meier, *The superfamily of organic anion transporting polypeptides.* Biochim Biophys Acta, 2003. **1609**(1): p. 1-18.
144. Campbell, S.D., S.M. de Morais, and J.J. Xu, *Inhibition of human organic anion transporting polypeptide OATP 1B1 as a mechanism of drug-induced hyperbilirubinemia.* Chem Biol Interact, 2004. **150**(2): p. 179-87.
145. Senafi, S.B., D.J. Clarke, and B. Burchell, *Investigation of the substrate specificity of a cloned expressed human bilirubin UDP-glucuronosyltransferase: UDP-sugar specificity and involvement in steroid and xenobiotic glucuronidation.* Biochem J, 1994. **303 (Pt 1)**: p. 233-40.
146. Stangier, J., et al., *Absorption, metabolism, and excretion of intravenously and orally administered [14C]telmisartan in healthy volunteers.* J Clin Pharmacol, 2000. **40**(12 Pt 1): p. 1312-22.
147. Ishiguro, N., et al., *Predominant contribution of OATP1B3 to the hepatic uptake of telmisartan, an angiotensin II receptor antagonist, in humans.* Drug Metab Dispos, 2006. **34**(7): p. 1109-15.
148. Kamisako, T., et al., *Transport of monoglucuronosyl and bisglucuronosyl bilirubin by recombinant human and rat multidrug resistance protein 2.* Hepatology, 1999. **30**(2): p. 485-90.
149. Cui, Y., J. Konig, and D. Keppler, *Vectorial transport by double-transfected cells expressing the human uptake transporter SLC21A8 and the apical export pump ABCC2.* Mol Pharmacol, 2001. **60**(5): p. 934-43.
150. Liu, X., V.H. Tam, and M. Hu, *Disposition of flavonoids via enteric recycling: determination of the UDP-glucuronosyltransferase isoforms responsible for the metabolism of flavonoids in intact Caco-2 TC7 cells using siRNA.* Mol Pharm, 2007. **4**(6): p. 873-82.
151. Tang, L., et al., *Use of glucuronidation fingerprinting to describe and predict mono- and dihydroxyflavone metabolism by recombinant UGT isoforms and human intestinal and liver microsomes.* Mol Pharm, 2010. **7**(3): p. 664-79.
152. Yang, Z., et al., *Simultaneous determination of genistein and its four phase II metabolites in blood by a sensitive and robust UPLC-MS/MS*

method: Application to an oral bioavailability study of genistein in mice. J Pharm Biomed Anal, 2010. **53**(1): p. 81-9.
153. Wong, Y.C., et al., *Intestinal first-pass glucuronidation activities of selected dihydroxyflavones.* Int J Pharm, 2009. **366**(1-2): p. 14-20.
154. Ahlin, G., et al., *Endogenous gene and protein expression of drug-transporting proteins in cell lines routinely used in drug discovery programs.* Drug Metab Dispos, 2009. **37**(12): p. 2275-83.
155. Enokizono, J., H. Kusuhara, and Y. Sugiyama, *Involvement of breast cancer resistance protein (BCRP/ABCG2) in the biliary excretion and intestinal efflux of troglitazone sulfate, the major metabolite of troglitazone with a cholestatic effect.* Drug Metab Dispos, 2007. **35**(2): p. 209-14.
156. Lee, J.K., et al., *Sex-dependent disposition of acetaminophen sulfate and glucuronide in the in situ perfused mouse liver.* Drug Metab Dispos, 2009. **37**(9): p. 1916-21.
157. Lengyel, G., et al., *Modulation of sinusoidal and canalicular elimination of bilirubin-glucuronides by rifampicin and other cholestatic drugs in a sandwich culture of rat hepatocytes.* Hepatol Res, 2008. **38**(3): p. 300-9.
158. Sakamoto, S., et al., *Identification of the transporters involved in the hepatobiliary transport and intestinal efflux of methyl 1-(3,4-dimethoxyphenyl)-3-(3-ethylvaleryl)-4-hydroxy-6,7,8-trimethoxy-2-na phthoate (S-8921) glucuronide, a pharmacologically active metabolite of S-8921.* Drug Metab Dispos, 2008. **36**(8): p. 1553-61.
159. Paoluzzi, L., et al., *Influence of genetic variants in UGT1A1 and UGT1A9 on the in vivo glucuronidation of SN-38.* J Clin Pharmacol, 2004. **44**(8): p. 854-60.
160. Court, M.H., et al., *Interindividual variability in acetaminophen glucuronidation by human liver microsomes: identification of relevant acetaminophen UDP-glucuronosyltransferase isoforms.* J Pharmacol Exp Ther, 2001. **299**(3): p. 998-1006.
161. Pritchett, L.E., et al., *Glucuronidation of the soyabean isoflavones genistein and daidzein by human liver is related to levels of UGT1A1 and UGT1A9 activity and alters isoflavone response in the MCF-7 human breast cancer cell line.* J Nutr Biochem, 2008. **19**(11): p. 739-45.
162. Kurkela, M., et al., *Expression and characterization of recombinant human UDP-glucuronosyltransferases (UGTs). UGT1A9 is more resistant to detergent inhibition than other UGTs and was purified as an active dimeric enzyme.* J Biol Chem, 2003. **278**(6): p. 3536-44.
163. Fujiwara, R., et al., *Effects of coexpression of UGT1A9 on enzymatic activities of human UGT1A isoforms.* Drug Metab Dispos, 2007. **35**(5): p. 747-57.
164. Benavente-Garcia, O., et al., *Beneficial action of Citrus flavonoids on multiple cancer-related biological pathways.* Curr Cancer Drug Targets, 2007. **7**(8): p. 795-809.
165. Comalada, M., et al., *In vivo quercitrin anti-inflammatory effect involves release of quercetin, which inhibits inflammation through down-regulation of the NF-kappaB pathway.* Eur J Immunol, 2005. **35**(2): p. 584-92.

166. Lee, E.R., G.H. Kang, and S.G. Cho, *Effect of flavonoids on human health: old subjects but new challenges.* Recent Pat Biotechnol, 2007. **1**(2): p. 139-50.
167. Chen, C.A. and H. Okayama, *Calcium phosphate-mediated gene transfer: a highly efficient transfection system for stably transforming cells with plasmid DNA.* Biotechniques, 1988. **6**(7): p. 632-8.
168. Ee, P.L., et al., *Modulation of breast cancer resistance protein (BCRP/ABCG2) gene expression using RNA interference.* Mol Cancer Ther, 2004. **3**(12): p. 1577-83.
169. Houston, J.B. and K.E. Kenworthy, *In vitro-in vivo scaling of CYP kinetic data not consistent with the classical Michaelis-Menten model.* Drug Metab Dispos, 2000. **28**(3): p. 246-54.
170. Hutzler, J.M. and T.S. Tracy, *Atypical kinetic profiles in drug metabolism reactions.* Drug Metab Dispos, 2002. **30**(4): p. 355-62.
171. Wang, S.W., et al., *Disposition of flavonoids via enteric recycling: structural effects and lack of correlations between in vitro and in situ metabolic properties.* Drug Metab Dispos, 2006. **34**(11): p. 1837-48.
172. Yamaoka, K., T. Nakagawa, and T. Uno, *Application of Akaike's information criterion (AIC) in the evaluation of linear pharmacokinetic equations.* J Pharmacokinet Biopharm, 1978. **6**(2): p. 165-75.
173. Yamaguchi, H., et al., *Secretory mechanisms of grepafloxacin and levofloxacin in the human intestinal cell line caco-2.* J Pharmacol Exp Ther, 2000. **295**(1): p. 360-6.
174. Saito, H., K. Inui, and R. Hori, *Mechanisms of gentamicin transport in kidney epithelial cell line (LLC-PK1).* J Pharmacol Exp Ther, 1986. **238**(3): p. 1071-6.
175. Liu, Y. and M. Hu, *Absorption and metabolism of flavonoids in the caco-2 cell culture model and a perused rat intestinal model.* Drug Metab Dispos, 2002. **30**(4): p. 370-7.
176. Mackenzie, P.I., *Identification of uridine diphosphate glucuronosyltransferases involved in the metabolism and clearance of mycophenolic acid.* Ther Drug Monit, 2000. **22**(1): p. 10-3.
177. Bernard, O. and C. Guillemette, *The main role of UGT1A9 in the hepatic metabolism of mycophenolic acid and the effects of naturally occurring variants.* Drug Metab Dispos, 2004. **32**(8): p. 775-8.
178. Wang, S.W., et al., *Disposition of flavonoids via enteric recycling: UDP-glucuronosyltransferase (UGT) 1As deficiency in Gunn rats is compensated by increases in UGT2Bs activities.* J Pharmacol Exp Ther, 2009. **329**(3): p. 1023-31.
179. Yao, X.L., et al., *Dexamethasone alters arachidonate release from human epithelial cells by induction of p11 protein synthesis and inhibition of phospholipase A2 activity.* J Biol Chem, 1999. **274**(24): p. 17202-8.
180. Chang, J.H., et al., *The role of pH in the glucuronidation of raloxifene, mycophenolic acid and ezetimibe.* Mol Pharm, 2009. **6**(4): p. 1216-27.
181. Breedveld, P., et al., *The effect of low pH on breast cancer resistance protein (ABCG2)-mediated transport of methotrexate, 7-*

hydroxymethotrexate, methotrexate diglutamate, folic acid, mitoxantrone, topotecan, and resveratrol in in vitro drug transport models. Mol Pharmacol, 2007. **71**(1): p. 240-9.
182. Narang, V.S., et al., *Dexamethasone increases expression and activity of multidrug resistance transporters at the rat blood-brain barrier.* Am J Physiol Cell Physiol, 2008. **295**(2): p. C440-50.
183. Zielonka, J., J. Gebicki, and G. Grynkiewicz, *Radical scavenging properties of genistein.* Free Radic Biol Med, 2003. **35**(8): p. 958-65.
184. Favaro, G., et al., *Acidichromism and ionochromism of luteolin and apigenin, the main components of the naturally occurring yellow weld: a spectrophotometric and fluorimetric study.* J Fluoresc, 2007. **17**(6): p. 707-14.
185. Chen, Z.S., et al., *Transport of methotrexate, methotrexate polyglutamates, and 17beta-estradiol 17-(beta-D-glucuronide) by ABCG2: effects of acquired mutations at R482 on methotrexate transport.* Cancer Res, 2003. **63**(14): p. 4048-54.
186. Xu, L., et al., *[Experimental study of the total flavonoid in Hypericum perforatum on depression].* Zhongguo Zhong Yao Za Zhi, 2005. **30**(15): p. 1184-8.
187. Merino, G., et al., *Transport of anthelmintic benzimidazole drugs by breast cancer resistance protein (BCRP/ABCG2).* Drug Metab Dispos, 2005. **33**(5): p. 614-8.
188. Kruijtzer, C.M., J.H. Beijnen, and J.H. Schellens, *Improvement of oral drug treatment by temporary inhibition of drug transporters and/or cytochrome P450 in the gastrointestinal tract and liver: an overview.* Oncologist, 2002. **7**(6): p. 516-30.
189. Breedveld, P., J.H. Beijnen, and J.H. Schellens, *Use of P-glycoprotein and BCRP inhibitors to improve oral bioavailability and CNS penetration of anticancer drugs.* Trends Pharmacol Sci, 2006. **27**(1): p. 17-24.

APPENDIX

Appendix A. Gene sequence analysis

```
Query  117  AGATTCCCAGCTGCTTGCTCTCAGCTGCAGTTCTCTGATGGCTTGCACAGGGTGGACCAG  176
            ||||||||||||||||||||||||||||||||||||||||||||||||||||||||||||
Sbjct  1    AGATTCCCAGCTGCTTGCTCTCAGCTGCAGTTCTCTGATGGCTTGCACAGGGTGGACCAG  60

Query  177  CCCCCTTCCTCTATGTGTGTGTCTGCTGCTGACCTGTGGCTTTGCCGAGGCAGGGAAGCT  236
            ||||||||||||||||||||||||||||||||||||||||||||||||||||||||||||
Sbjct  61   CCCCCTTCCTCTATGTGTGTGTCTGCTGCTGACCTGTGGCTTTGCCGAGGCAGGGAAGCT  120

Query  237  ACTGGTAGTGCCCATGGATGGGAGCCACTGGTTCACCATGAGGTCGGTGGTGGAGAAACT  296
            ||||||||||||||||||||||||||||||||||||||||||||||||||||||||||||
Sbjct  121  ACTGGTAGTGCCCATGGATGGGAGCCACTGGTTCACCATGAGGTCGGTGGTGGAGAAACT  180

Query  297  CATTCTCAGGGGGCATGAGGTGGTTGTAGTCATGCCAGAGGTGAGTTGGCAACTGGGAAG  356
            ||||||||||||||||||||||||||||||||||||||||||||||||||||||||||||
Sbjct  181  CATTCTCAGGGGGCATGAGGTGGTTGTAGTCATGCCAGAGGTGAGTTGGCAACTGGGAAG  240

Query  357  ATCACTGAATTGCACAGTGAAGACTTATTCAACTTCATATACCCTGGAGGATCTGGACCG  416
            ||||||||||||||||||||||||||||||||||||||||||||||||||||||||||||
Sbjct  241  ATCACTGAATTGCACAGTGAAGACTTATTCAACTTCATATACCCTGGAGGATCTGGACCG  300

Query  417  GGAGTTCAAGGCTTTTGCCCATGCTCAATGGAAAGCACAAGTACGAAGTATATATTCTCT  476
            ||||||||||||||||||||||||||||||||||||||||||||||||||||||||||||
Sbjct  301  GGAGTTCAAGGCTTTTGCCCATGCTCAATGGAAAGCACAAGTACGAAGTATATATTCTCT  360

Query  477  ATTAATGGGTTCATACAATGACATTTTTGACTTAttttttCAAATTGCAGGAGTTTGTT  536
            ||||||||||||||||||||||||||||||||||||||||||||||||||||||||||||
Sbjct  361  ATTAATGGGTTCATACAATGACATTTTTGACTTATTTTTTTCAAATTGCAGGAGTTTGTT  420

Query  537  TAAAGACAAAAAAATTAGTAGAATACTTAAAGGAGAGTTCTTTTGATGCAGTGTTTCTCGA  596
            ||||||||||||||||||||||||||||||||||||||||||||||||||||||||||||
Sbjct  421  TAAAGACAAAAAAATTAGTAGAATACTTAAAGGAGAGTTCTTTTGATGCAGTGTTTCTCGA  480

Query  597  TCCTTTTGATAACTGTGGCTTAATTGTTGCCAAATATTTCTCCCTCCCCTCCGTGGTCTT  656
            ||||||||||||||||||||||||||||||||||||||||||||||||||||||||||||
Sbjct  481  TCCTTTTGATAACTGTGGCTTAATTGTTGCCAAATATTTCTCCCTCCCCTCCGTGGTCTT  540

Query  657  CGCCAGGGGAATACTTTGCCACTATCTTGAAGAAGGTGCACAGTGCCCTGCTCCTCTTTC  716
            ||||||||||||||||||||||||||||||||||||||||||||||||||||||||||||
Sbjct  541  CGCCAGGGGAATACTTTGCCACTATCTTGAAGAAGGTGCACAGTGCCCTGCTCCTCTTTC  600

Query  717  CTATGTCCCCAGAATTCTCTTAGGGTTCTCAGATGCCATGACTTTCAAGGAGAGAGTACG  776
            ||||||||||||||||||||||||||||||||||||||||||||||||||||||||||||
Sbjct  601  CTATGTCCCCAGAATTCTCTTAGGGTTCTCAGATGCCATGACTTTCAAGGAGAGAGTACG  660
```

Polypeptide 1A9 (UGT1A9), mRNA Length=2395 Identities = 787/788 (99%), Gaps = 0/788 (0%)

Figure I Gene sequence analysis. *UGT1A9* gene (NM_021027.2) cloned in pcDNA 3.1(+/-) was sequenced (Query) and compared with the normal sequence (Sbjct) in NIH data base by blast.

Appendix B. The G418 concentration selection for development of engineered HeLa cells

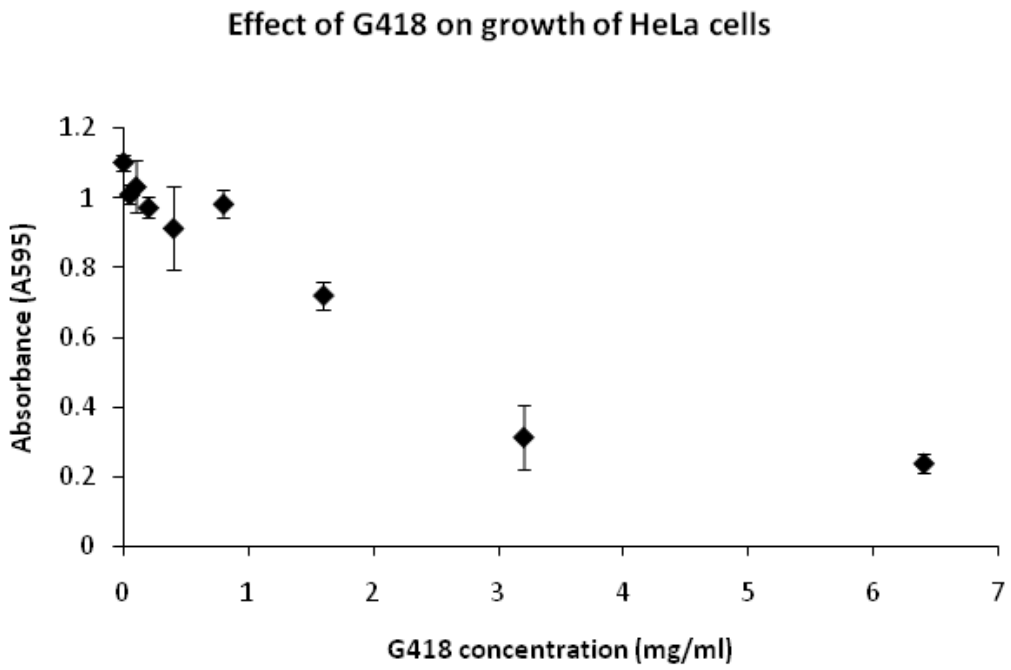

Figure II Effects of G418 on growth of HeLa cells. Wild type HeLa cells were seeded at density of 4000/well in 96-well plate. G418 was added from highest 6.4mg/ml to 0.0125mg/ml by half-half dilution. Each bar is the average of at least three determinations (n>=3) and error bars are the standard deviations of the mean.

Appendix C. UGT1A9 siRNA selection

Table C-1a. Effects of siRNA type and dose on excretion rates of apigenin glucuronides

	siRNA	Dose of siRNA (pmole)	
		10	30
Excretion rate inhibition (%)	**1A9_1**	42.80±6.29	47.72±9.31
	1A9_2	35.39±2.76	* 67.3±3.31

Table C-1b. Effects of siRNA type on excretion rates of wogonin glucuronides

	siRNA (30pmole)	**Loading concentration of wogonin (μM)**			
		2	**10**	**20**	**30**
Excretion rate inhibition (%)	**1A9_1**	26.20±2.16	25.53±2.08	26.22±4.39	-
	1A9_2	**44.90±1.70	**46.81±2.01	**44.46±3.21	**44.90±1.70

Appendix D. The siRNA-mediated UGT1A9 silencing using scrambled siRNA as negative control

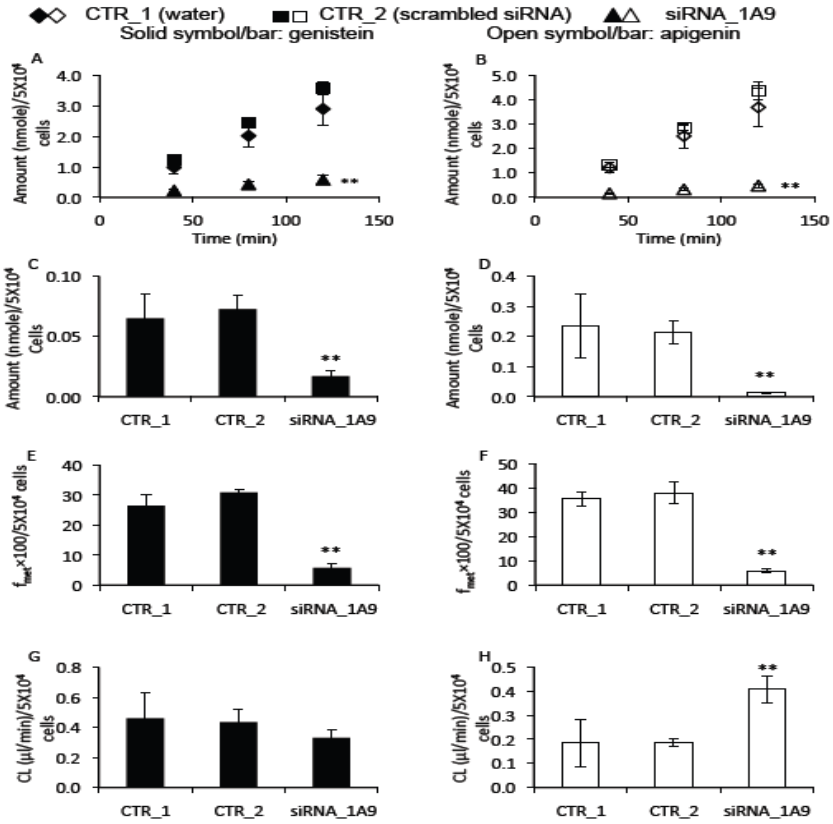

Figure III Effects of siRNA-mediated UGT1A9 silencing on the excretion rates, intracellular amounts, fraction metabolized (f_{met}), and clearance (CL) of flavonoidglucuronides. Engineered HeLa cells stably overexpressing UGT1A9 grow on 12-well plates were treated with 10µM genistein or apigenin in the absence of siRNA (30µl water per well) or presence of 30pmole/well scrambled siRNA or siRNA targeting UGT1A9. The amounts of excreting glucuronides as a function of time was shown in the A and B and the intracellular amounts (determined at 120min) were shown in the C and D. The f_{met} values (determined at 120min) were shown in the E and F, and the CL values were given in the G and H. For the control group treated with equal volume of water, each data point was the average of six determinations (n=6); for the control group transfected with scrambled siRNA or the group treated with siRNA targeting UGT1A9, each data point was the average of three determinations (n=3). The error bar represents the standard deviation. $p<0.05$, *; $p<0.01$,. There was no statistically significant difference observed between the scrambled control and water transfection.**

Appendix E. pH effects on excretion of genistein glucuronides

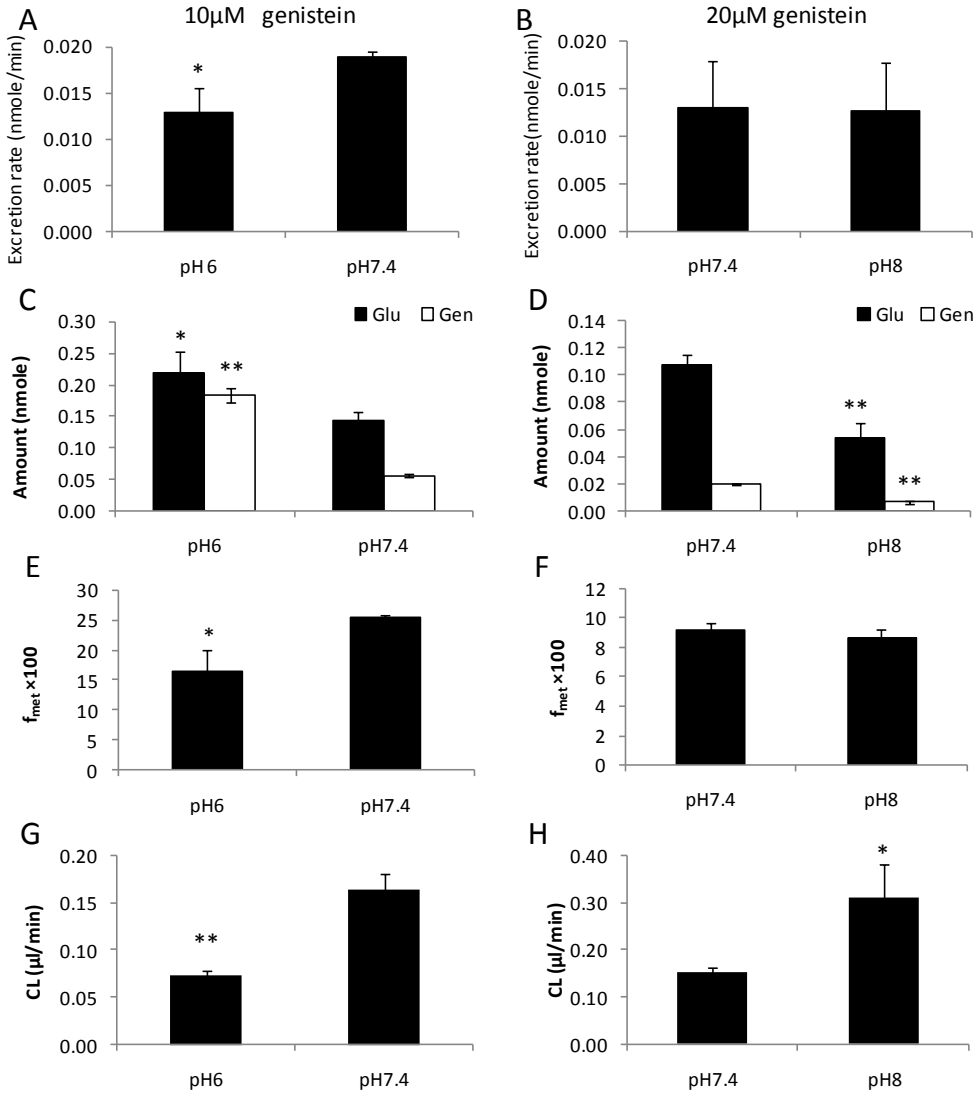

Figure IV Effects of pH on the excretion rates, intracellular amounts, fraction metabolized (f_{met}) and clearance (CL) of genistein glucuronides. Engineered HeLa cells stably overexpressing UGT1A9 were treated with 10μM genistein under pH6 and pH7.4, and treated with 20μM under pH7.4 and pH8. The intracellular amounts and the f_{met} values were determined at 120min. Each data point was the average of three determinations with error bar representing the standard deviation (n=3). P<0.05, *; P<0.01, Glu was short for glucuronides whereas Gen was short for genistein.**

Appendix F. Effects of dexamethasone on excretion of glucuronides

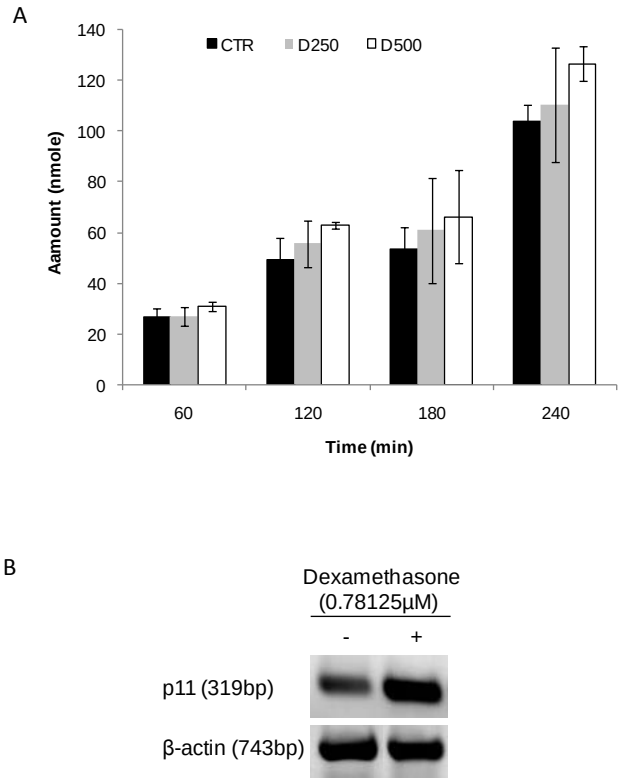

Figure V Effects of dexamethasone on the excretion of apigenin glucuronides (A) and inducation of p11 (B). Engineered HeLa cells pretreated with or without dexamethasone for 24 hours were incubated with 10μM apigenin. Each data point was the average of three determinations with error bar representing the standard deviation of the mean (n=3). P<0.05, *; P<0.01, . D250 and D500 represented 250nM and 500nM dexamethasone, respectively.**